



TARGETING THE CAROTID BODIES TO TREAT OBESITY

BERNARDETE SOFIA DE FREITAS MELO

Tese para obtenção do grau de Doutor em Mecanismos de Doença e Medicina Regenerativa

Doutoramento em associação entre:

Universidade NOVA de Lisboa (Faculdade de Ciências Médicas | NOVA Medical School)

Universidade do Algarve (UAlg)

Junho, 2021





TARGETING THE CAROTID BODIES TO TREAT OBESITY

Bernardete Sofia de Freitas Melo
Orientadores: Silvia Vilares Conde, Professora Auxiliar
Faculdade de Ciências Médicas | NOVA Medical School – FCM | NMS/UNL
Paulo Matafome, Investigador
iCBR, Faculdade de Medicina da Universidade de Coimbra

Tese para obtenção do grau de Doutor em Mecanismos de Doença e Medicina Regenerativa

Doutoramento em associação entre: Universidade NOVA de Lisboa (Faculdade de Ciências Médicas | NOVA Medical School) Universidade do Algarve (UAlg)

The experimental work was performed at: Chronic Diseases Research Center (CEDOC), Nova Medical School|Faculdade de Ciências Médicas da Universidade Nova de Lisboa; Departamento de Bioquímica y Biología Molecular y Fisiología, Universidad de Valladolid, Facultad de Medicina, Espanha; Laboratório de Fisiologia, Coimbra Institute for Clinical and Biomedical Research

(iCBR), Faculdade de Medicina, Universidade de Coimbra, Portugal;

Recherche Scientifique (CNRS) and Universidade de Côte d'Azur

- Institut de Pharmacologie Moléculaire et Cellulaire , Centre National de la

The present work was funded by Portuguese Foundation for Science and Technology (FCT – Portugal), grant reference PD/BD/128336/2017; PEst UID/NEU/04539/2013 and UID/NEU/04539/2019: CNC.IBILI; PEst UIDB/04539/2020 and UIDP/04539/2020: CIBB; and by European Foundation for the Study of Diabetes (EFSD) Albert Renold Travel Fellowship Programme attributed to Bernardete F. Melo (2020).

All animal studies described in this thesis were carried out in accordance with the European Union Directive for Protection of Vertebrates Used for Experimental and Other Scientific Ends (2010/63/EU). Experimental protocols were part of the project "Estudo das vias neuronais envolvidas nas doenças metabólicas associadas a sobreativação dos corpos carotídeos: definindo o caminho para o uso de dispositivos bioeletrónicos" (nº08/2015/CEFCM) approved by the NOVA Medical School|Faculdade de Ciências Médicas Ethics Committee (CEFCM) and by the Direção-Geral de Alimentação e Veterinária (DGAV).

The present work:

Originated the following publications:

Melo BF, Sacramento JF, Ribeiro MJ, Prego CS, Correia MC, Coelho JC, Cunha-Guimarães JP, Rodrigues T, Martins IB, Guarino MP, Seiça RM, Matafome P, Conde SV. Evaluating the Impact of Different Hypercaloric Diets on Weight Gain, Insulin Resistance, Glucose Intolerance, and its Comorbidities in Rats. Nutrients. 2019 May 28;11(6).

Originated the following conference proceedings:

B.F. Melo, C.S. Prego, J.F. Sacramento, S.V. Conde. Carotid body modulation: a therapeutic approach to induce adipose tissue browning and ameliorate metabolism promoting weight loss. Diabetologia (2019) 62 (Suppl 1):S1–S600.

Melo, Bernardete F.; Cláudia S. Prego; Joana F. Sacramento; Silvia V. Conde. "Bilateral carotid sinus nerve resection decreases weight gain, body fat mass and obesity associated co-morbidities in rodents.". Obesity Facts (2019) Vol. 12, Supplement 1:1–298.

Melo BF*, Prego CS*, Sacramento JF, Conde SV. Bilateral carotid sinus nerve resection decreases weight gain, body fat mass and obesity associated co-morbidities in rodents. Obesity Facts (2018) Vol. 11, Supplement 1, 1-364.

Prego CS*, Melo BF*, Sacramento JF, Conde SV. A ressecção do nervo do seio carotídeo diminuiu o ganho de peso, a massa gorda corporal e melhora as comorbilidades associadas à obesidade. Revista Portuguesa de Diabetes. (2018) Vol. 13(1) suppl:105.

Melo, Bernardete F.; Cláudia S. Prego; Miguel C. Correia; Marlene D. Cabral; Joana F. Sacramento; Silvia V. Conde. "Beneficial effects of carotid body denervation in obesity co-morbilities". Diabetologia (2018) Vol. 61:1–620

Melo BF*, Prego CS*, Correia MC, Cabral MD, Sacramento JF, Conde SV. Beneficial effects of carotid body denervation in obesity co-morbilities. Diabetologia (2017) 60 (Suppl 1):S1–S608.

Won the following awards:

Best poster communication at the Early Career Physiologists' Symposium. London, UK, 2018.

Best poster communication at the IV SPCAL Congress - Sociedade Portuguesa de Ciências em Animais de Laboratório, Portugal (2018).

Dr. Machiko Shirahata Trainee Award at the XX Meeting of the International Society for Arterial Chemoreception (ISAC), Baltimore (USA) 2017.

Originated the following communications:

Oral communications in international meetings:

Bernardete F. Melo, Cláudia S. Prego, Joana F. Sacramento, Sílvia V. Conde. The beneficial effects of carotid sinus nerve resection on obesity and glucose homeostasis are related with adipose tissue browning. 7th Meeting of the EASD-EGIR Study Group. Lisboa, Portugal, 2019.

Melo BF*, Prego CS*, Correia CS, Cabral MD, Sacramento JF, Conde SV. Carotid Sinus Nerve resection decreases weight gain and fat mass in a rodent model of obesity. XX Meeting of the International Society for Arterial Chemoreception (ISAC), Baltimore (USA) 2017.

Oral communications in national meetings:

Bernardete F. Melo, Cláudia S. Prego, Joana F. Sacramento, Sílvia V. Conde. Os efeitos benéficos da desnervação do nervo do seio carotídeo na obesidade e na homeostasia da glucose devem-se à indução do browning do tecido adiposo. 15th Portuguese Congress on Diabetes. Vilamoura, Portugal, 2019.

Melo BF, Prego CS, Sacramento JF, Conde SV. Carotid body modulation to treat obesity: inducing adipose tissue browning. 22nd Portuguese Congress on Obesity. Lisbon, Portugal, 2018.

Melo BF*, Prego CS*, Correia MC, Cabral MD, Sacramento JF, Conde SV. Carotid sinus nerve resection ameliorates glucose homeostasis and insulin secretion and action in an animal model of obesity. XLVIII Annual meeting of the Portuguese Society of Pharmacology, Lisbon, Portugal, 2018.

Prego CS*, Melo BF*, Correia MC, Cabral MD, Sacramento JF, Conde SV. Bilateral carotid sinus nerve resection decreases weight gain and body fat mass in a rat model of obesity. XLVIII Annual meeting of the Portuguese Society of Pharmacology, Lisbon, Portugal, 2018.

Poster communications in international meetings:

B.F. Melo, C.S. Prego, J.F. Sacramento, S.V. Conde. Carotid body modulation: a therapeutic approach to induce adipose tissue browning and ameliorate metabolism

promoting weight loss. Annual Meeting of the European Association for the Study of Diabetes (EASD). Barcelona, Spain, 2019.

Bernardete F. Melo*, Cláudia S. Prego*, Joana F. Sacramento, Silvia V. Conde. Carotid body modulation: a therapeutic target to produce adipose tissue browning and ameliorate metabolism promoting weight loss. 26th European Congress on Obesity (ECO2019). Glasgow, Scotland, 2019.

Melo BF*, Prego CS*, Sacramento JF, Conde SV. Beneficial effects of carotid sinus nerve resection on white adipose tissue metabolism. Europhysiology 2018 Congress. London, UK, 2018.

Melo BF*, Prego CS*, Sacramento JF, Conde SV. Beneficial effects of carotid sinus nerve resection on white adipose tissue metabolism. Early Career Physiologists' Symposium. London, UK, 2018.

Prego CS*, Melo BF*, Sacramento JF, Conde SV. Carotid sinus nerve resection reduces weight gain and improves metabolic function in high-fat animals via an increase in brown adipose tissue function and decrease in its inflammation. Europhysiology 2018 Congress. London, UK, 2018.

Melo BF*, Prego CS*, Sacramento JF, Conde SV. Bilateral carotid sinus nerve resection decreases weight gain, body fat mass and obesity associated co-morbidities in rodents. XXV European Congress on Obesity (ECO2018). Vienna, Austria, 2018.

Poster communications in national meetings:

Melo BF*, Sacramento JF*, Prego CS, Ribeiro MJ, Martins IB, Guarino MP, Conde SV. What is the most appropriate rat model to study type 2 diabetes? IV Congress Portuguese Society of Sciences in Laboratory Animals (SPCAL). Braga, Portugal, 2018.

Prego CS*, Melo BF*, Sacramento JF, Conde SV. A ressecção do nervo do seio carotídeo diminuiu o ganho de peso, a massa gorda corporal e melhora as comorbilidades associadas à obesidade. 14th Portuguese Congress of Diabetes. Albufeira, Portugal, 2018.

Para os meus pais José e Lília

Em memória dos meus avós

Acknowledgements

Em primeiro lugar gostaria de agradecer à Professora Doutora Sílvia Conde por me ter dado a oportunidade de desenvolver este projeto, orientando-me ao longo destes 4 anos. Queria também agradecer pela sua disponibilidade, pelo conhecimento transmitido, por todas as oportunidades que me proporcionou desde o momento em que integrei o seu grupo de investigação e pela sua positividade, mesmo quando os resultados não são propriamente o que esperávamos.

Gostaria também de agradecer ao meu co-orientador, o Professor Doutor Paulo Matafome, pelas palavras de incentivo e pela ajuda no mundo ingrato dos Western Blots.

À minha companheira de laboratório, Joana Sacramento, agradeço pela disponibilidade para me ajudar ao longo destes anos, pelas alegres manhãs passadas no biotério, pelas idas à Feira do Livro (que esperamos que possam voltar a acontecer em breve) e pelo conhecimento transmitido ao longo de 8 anos de vida em laboratório.

Gostaria também de agradecer às minhas companheiras de grupo Solange, Fátima e Adriana, pelos momentos divertidos, pelas gargalhadas e boa disposição que normalmente vos acompanham.

Aos meus companheiros de jornada, a "maltinha xalente" e em especial à Daniela Pedroso e à Juliana Gonçalves, pela companhia, pelos cafés e pelos lanches de final de tarde.

Deixo também um agradecimento à Professora Doutora Joana Batuca, Professora Doutora Maria Guarino e às Professoras Doutoras Emília Monteiro e Sofia Pereira, e restantes membros da Farmacologia, em especial à Maria João Correia e à Catarina Serqueira, não esquecendo também os ex-vizinhos Nuno Coelho, Clara Dias e Nádia Grilo. Obrigada por todos os momentos de alegria e pela companhia.

Não posso deixar de agradecer à Cláudia Prego por toda a sua dedicação a este projeto, pela ajuda, companhia e por todos os momentos de boa disposição.

Agradeço também à Filipa Freitas, pela companhia e pelos passeios, que agora já se fazem acontecer por terras Lisboetas!

Ao Gilberto gostaria de agradecer-te por todo o amor, pelo apoio que me deu ao longo destes anos, pelas palavras de conforto que nunca faltaram e por nunca duvidar das minhas capacidades. Agradeço acima de tudo a tua paciência e a capacidade de sempre me fazeres rir, por estares sempre disponível para mim e por me conseguires sempre acalmar!

Aos meus avós, que sempre cuidaram de mim com todo o amor e que infelizmente já não puderam acompanhar fisicamente esta caminhada, o meu imenso obrigada. As saudades são infinitas!

Por último, deixo aqui um agradecimento muito especial aos meus pais, por todo o amor que têm por mim e por todo o esforço que fizeram para que eu sempre pudesse seguir os meus "sonhos"; por todo o apoio, por me ouvirem e aconselharem e acima de tudo, por serem um exemplo a seguir! Obrigada!

List of Contents

	Page
List of Figures	iii
List of Tables	٧
Abbreviations	vii
Abstract	ix
Resumo	хi
Chapter I – The state of art	
Obesity	3
The white adipose tissue	4
Endocrine properties of adipose tissue	6
White adipose tissue distribution and types of obesity	10
White adipose tissue dysfunction in obesity	10
Insulin resistance, impaired glucose metabolism and T2D	14
The brown adipose tissue	16
Brown adipose tissue activation	19
Brown adipose tissue in obesity	23
The SNS in obesity	24
The carotid body	26
Physiology of the CB	27
Role of carotid body as a metabolic sensor	28
Carotid body and the sympathetic-mediated diseases	30
Therapeutic options for the treatment of obesity	32
Chapter II- General and specific aims	35
Chapter III- Evaluating the Impact of Different Hypercaloric Diets on Weight Gain,	
Insulin Resistance, Glucose Intolerance, and its Comorbidities in Rats	
Abstract	38
Introduction	38
Methods	41
Results	45
Discussion	58
Chapter IV - Carotid body and adipose tissue in obesity and type 2 diabetes: an	66
intricate link involving browning and sympathetic integration modulation	00
Abstract	68
Introduction	69
Methods	71
Results	79
Discussion	92
Chapter V- General discussion	100
Final considerations and futures directions	108
References	110

List of Figures

	Page
Chapter I – The state of art	
Figure 1- Lipogenesis and lipolysis pathways in the adipocytes	6
Figure 2- Possible mechanisms of obesity-induced insulin resistance development	16
Figure 3- Anatomical location of brown adipose tissue (BAT) depots	18
Figure 4- Activation of BAT thermogenesis by the SNS	20
Figure 5- Sympathetic neurons and neurotransmitters released	24
Figure 6- Carotid Body (CB) morphology	27
Chapter III- Evaluating the Impact of Different Hypercaloric Diets on Weight Gain,	
Insulin Resistance, Glucose Intolerance, and its Comorbidities in Rats	
Figure 1- Weight gain in animal models of type 2 diabetes and obesity.	46
Figure 2- Glucose metabolism and insulin action and secretion in animal models of type	51
2 diabetes and obesity	31
Figure 3- Alterations in the expression of proteins involved in insulin signaling in insulin-	53
sensitive tissues in animal models of obesity and type 2 diabetes.	33
Figure 4- Mean arterial pressure levels in the distinct models of obesity and type 2	55
diabetes.	33
Figure 5- Lipid deposition in the liver in the distinct models of obesity and type 2	55
diabetes	55
Figure 6- Effect of hypercaloric diets and genetic deletion of leptin receptors on	57
sympathetic activity evaluated by spectral analysis of the heart rate.	57
Chapter IV - Carotid body and adipose tissue in obesity and type 2 diabetes: an	
intricate link involving browning and sympathetic integration modulation	
Figure 1- Carotid sinus nerve (CSN) resection decreases weight gain and adipose tissue	80
deposition in obese rodents	00
Figure 2- Carotid Sinus Nerve (CSN) resection decreases respiratory responses to	81
hypoxia	01
Figure 3- Carotid sinus nerve (CSN) resection ameliorates visceral white adipose tissue	85
(WAT) metabolism in obese rodents	03
Figure 4- Carotid sinus nerve (CSN) resection improves brown adipose tissue	88
metabolism and re-establish sympathetic integration in rodents	00
Figure 5- Linking the carotid body with obesity associated-adipose tissue inflammation	90
and hypoxia	50
Figure 6- Carotid sinus nerve (CSN) resection restores sympathetic integration in	92
visceral white and brown adipose tissues	52

List of tables

	Page
Chapter III- Evaluating the Impact of Different Hypercaloric Diets on Weight Gain,	_
Insulin Resistance, Glucose Intolerance, and its Comorbidities in Rats	
Table 1- Adipose tissue depots and lipid profile (total cholesterol, triacylglycerols, high-	
density lipoprotein (HDL)—cholesterol and low-density lipoprotein (LDL)—cholesterol) in	48
animal models of obesity and type 2 diabetes.	
Table 2- Catecholamine (epinephrine and norepinephrine) levels in plasma and in	57
adrenal medulla in animal models of obesity and type 2 diabetes.	
Table 3- Summary of the main pathological features of animal models of	59
dysmetabolism.	
Chapter IV - Carotid body and adipose tissue in obesity and type 2 diabetes: an	
intricate link involving browning and sympathetic integration modulation	
Table 1- Effect of CSN resection on metabolism and lipid profile on obese rats and mice	82

Abbreviations

ACC1 - Acetyl-CoA carboxylase 1

ADIPOR1 - Adiponectin receptor 1

ADIPOR2 - Adiponectin receptor 2

AgRP - Agouti-related peptide

Akt2 - Serine/threonine-protein kinase 2

ATGL - Adipocyte triglyceride lipase

ATP - Adenosine triphosphate

b-AR - Beta adrenergic receptor

 $\beta_1\text{-AR}$ - $\ \beta_1$ adrenergic receptor

 β_2 -AR - β_2 adrenergic receptor

β3-AR - b-3 adrenergic receptors

BAT – Brown adipose tissue

BMI - Body mass index

C/EBPβ - CCAAT/enhancer-binding protein beta

Ca²⁺ - Calcium

cAMP - Cyclic AMP

CB – Carotid body

cBAT - Cervical brown adipose tissue

CD36 - Cluster of differentiation 36

CSN - Carotid sinus nerve

DGAT - Diacylglycerol acyltransferase

DIO – Diet-induced obese

FAS - Fatty acid synthase

FFA - Free fatty acids

FOXO1 - Forkhead box protein O1

G6P - glucose-6-phosphate

G6pc - Glucose-6-phosphatase

GLP-1 - glucagon-like peptide 1

GLUT4 – Glucose transporter type 4

GSK3 – Glycogen synthase kinase-3

GSVs - GLUT4 containing storage vesicles

GYS2 - Glycogen Synthase 2

HIF - Hypoxia-inducible factors

HIF-1 β - Hypoxia-inducible factor 1-beta

 $HIF1\alpha$ - Hypoxia-inducible factor 1-alpha

 $\mathsf{HIF2}\alpha$ - Hypoxia-inducible factor 2-alpha

HSL – Hormone sensitive lipase

iBAT - Interscapular brown adipose tissue

IL-1β - interleukin-1b

IL-6 - interleukin-6

IR - Insulin receptor

IRS - insulin receptor substrate

IRS1 - Insulin receptor substrate 1

IRS2 – Insulin receptor substrate 2

LEP - Leptin gene

LEPR or OBR – Leptin receptor

LPL - Lipoprotein lipase

MCP-1 - Monocyte chemotactic protein-1

MGL - Monoacylglycerol lipase

mmHg - Millimeter of mercury

MTORC2 - mTOR Complex 2

Myf5 - Myogenic factor 5

NA - Noradrenaline

NADPH - Nicotinamide adenine dinucleotide phosphate

NE – Norepinephrine

NPY - Neuropeptide Y

O₂ – Oxygem

OSA - Obstructive sleep apnea

Pck1 - Phosphoenolpyruvate carboxykinase 1

PDE3B - Phosphodiesterase 3

PDK1 - 3-phosphoinositide-dependent protein kinase 1

PGC-1α - peroxisome proliferator-activated receptor gamma coactivator 1-alpha

PI3K - phosphoinositide 3-kinase

PIP2 - phosphatidylinositol 4,5-bisphosphate

PIP3 - phosphatidylinositol (3,4,5)-trisphosphate

PKA - Protein kinase A

PKC - protein kinase C

PLIN1 - Perilipin1

PNS - Parasympathetic nervous system ACh - Acetylcholine

PO₂ - Partial pressure of oxygen

POMC - Pro opiomelanocortin

PPAR-γ - peroxisome proliferator-activated receptor gamma

PPARα - Peroxisome proliferator-activated receptor alpha

PRDM16 - Transcriptional regulators PR domain containing 16

Rab GAP TBC1D - RabGTPase-activating Protein TBC1D

SAT - Subcutaneous adipose tissue

sBAT - Sub-scapular brown adipose tissue

SNS – Sympathetic nervous system

T2D – Type 2 diabetes

TAG - Triacylglycerol

TK - Tyrosine kinase

TNF α - Tumor necrosis factor α

TRP - Transient receptor potential

UCP1 - Uncoupling protein 1

VAT - visceral/omental adipose tissue

VEGF - Vascular endothelial growth factor

WAT – White adipose tissue

WHO - World Health Organization

Abstract

Obesity is a major public health concern, which contributes significantly to morbidity and mortality due to the associated comorbidities. Therapeutics to obesity are often unsuccessful and therefore there is an urgent need for novel approaches that would help to find more effective therapeutic interventions for obesity.

Currently, the carotid bodies (CBs), which are peripheral chemoreceptors that respond to hypoxia by increasing chemosensory activity in its sensitive nerves, are considered metabolic sensors, being consensual that these organs control sympathetic activity. Moreover, CBs overactivation, via an increase in the whole-body sympathetic nervous system (SNS), have been shown in several metabolic diseases that are strongly associated with obesity. It was already described that the resection of CB sensitive nerve, the carotid sinus nerve (CSN), prevented weight gain and improved glucose homeostasis by positively impacting insulin signaling and glucose uptake in the liver and adipose tissue. Herein, we characterized several hypercaloric rat models of obesity and type 2 diabetes, comparing each with a genetic model, the Zucker fatty diabetic rat, with the aim of identifying the most appropriate model to study these disorders. Moreover, we tested the innovative hypothesis that the CBs are key players in the neural sympathetic circuit controlling the white and brown adipose tissue metabolism and that the abolishment of CB activity will have an anti-obesity effect, associated with increased function of the adipose tissues and the recovery of sympathetic integration. To test this hypothesis, we have abolished CB activity by resecting the CSN in control and obese animals, achieved by submitting Wistar rats and C57/BL6 mice to 60% lipid-rich diet during 10 and 12 weeks; and studied its impact on weight gain and fat deposition and its comorbidities as well as on white and brown adipose tissue metabolism and its sympathetic activation.

We found that the best rat model to study obesity and comorbidities is the diet-induced rat, particularly the animal submitted to 60% lipid-rich diet for 19 weeks, since it exhibits a phenotype more similar to human obesity, with increased weight gain, fat deposition and metabolic dysfunction. Additionally, we found that CSN resection decreased weight gain, adipose tissue deposition and adipocytes perimeter, as well as reversed insulin

resistance, ameliorated glucose intolerance and decreased hyperinsulinemia. Also, CSN resection restored the decreased basal visceral WAT metabolism induced by HF diet, measured by the oxygen consumption rate (OCR), mitochondrial activity evaluated by the mitotraker, UCP1 expression, in vivo glucose uptake, the expression of PGC1lpha and PPARγ and AMPK phosphorylation. In addition, CSN resection while did not modified basal OCR within the BAT, it increased its thermogenic activity in control and HF animals in response to norepinephrine, and increased mitochondrial activity, UCP1 expression, glucose uptake and AMPK phosphorylation. We also found that, albeit inflammation and hypoxia usually represent important mechanisms in promoting adipose tissue dysfunction, in this case HF diet did not induced significant alteration in the expression of IL-6 or IL-1 β receptors within the adipose tissue both WAT and BAT neither in circulating levels of TNF α levels or IL-10. Also, CSN resection did not impact HIF1 α or HIF2 α expression. Moreover, CSN resection restored catecholaminergic signaling and integration in the WAT of HF animals, shown by the restoration of the decreased levels of catecholamines within the WAT and decreased intensity of TH expression by lightsheet microscopy and western blot induced by HF diet.

Therefore, we can conclude that the CB plays an important role in development of obesity and in the control of adipose tissue metabolism being a new player in the neurocircuitry sympathetic nervous system-adipose tissue connection. The results obtained in the present thesis introduce a new therapeutic target for obesity management.

Resumo

A obesidade é um importante problema de saúde pública que contribui para elevada mortalidade e morbilidade a nível mundial devido às suas comorbilidades. As terapêuticas para a obesidade são frequentemente ineficazes e como tal, há a necessidade de encontrar novas abordagens terapêuticas para a mesma.

Os corpos carotídeos (CBs) são quimiorreceptores periféricos que respondem à hipóxia através de um aumento da atividade quimiossensitiva dos seus nervos sensitivos. Atualmente, os CBs são também considerados sensores metabólicos, sendo consensual que estes controlam a atividade do sistema nervoso simpático.

Para além disso, a sobre-ativação destes, através do aumento da atividade do sistema nervoso simpático, tem sido demonstrada em diversas doenças metabólicas associadas à obesidade. Em adição, já foi descrito que o corte do nervo do seio carotídeo, o nervo sensitivo do CB, previne o ganho de peso e melhora a homeostasia da glucose através de uma melhoria na sinalização de insulina e no captação de glucose no fígado e no tecido adiposo.

Com este trabalho, foram caracterizados vários modelos animais de obesidade e diabetes tipo 2, induzidos por dieta hipercalórica, os quais foram comparados com um modelo genético, os ratos diabéticos Zucker, com o objetivo de identificar o modelo mais apropriado para estudar estas patologias. Para além disso, testamos a hipótese de que os CBs são elementos essenciais no circuito neuronal simpático, controlando o metabolismos dos tecidos adiposos branco e castanho, e que a supressão da atividade destes terá um efeito anti-obesidade, associado a um aumento da atividade do tecido adiposo e a uma recuperação da integração simpática no mesmo. De forma a testar esta hipótese, a atividade do CB foi abolida através da ressecção do nervo do seio carotídeo, em ratos Wistar e ratinhos C57/BL6 submetidos a uma dieta hipercalórica (60% de lípidos), sendo depois avaliado o seu efeito no ganho de peso e comorbidades associadas a este, bem como no metabolismo e na ativação simpática dos tecidos adiposos branco e castanho. Assim, observamos que o melhor modelo animal para estudar a obesidade, e comorbidades a esta associadas, é o modelo submetido a 19 semanas de dieta HF, dado que exibiu um fenótipo mais semelhante à obesidade

observada nos humanos, com um aumento no ganho de peso, na deposição de gordura e na disfunção metabólica. Adicionalmente, observamos que o corte do nervo do seio carotídeos diminui o ganho de peso, a deposição de gordura e o perímetro dos adipócitos, revertendo a resistência à insulina, melhorando a tolerância à glucose e diminuindo os níveis de insulina. Em adição, a ressecção do nervo do seio carotídeo melhorou o metabolismo do tecido adiposo branco, através do aumento do seu metabolismo basal e/ou do seu metabolismo em resposta a uma ativação simpática, bem como através da melhoria nas vias envolvidas na termogénese, com aumento na expressão das proteínas UCP1, PGC1 α e PPAR γ e ainda com um aumento do conteúdo mitocondrial, e uma melhoria da captação de glucose e aumento da expressão da proteína AMPK fosforilada, melhorando também o metabolismo do tecido adiposo castanho. Para além disso, apesar de estar descrito a presença de inflamação e hipóxia em estados de obesidade, não observamos qualquer alteração da expressão de marcadores inflamatórios, como por exemplo, nos receptores de IL-6 e de IL-1 β bem como nos níveis de TNFlpha ou da citocina anti-inflamatória, IL-10, sendo que também não foi observada qualquer alteração na expressão dos fatores HIF1 α e HIF2 α . Finalmente, demonstramos que o CB controla a ação do sistema catecolaminérgico no tecido adiposo dado que o corte do nervo do seio carotídeo restaurou a atividade do SNS, através da diminuição das catecolaminas plasmáticas e do índice de ativação simpática do organismo, contribuindo também para o restauro do conteúdo de catecolaminas. Mais, a abolição da atividade do CB aumentou a expressão de tirosina hidroxilase no tecido adiposo e restaurou a integração simpática neste.

Assim, com este trabalho, demonstramos que o CB é um interveniente chave na ligação sistema nervoso simpático-tecido adiposo sendo, como tal, um possível alvo terapêutico para a obesidade e suas comorbidades.

	Cha	pter	ı
--	-----	------	---

The state of art

Obesity

Obesity is defined by the World Health Organization (WHO) as an excess in the fat mass enough to increase the risk of morbidity, of altered physical or psychological well-being, and/or mortality (Angi & Chiarelli, 2020; *World Health Organization - Obesity and overweight*, 2021). Epidemiological studies demonstrate that obesity and overweight are significant growing problems that have reached the status of global epidemics (Kojta et al., 2020) and according to WHO, the numbers of obese people have tripled in the last 20 years (*World Health Organization - Obesity and overweight*, 2021).

Obesity is a multifactorial disease whose development can be affected by several genetic, sociocultural and behavioral factors, and is a primary cause of metabolic disorders such as type 2 diabetes (T2D), dyslipidemia and hypertension (F. Liu et al., 2020). In fact, recently, epidemiological evidence showed that from type 2 diabetic adults, 85% are also obese, and is predicted that, by 2025, more than 300 million people will have T2D as consequence of obesity (Chait & den Hartigh, 2020).

The adipose tissue

Historically, the adipose tissue has been classified in two types, the white adipose tissue (WAT) and the brown adipose tissue (BAT). The WAT comprises the largest adipose tissue in most mammals and it is essential for energy storage, insulin sensitivity and endocrine regulation (Chait & den Hartigh, 2020). On the other hand, the BAT, which is critical for body temperature maintenance through non-shivering thermogenesis, is mostly present in mammals postnatally and during hibernation.

The adipose tissue is composed of many different cell types, which secrete numerous cytokines, chemokines and hormones. The adipocytes constitute approximately 33% of the adipose tissue, with the rest being endothelial cells, macrophages, fibroblasts, stromal cells, immune cells and pre-adipocytes (Chait & den Hartigh, 2020).

White and brown adipocytes differ in size, shape and in the intracellular structure of the organelles. While the white adipocytes are generally spherical and contain one large and single lipid droplet, that pushes the organelles to the cell's periphery, the brown

adipocytes are ellipsoidal-shaped cells that are composed of dispersed multiple lipid droplets and iron-containing mitochondria (Richard et al., 2000).

Recently, the beige adipocytes were also described as having characteristics of both white and brown adipocytes. They develop within WAT depots, from a distinct subset of preadipocytes or through transdifferentiation of existing adipocytes. This type of adipocytes can arise in response to many stimuli such as cold exposure, diet and exercise, among others (Chait & den Hartigh, 2020; Seale et al., 2008; Shao et al., 2019; J. Wu et al., 2012).

The white adipose tissue

The adipose tissue functions as a focal point of energy balance where the adipocytes store triacylglycerol (TAG) and release fatty acids to supply to other tissues during fasting or in situations of high-energy demand as, for example, exercise. Stored triglycerides are in a constant state of flux because energy storage and mobilization are determined largely by hormone fluctuations (Chait & den Hartigh, 2020; Qatanani & Lazar, 2007) which occur with circadian rhythms or in response to nutrient availability. Also, the WAT is innervated by sympathetic nerve endings, being the sympathetic nervous system the principal physiological mediator of lipolysis (Siddle & Hales, 1975; Trayhurn, 2013).

Lipogenesis

The adipocytes can accumulate lipids via two processes: 1) by removing dietary lipids from circulation in the form of free fatty acids (FFA) released from circulating TAGs, through action of the lipoprotein lipase (LPL) (Kersten, 2014). LPL is secreted by the adipocytes and transported to the adjacent capillary lumen to catalyze the hydrolysis of the FFAs from circulating lipoproteins, such as very low density proteins or chylomicrons produced in the small intestine and these FFAs will then enter the cell through action of the cluster of differentiation 36 (CD36) (Fielding & Frayn, 1998; K. Frayn, 2002). The adipocytes also take up glucose, through glucose transporter type 4 (GLUT4), which is

converted into glycerol that is essential for the sequential esterification of the fatty acids to form TAG. The final step of this process of TAG formation is the re-esterification of the circulating FFAs, mediated by diacylglycerol acyltransferase (DGAT) (Harris et al., 2011; Luo & Liu, 2016; Richard et al., 2000); 2) by *de novo* lipogenesis that occurs within the adipocytes, in fasting or in fed states (Luo & Liu, 2016). Therefore, after a meal, the excess of glucose oxidation activates acetyl-CoA carboxylase 1 (ACC1) and fatty acid synthase (FAS) to convert acetyl-CoA to palmitate, which can be elongated and desaturated to originate other fatty acid species (Figure 1).

Under physiological conditions, *de novo* lipogenesis is relatively low in WAT, compared with BAT and liver, both in humans and rodents (Richard et al., 2000).

Lipolysis

Lipolysis is a process that generates glycerol and FFAs from the cleavage of TAGs by lipases (Braun et al., 2018). This process happens when energy demand is high and/or the metabolic fuels are low and it can occur in all tissues being more prevalent in the adipose tissue. Briefly, the TAGs are broken down into diacylglycerols and monoacylglycerols by the sequential action of the adipocyte triglyceride lipase, hormone sensitive lipase and monoacylglycerol lipase (Braun et al., 2018; Luo & Liu, 2016). From each step is released a FFA and at the end the monoacylglycerol lipase also releases glycerol from the last FFA released. These products can be released into circulation to be used by other tissues or can be re-esterified within the adipocytes (Braun et al., 2018; Luo & Liu, 2016). This process is controlled by both sympathetic nervous system input and a variety of hormones. Norepinephrine (NE) is a well-studied regulator of lipolysis and it acts by stimulating b-adrenergic receptors (b- AR) which lead to stimulation of the protein kinase A (PKA) via adenyl cyclase-mediated production of cyclic AMP (cAMP) (Braun et al., 2018). PKA in turn activates adipocyte triglyceride lipase, by phosphorylating perilipin1 (PLIN1), and hormone sensitive lipase, by direct phosphorylation (Hsieh et al., 2012; Nielsen et al., 2014) (Figure 1).

Lipolysis is suppressed by the postprandial increase in circulating insulin levels through increased phosphodiesterase 3 (PDE3B) activity and decreased cAMP levels. On the

other side, in a fasting state, insulin levels decrease and NE is released, promoting lipolysis (Braun et al., 2018; Nielsen et al., 2014; Richard et al., 2000; Sztalryd & Brasaemle, 2017).

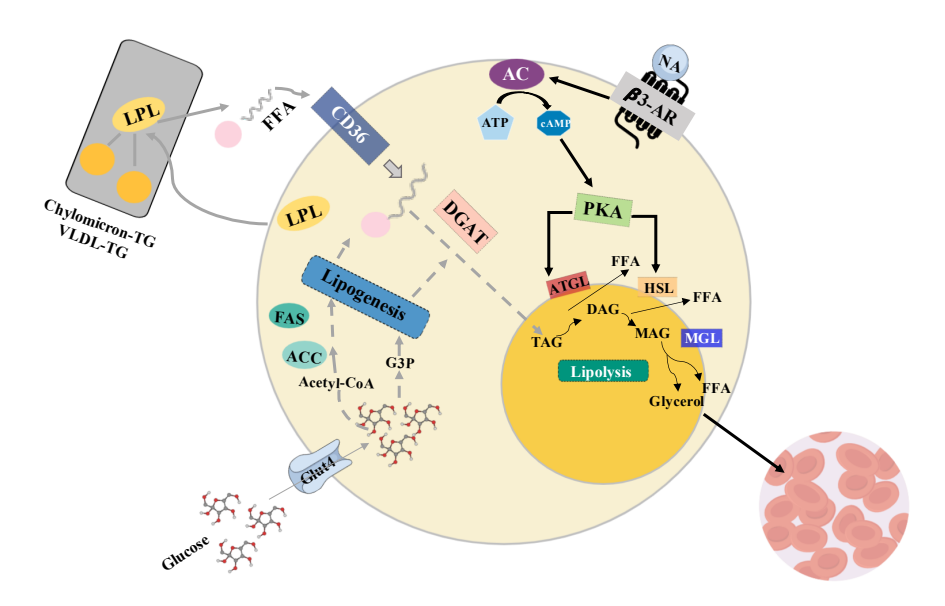


Figure 1 -Lipogenesis and lipolysis pathways in the adipocytes. Lipogenesis is shown with gray arrows: free fatty acids (FFA) enter the cell through action of the fatty acid transporter, cluster of differentiation 36 (CD36); insulin stimulates glucose uptake by increasing glucose transporter type 4 (GLUT4) in the plasma membrane, which is converted into glycerol that is essential for the sequential esterification of the fatty acids to form TAG; re-esterification of the circulating FFAs, mediated by diacylglycerol acyltransferase (DGAT). Lipolysis is shown by black arrows: Norepinephrine (NE) stimulates ß-adrenergic receptors (ß3-AR) which leads to stimulation of the protein kinase A (PKA) production of cyclic AMP (cAMP); PKA activates adipocyte triglyceride lipase (ATGL), by phosphorylating perilipin1 and hormone sensitive lipase (HSL); TAGs are broken down into diacylglycerols and monoacylglycerols by the sequential action of the ATGL, HSL and monoacylglycerol lipase (MGL), releasing FFA and glycerol, from the last FFA released. Adapted from Richard et al., (2000).

Endocrine properties of adipose tissue

Adipocytes and other cells of the adipose tissue secrete several mediators, including inflammatory cytokines, lipids and peptide hormones, among others. Leptin and adiponectin are two hormones that are almost exclusively secreted in the adipocytes and that have several functions, such as regulation of food intake, insulin sensitivity and immune responses.

1. Leptin

Leptin is a peptide hormone, encoded by the LEP gene, essential for body weight regulation. After its release by the adipose tissue into the bloodstream, it crosses the blood brain barrier and, by binding to its receptors (LEPR or OBR), will mainly act in the arcuate nucleus of the hypothalamus to activate pro opiomelanocortin (POMC)containing neurons, which produce anorexigenic molecules, and to deactivate the orexigenic neuropeptide Y (NPY)- and agouti-related peptide (AgRP)-containing neurons (Chait & den Hartigh, 2020; Klok et al., 2007). Briefly, when energy stores are low, leptin levels decrease, leading to lower activity of POMC neurons and increased activity of NPY and AgRP neurons, increasing appetite and food intake. On the other hand, when energy stores are abundant, for example in obesity, it is expected that elevated leptin levels result in decreased energy intake (Nikolaos Perakakis et al., 2021). Leptin has also an important impact on hypothalamic pituitary axes in both animals and humans (Chan et al., 2003) and, in preclinical studies (Haynes et al., 1997b; Rahmouni et al., 2005), has also been proposed to be linked with sympathetic nervous system (SNS) activity. In fact, it was demonstrated that leptin increases NE turnover in interscapular BAT (Collins et al., 1996) and sympathetic nerve activity in lean Sprague-Dawley rats (Haynes et al., 1997a). Furthermore, leptin also increases sympathetic nerve activity to the kidney, hindlimb, and adrenal gland (Haynes et al., 1997b) and plasma concentration of NE and epinephrine (Satoh et al., 1999) and it has been proposed to be one of the major contributors to the increased SNS activity observed in obesity and obesityinduced cardiometabolic disturbances, since it was observed a positive correlation between whole-body NE spillover and plasma leptin levels in overweight and obese metabolic syndrome subjects (Straznicky et al., 2005), with similar results in rats (Muntzel et al., 2012). Apart from its direct role on SNS, it was also demonstrated that the carotid body (CB), which is known to increase SNS activity when activated (for detailed description please see page 26), expresses the receptor LEPR in type I cells. This finding has been associated with a physiological role of circulating or locally produced leptin in the regulation of CB function (Messenger et al., 2012; Porzionato et al., 2011; Ribeiro et al., 2018). In fact, it was proposed that leptin is also involved in the control of breathing, since it was described that the administration of leptin reverses hypoxia and hypercapnia in animal models with a mutation in the leptin gene (Ip et al., 2000; Tankersley et al., 1998), and that leptin increases minute ventilation in rats and mice during normoxia (O'Donnell et al., 1999; Ribeiro et al., 2018; Yao et al., 2016) and hypoxic exposure (Ribeiro et al., 2018). Also, leptin levels are increased in obstructive sleep apnea (OSA) patients (Ip et al., 2000), correlating with its severity, which may denote leptin resistance, a condition commonly observed in obese patients. Furthermore, it was demonstrated that leptin plays a role on hypertension since it was shown that leptin infusion, in lean mice, increased blood pressure, an effect that was abolished by CB denervation (M.-K. Shin et al., 2019). Moreover, in a study with transgenic mice overexpressing leptin, mice exhibited an increase of 10-15 mmHg in blood pressure relative to wildtype ones, which was normalized after treatment with α -adrenoceptor, β -adrenoceptor, and sympathetic ganglionic blockers (Ogawa et al., 2002).

Most animal studies with leptin have been performed in the ob/ob mice or in the dietinduced obese (DIO) mice. The ob/ob mice have no leptin, are severely obese, hyperphagic, have lower body temperature and energy expenditure, are hyperglycemic, hyperinsulinemic, hyperlipidemic and have hepatic steatosis (Cohen et al., 2001; Lindström, 2007; Singh et al., 2009; M. Zhang et al., 2007). In these mice, leptin administration completely reversed most of the observed abnormalities (J. Halaas et al., 1995; Singh et al., 2009; Weigle et al., 1995) and normalized body weight by reducing fat mass without affecting lean mass (J. Halaas et al., 1995; Weigle et al., 1995), showing the role of leptin on regulating food intake and energy consumption and on promoting lipolysis. However, leptin administration may also promote side effects such as atherogenesis, platelet aggregation, inflammation, oxidative stress and endothelial dysfunction, among others (Beltowski, 2006; Konstantinides et al., 2001; Simonds et al., 2017). Leptin administration was also tested in DIO mice however the beneficial effects of leptin observed in the ob/ob mice were not replicated (J. L. Halaas et al., 1997; Masuzaki et al., 1995) and the same was also observed in human studies with obese patients suggesting the presence of leptin tolerance/resistance (Hukshorn et al., 2000; Mittendorfer et al., 2011). In fact, studies showed that serum and plasma leptin levels are higher in subjects with a higher body mass index (BMI) and a higher percentage of total body fat (Considine et al., 1996; J. A. Marshall et al., 2000) and also in subjects with insulin resistance and T2D (Bidulescu et al., 2020), which could explain leptin resistance. Leptin resistance may involve reduced leptin transport across the blood brain barrier, impaired receptor trafficking, suppression of leptin receptor signaling or it may indicate that leptin functions only in hypoleptinemic and normoleptinemic states. However, leptin resistance remains unclear, especially in humans, due to the technical limitations of the studies and most of the information is acquired from animal-based studies.

2. Adiponectin

Adiponectin is an insulin-sensitizing hormone that acts in a wide range of tissues. Its expression and circulating levels vary between adipose tissue depots and with higher expression in the subcutaneous depot. Adiponectin signals through ADIPOR1 and ADIPOR2 receptors, which are expressed predominantly in muscle and liver (Cantarin et al., 2013). The resulting signaling pathway, mediated through peroxisome proliferator-activated receptor alpha (PPARα), leads to increased glucose uptake in WAT, decreased WAT inflammation, decreased hepatic gluconeogenesis and increased liver and skeletal muscle fatty acid oxidation (Chait & den Hartigh, 2020). In fact, clinical data showed an association between low plasma adiponectin levels and obesity, insulin resistance, metabolic syndrome and T2D (Kadowaki et al., 2006). Furthermore, low adiponectin levels were also associated with increased atherosclerotic cardiovascular events, hypertension, and dyslipidemia (Wang & Scherer, 2008).

White adipose tissue distribution and types of obesity

The WAT can be classified by location into subcutaneous (SAT; located under the skin, in gluteofemoral, back and anterior abdominal region) or visceral/omental (VAT; located intra-abdominally) adipose tissue (Chait & den Hartigh, 2020). These tissues are also distinguished taking into account their morphology as well as their functionality, with

the VAT containing small amounts of pre-adipocytes and larger adipocytes whereas the SAT tends to have a higher number of smaller adipocytes in physiological conditions (Kojta et al., 2020; A. Liu et al., 2009; F. Liu et al., 2020). Furthermore, the SAT is characterized by having higher insulin sensitivity therefore, metabolically, the SAT is suggested to have a protective role in metabolic risk whereas VAT accumulation is an independent risk factor for obesity comorbidities. In fact, studies have shown that VAT is more related with adipose tissue inflammation and that VAT-related obesity promotes the development of insulin resistance and T2D and is often accompanied by dyslipidemia and hypertension (Kojta et al., 2020)

Taking into account the different locations and functionalities of the WAT, two types of obesity have been described, the android obesity and gynoid obesity. Android obesity is characterized by central/abdominal accumulation of adipose tissue whereas gynoid obesity is characterized by gluteo-femoral accumulation of adipose tissue, being the first dominant in men whereas subcutaneous fat in the hip and thigh regions is dominant in women (Vague, 1996). Furthermore, android obesity has been shown to be associated with a higher risk of cardiovascular disease, of development of insulin resistance and T2D, hypertension, dyslipidemia and inflammation (Kojta et al., 2020).

White adipose tissue dysfunction in obesity

Obesity is often characterized by dysfunctional WAT in which, initially, adipocytes become hypertrophic in periods of caloric excess and secrete adipokines that result in the recruitment of pre-adipocytes, which will differentiate into mature adipocytes (Chait & den Hartigh, 2020; Goossens & Blaak, 2015). However, for reasons that are currently under investigation, when the capacity for adipocytes recruitment and hypertrophy is overloaded, fat will accumulate in ectopic sites such as liver, visceral depots and skeletal muscle, among others (S. M. Kim et al., 2014). This accumulation of fat is accompanied by inflammation, by an exacerbation of regional hypoxia and consequent excessive collagen deposition (F. Liu et al., 2020). Also, these pathophysiological alterations contribute to adipokine dysregulation and can induce insulin resistance, dyslipidemia,

dysglycemia, hypertension, non-alcoholic fatty liver disease and T2D, as already mentioned (Chait & den Hartigh, 2020).

1. WAT Inflammation and immune cells infiltration

Over the years, it has been recognized that obesity is associated with a chronic, lowgrade inflammation in a variety of tissues including skeletal muscle, liver, pancreas islet, intestine, brain and WAT (H. Wu & Ballantyne, 2020). The expansion of the adipose tissue depots is accompanied by an infiltration of immune cells, namely monocytes, which are recruited in response to chemokines produced by the hypertrophic adipocytes, such as monocyte chemotactic protein-1 (MCP-1). Once the monocytes arrive to the inflammation sites on the WAT, they differentiate into macrophages M1, which produce pro-inflammatory cytokines such as tumor necrosis factor α (TNF α), interleukin-6 (IL-6) and interleukin-1b (IL-1β). This macrophage accumulation occurs especially in the visceral depot, both in rodents and humans, and is thought that these represent an immune response to dead or dying adipocytes or as a buffer for ectopic lipids that surpass adipocyte storage capacity (Cancello et al., 2006; Murano et al., 2008; Subramanian et al., 2008). Indeed, the adipose tissue in obesity is characterized by the presence of foam cells similar to those observed in atherosclerotic plaques, resulting from lipid phagocytosis by macrophages (Shapiro et al., 2013). Other pro-inflammatory cells that were found increased in the WAT in obesity states are TH2 T-cells, B-cells and dendritic cells (Cho et al., 2016; J. Liu et al., 2009; O'Rourke et al., 2009; Winer et al., 2011). In addition, hypertrophic adipocytes overexpress inflammatory cytokines such as IL-6, MCP1 and TNF α , independently of the total body fat mass content and BMI. Evidences suggest that the systemic inflammation that is present in obesity and that contributes to insulin resistance begins with the inflammation of the WAT and in fact, is thought that the regulation of hepatic c-reactive protein, which is a biomarker for insulin resistance and cardiovascular disease, occurs in response to IL-6 secretion from WAT (Chait & den Hartigh, 2020; F. Liu et al., 2020; Longo et al., 2019; Yudkin et al., 2000).

2. WAT hypoxia

A well-known oxygen (O₂) sensing mechanism in cells is the transcription of hypoxiainducible factors (HIF), the O_2 -sensitive subunits HIF-1 α and HIF-2 α , and the O_2 insensitive HIF-1 β subunit (Semenza, 1999). In normoxic conditions, HIF α is hydroxylated by prolyl hydroxylases and degraded by proteasomes, through interaction with the von Hippel-Lindau protein (W. Kim & Kaelin, 2003). However, under hypoxic conditions, the hydroxylation of HIF α is inhibited, it becomes stabilized and dimerizes with the HIF-1 β (which is constitutively expressed) to activate the transcription of genes involved in the regulation of angiogenesis and energy metabolism (Semenza, 1999). It is known that both $HIF1\alpha$ and $HIF2\alpha$ are expressed in adipocytes, with $HIF1\alpha$ being expressed in mature adipocytes and progenitor cells whereas $HIF2\alpha$ is expressed only in mature adipocytes (Lin et al., 2006). Also, it has been proposed that the adipocytes' hypertrophy limits oxygen diffusion in the WAT, triggering regional hypoxia and leading to the activation of HIF- 1α and HIF- 2α subunits. In fact, it was already showed that HIF-2α protein levels are increased in adipocytes of mice submitted to 4 weeks of high-fat diet (Shimba et al., 2004) and that the adipose tissue of obese mice presents increased levels of HIF-1 α (Ye et al., 2007).

In obese rodents, it was observed, by immune-staining, that hypoxic areas within WAT are colocalized with macrophages, suggesting a link between hypoxia and the inflammatory response (Rausch et al., 2008). Furthermore, when comparing the partial pressure oxygen (PO₂) levels on the WAT of lean and obese mice, it was observed that in lean mice WAT presented levels of 48 mmHg, similar to the general level of tissue oxygenation but that in obese mice, the PO₂ was threefold lower, being approximately 15.2 mmHg (Ye et al., 2007). In humans, it was already demonstrated that in obese states, the WAT blood flow is lower than in lean subjects (A. Engin, 2017; F. Liu et al., 2020), with the PO₂ levels in the SAT being lower in obese than in lean subjects (a difference of around 20 mmHg) (Blaak et al., 1995; Lempesis et al., 2020). However, contrasting results were recently reported showing higher PO₂ levels in the WAT of obese subjects than in the lean subjects (Goossens et al., 2011). These results were surprising since, in the same study, the fasting blood flow to WAT was reduced in the

obese relative to the lean subjects and the obese did not exhibit the postprandial increase in flow that occurs with the lean. Furthermore, in vivo measurements of O2 consumption in the abdominal SAT, as well as markers of mitochondrial function, were lower in the obese subjects (Goossens et al., 2011). These contrasting results can be explained by differences related with the degree of obesity of the subjects or in the techniques employed and in general, taking into account the studies performed so far, particularly in animals, there is strong evidence of hypoxia in WAT depots in obesity. It is proposed that regional hypoxia and activation of HIF1 α will culminate in increased fiber deposition remodeling and pro-inflammatory phenotype, contributing to WAT dysfunction and progression of insulin resistance (Hosogai et al., 2007; F. Liu et al., 2020; Trayhurn et al., 2008). So far, it is known that hypoxia promotes alterations in the expression of key genes in the adipocytes, with an increase in the expression of genes encoding for leptin, IL-6, vascular endothelial growth factor (VEGF), glucose transporter types 1,3 and 5 and aquaporins 3 and 5, among others, and a decrease in the expression of genes encoding for adiponectin, catalase, uncoupling protein 2, peroxisome proliferator-activated receptor gamma (PPAR-γ) and peroxisome proliferator-activated receptor gamma coactivator 1-alpha (PGC-1α), among others (Trayhurn, 2013). Furthermore, in response to low levels of PO₂, a switch from oxidative metabolism to anaerobic glycolysis occurs being this translated into an increase in glucose uptake and utilization and consequently, in an increase in lactate release, which is known to stimulate inflammation in macrophages (Hashimoto et al., 2007) to induce insulin resistance in the muscle (Choi et al., 2002) and to inhibit lipolysis in the adipocytes (C. Liu et al., 2009) and also to be increased in obesity states. Therefore, adipose tissue hypoxia may dysregulates the local lactate autocrine/paracrine loop and consequently impair the antilipolytic action of insulin, since recent evidence suggests that the inhibition of lipolysis by lactate mediates the classical antilipolytic action of insulin (Ahmed et al., 2010; Rooney & Trayhurn, 2011). In addition, although controversial, studies have shown an increase in basal lipolysis in murine adipocytes, with hypoxia (Yin et al., 2009), which would be consistent with hypoxia-induced insulin resistance leading to a loss of the antilipolytic action of insulin. On the other hand, fatty acids uptake, by adipocytes, is decreased by hypoxia which, together with increased lipolysis, may explain the increased plasma FFA levels in obesity (K. N. Frayn et al., 2003) and their increased ectopic deposition in liver and skeletal muscle.

Insulin resistance, impaired glucose metabolism and T2D

Physiologically, the insulin receptor (IR) is located in caveolae and when insulin binds to IR, it activates tyrosine kinase (TK) and this will lead to the recruitment of intracellular docking proteins such as insulin receptor substrate (IRS) proteins (F. Liu et al., 2020; Peterson & Schreiber, 1999). In the skeletal muscle, IR stimulation triggers a phosphorylation-dephosphorylation cascade that is mediated by several kinases such as S6 kinase, protein kinase B, 3-phosphoinositide-dependent protein kinase 1 (PDK1), and isoforms of protein kinase C (PKC) (Boucher et al., 2014). These proteins regulate the pathways in the skeletal muscle that contribute to glucose metabolism, such as the translocation of GLUT4 containing storage vesicles (GSVs) to the plasma membrane, which is regulated by Serine/threonine-protein kinase 2 (Akt2), an increase in glucose-6-phosphate (G6P), dephosphorylation of glycogen metabolic proteins, and glycogen synthesis (DeFronzo & Tripathy, 2009; Taniguchi et al., 2006).

In the liver, insulin signaling is initiated by IR trans-autophosphorylation and activation, which results in the recruitment of signaling proteins (Mugabo & Lim, 2018) such as IRS1 and activation of phosphoinositide 3-kinase (PI3K) that will phosphorylate the signaling lipid molecule phosphatidylinositol 4,5-bisphosphate (PIP2) into phosphatidylinositol (3,4,5)-trisphosphate (PIP3). In turn, PIP3 activates PDK1, which phosphorylates Akt, at Thr308, which to be fully activated needs also to be phosphorylated at Ser473 by mTOR Complex 2 (mTORC2) (Santoleri & Titchenell, 2018). From here, different pathways for controlling glucose and lipid homeostasis proliferate, such as glycogen synthesis [through Akt inhibition of Glycogen synthase kinase-3 (GSK3) or in a manner independent of it, by activation of Glycogen Synthase 2 (GYS2)], lipogenesis and inhibition of gluconeogenesis [through inhibition of Forkhead box protein O1 (FOXO1) by Akt, which suppresses the expression of the proteins glucose-6-phosphatase (G6pc) and Phosphoenolpyruvate carboxykinase 1 (Pck1] (Santoleri & Titchenell, 2018). In the

WAT, and similarly to the muscle, insulin exerts its effects via the IRS-PI3K-Akt2-GLUT4 signaling pathways, with both IRS1 and IRS2 involved in adipocyte insulin signaling, in contrast with hepatocytes, where IRS1 has a more significant role. Also, RabGTPase-activating Protein TBC1D (Rab GAP TBC1D) contributes to the regulation of insulin signaling through vesicle trafficking and translocation of GLUT4 to the plasma membrane (Chadt et al., 2015).

Insulin resistance is identified as an impairment of response to insulin stimulation of target tissues. It impairs glucose disposal, resulting in a compensatory increase in the production of insulin by pancreatic beta-cell and consequent hyperinsulinemia. This vicious cycle continues until beta-cells activity can no longer meet the insulin demand, resulting in hyperglycemia. As this cycle continues, glycemia levels rise to levels that are consistent with T2D (Freeman & Pennings, 2021).

With the accumulation of WAT, the glucose uptake rate of hypertrophic adipocytes significantly changes and in fact, it was already showed that hypertrophic adipocytes may have a persistent decrease in the response to insulin and that smaller adipocytes have increased glucose uptake rate (Franck et al., 2007; F. Liu et al., 2020; Salans et al., 1968).

Several hypotheses have been suggested for the relationship between WAT dysfunction and body insulin resistance, which include elevated levels of FFA, inflammatory cytokines, decreased adiponectin, increased resistin, ceramide accumulation and ectopic fat accumulation in tissues like the liver and skeletal muscle (Chait & den Hartigh, 2020; Tchkonia et al., 2013) (Fig. 2).

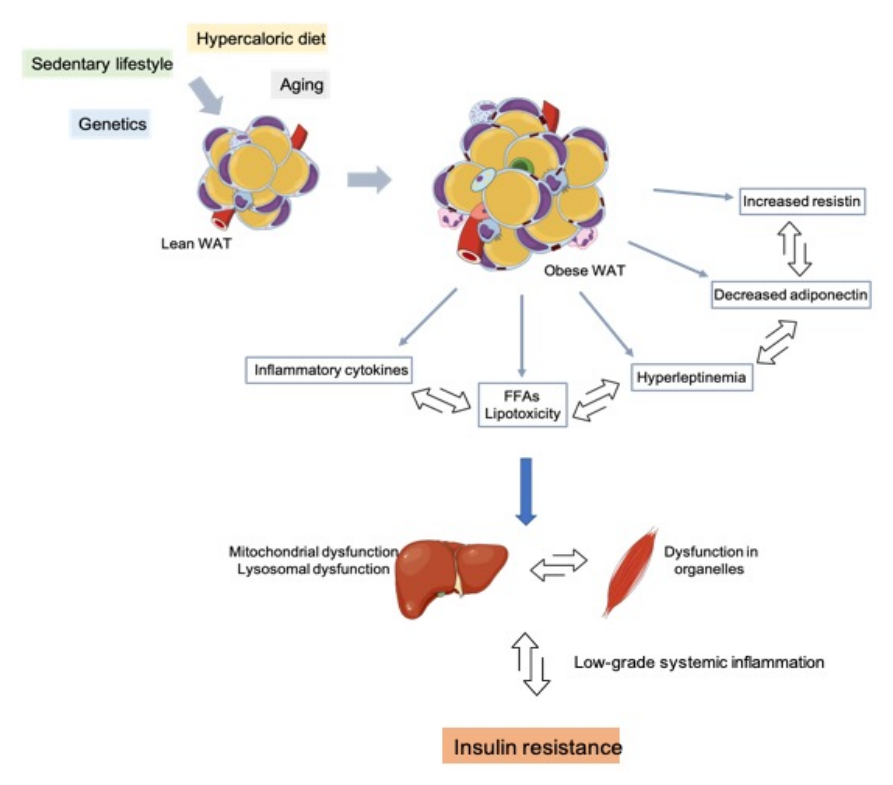


Figure 2 - Possible mechanisms of obesity-induced insulin resistance development. Risk factors as hypercaloric diets consumption, sedentary lifestyle, aging and genetics, among others, contribute to white adipose tissue (WAT) dysfunction and consequent development of obesity. The dysfunctional WAT secretes low levels of adiponectin and contributes to increased levels of leptin (hyperleptinemia) and resistin, releasing free fatty acids (FFA) and pro-inflammatory cytokines into circulation. FFA and other lipids accumulate in other organs, such as liver and skeletal muscle, leading to lipotoxicity and dysregulating mitochondria, lysosomes and the endoplasmic reticulum. These alterations, accompanied by a low-grade systemic inflammation will culminate in the development of insulin resistance. Adapted from B. Ahmed et al., (2021).

The brown adipose tissue

The BAT is a highly innervated, vascularized and metabolically active tissue that dissipates energy, in a heat-producing process called non-shivering thermogenesis, through the uncoupling protein 1 (UCP1), which uses the mitochondrial proton gradient to produce heat instead of adenosine triphosphate (ATP) (Ladoux et al., 2021).

As already mentioned, brown adipocytes are small and hexagonal cells that contain multiple lipid droplets of varied sizes and that are rich in mitochondria. Brown adipocytes have an extensive endoplasmic reticulum network that forms contact points with the mitochondria, the mitochondria-associated endoplasmatic reticulum membrane (Cohen & Spiegelman, 2015; de Meis et al., 2010). Furthermore, these cells

constitute a very heterogeneous population with variations in the expression of classic marker genes such as UCP1, fatty acid glutamate and amino acid, among others.

Classical brown adipocytes develop from myoblastic-like Myogenic factor 5 (Myf5) positive precursors that differentiate into brown adipocytes through the action of the transcriptional regulators PR domain containing 16 (PRDM16) and CCAAT/enhancer-binding protein beta (C/EBPβ) (Kajimura et al., 2009; Seale et al., 2008). On the other hand, distinct types of UCP1-positive adipocytes are found sporadically in the WAT of adult animals that have been exposed to several stimuli. These inducible brown-like adipocytes (beige or brite cells) possess many of the biochemical and morphological characteristics of classical brown adipocytes, including the presence of multilocular lipid droplets (Frontini & Cinti, 2010). However, they arise from a non-Myf5 cell lineage and hence, have distinct origins from the classical brown adipocytes.

In rodents, BAT depots are located in the interscapular (iBAT), sub-scapular (sBAT) and cervical (cBAT) regions, and smaller depots have been reported in association with the kidneys and aorta (Fig. 3). Several years ago, the long-standing prevailing view was that larger mammals lose their prominent brown fat depots after infancy. However, recently, [18F]fluorodeoxyglucose positron emission tomography-computed tomography scans demonstrated that active BAT exists in adult humans and subsequent studies indicated that these active BAT depots can be activated with cold exposure (Frontini & Cinti, 2010; Hany et al., 2002; Sidossis & Kajimura, 2015; F. Zhang et al., 2018).

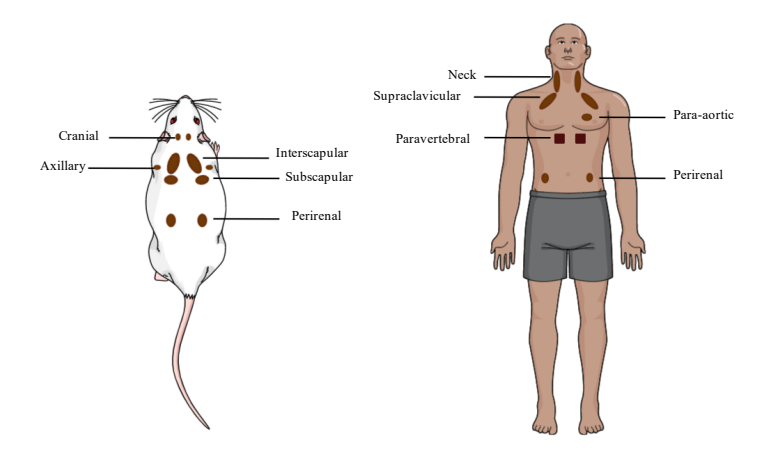


Figure 3 - Anatomical location of brown adipose tissue (BAT) depots. Rodents BAT depots are located in the interscapular (iBAT), sub-scapular (sBAT) and cervical (cBAT) regions with smaller associated to kidneys area and aorta; human BAT is mainly located in the neck, supraclavicular and paravertebral areas. Adapted from Pollard & Carling (2020).

In contrast to rodents, human BAT is mainly located in the deep neck and clavicular regions (Fig. 3). The most well-studied human BAT depot is the supraclavicular BAT depot, which is positioned above the clavicle bone. Additionally, some individuals also possess BAT depots in the axillary, prevertebral regions and kidneys (Kuryłowicz & Puzianowska-Kuźnicka, 2020).

UCP1-mediated thermogenesis

UCP1 generates heat by dissipating the energy proton gradient from the electron transport chain in mitochondrial respiration, which expression is induced by PGC1 α . PGC1 α is the master regulator of UCP1-mediated thermogenesis and initially it was identified as a cofactor that directly interacts with PPAR γ in brown adipocytes. However, later studies showed that, in addition to UCP1 and PPAR γ , PGC1 α also activates several transcription factors and function as the central regulator of numerous pathways involved in mitochondrial biogenesis and thermogenesis (Castillo-Quan, 2012; Sharma et al., 2014). Several studies have investigated the essential role of UCP1 in thermogenesis and it was already showed that UCP1 knockout mice are unable to

maintain their body temperature and develop hypothermia upon acute cold challenge (Enerbäck et al., 1997)

It is known that adrenergic stimulation activates brown adipocyte lipolysis and mitochondrial respiration in an UCP1-dependent manner (Li et al., 2014). However, recent studies in mice with BAT-specific deficiencies in key lipolytic enzymes revealed that the absence of lipolysis in BAT does not alters non-shivering thermogenesis, which suggest the existence of compensatory pathways that require further investigation (Schreiber et al., 2017; H. Shin et al., 2017)

UCP1-independent thermogenesis

For years, UCP1 had been thought to be the only thermogenic protein responsible for non-shivering thermogenesis. However, many observations support the existence of metabolic mechanisms independent of UCP1. In fact, the inguinal WAT of knockout mice for Ucp1, maintained in a chronic cold environment, showed greater respiration than knockout mice maintained under thermoneutrality (Ukropec et al., 2006). In addition, chronic β₃ adrenergic agonist treatment increased oxygen consumption in the epididymal WAT in these mice (Granneman et al., 2003). Therefore, other mechanisms were studied and it was recently found that creatine substrate cycling stimulates mitochondrial respiration and serves as a thermogenic pathway in thermogenic adipocytes (Bertholet et al., 2017; Kazak et al., 2015) since, for example, it was showed that creatine kinase U-type and creatine kinase B double knockout mice present cold intolerance and reduced norepinephrine responses to activate thermogenic respiration (Streijger et al., 2009). Another mechanism that was also identified as an UCP1independent thermogenic pathway is the calcium (Ca²⁺) cycling that contributes to nonshivering thermogenesis through sarco-endoplasmic reticulum ATPase activity (Meis, 2003; Meis et al., 2006, p. 2; Periasamy et al., 2017).

Brown adipose tissue activation

BAT thermogenesis is primarily driven by the SNS, with the release of norepinephrine (NE), also called noradrenaline (NA), and subsequent stimulation of β -AR. Briefly, NE-induced adrenergic signaling enhances the expression of proteins that are involved in

thermogenesis and stimulates intracellular lipolysis (Cannon & Nedergaard, 2004). After, the FFAs that were released are directed to the mitochondria to be used or to activate UCP1 (Fig. 4) (Fedorenko et al., 2012). In the last decades, it was demonstrated that several stimuli can contribute to the activation of BAT through SNS activation, among which are administration of β_3 -AR agonists, hypercaloric diet and cold exposure.

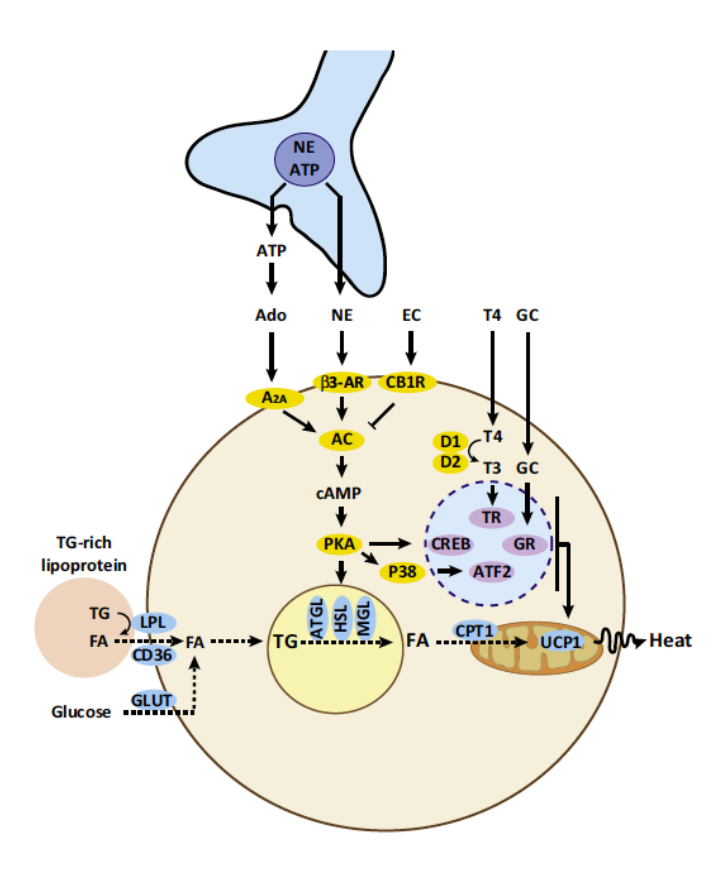


Figure 4 - Activation of BAT thermogenesis by the SNS. The NE released from the nerve endings near the brown adipocytes stimulates β 3-adrernergic receptor(β 3-AR) that, in turn, stimulates cyclic AMP (cAMP) production by adenylyl cyclase (AC). cAMP activates protein kinase A (PKA), which drives lipolysis through phosphorylation of hormone sensitive lipase (HSL) and induces transcription of genes involved in mitochondrial bio-synthesis and thermogenesis. Fatty acids that are released from lipid droplets are directed to the mitochondria to be combusted or may allosterically activate uncoupling protein1 (UCP1). Other mechanism involved in BAT activation is through the release of ATP from the nerve endings that will be converted into adenosine that in turn will activate adenosine A_{2A} receptors and stimulate cAMP (not discussed in this work). From Kooijman et al., (2015).

1. β₃-Receptors agonists administration

Rodent and human adipose tissue present different β -adrenergic receptors expression profiles. In rodents, the β_3 -AR is highly expressed in both BAT and WAT whereas in the

adult human, the β_3 -AR is only expressed in BAT. In human WAT, β_1 -AR is more abundant than β_3 -AR (Granneman, 1995). It was already reported that the binding affinity of NE to β_3 -AR in in the low micromolar range and it is known that β_1 -AR desensitizes more rapidly than β_3 -AR after exposure to agonists. All this indicates that the activation of β_3 -AR may require higher levels of sympathetic stimulation but, after activation, it seems to deliver a more sustained effect (Granneman, 1995).

Several β_3 -AR agonists such as BRL-37344, CL-316,243 and CGP-12177A, that stimulate brown and white adipocyte lipolysis, showed potent anti-obesity and anti-diabetic effects in rodent models of obesity, although none of these compounds presented efficacy when tried in humans. On the other side, a study with CL-316,243 treatment in lean healthy men increased in 45% the insulin-mediated glucose disposal and reduced 24-h respiratory quotient, which may indicate enhanced fat oxidation but with no increase in the energy expenditure (Weyer et al., 1998). Similarly, no increase in energy expenditure was observed in studies where ZD7114 and ZD2079 β_3 -AR agonists were used (Buemann et al., 2000).

In contrast, in a study with high therapeutic doses of β_3 -AR agonist mirabegron, in healthy young male subjects, it was observed an increase of around 13% in resting metabolic rate, indicating BAT activation (Cypess et al., 2015). However, another recent study provided evidence supporting the idea that BAT thermogenesis in humans is mediated by the stimulation of the β_2 -AR instead of β_3 -AR. In this study, it was demonstrated that, *in vivo*, only a maximal dose of mirabegron, promoting cross-activation and leading to stimulation of β_1 -AR mediated cardiovascular responses and β_2 -AR mediated WAT lipolysis, could stimulate BAT activation (Blondin et al., 2020). Furthermore, *in vitro* experiments from the same study demonstrated that brown adipocytes and immortalized brown adipocytes stimulated with β_2 -AR agonists, exhibited increased uncoupled respiration and lipolysis, respectively, which did not occur upon β_3 -AR agonists stimulation. This effect was abolished after stimulation with a β_2 -AR antagonist., meaning that, in human brown adipocytes, thermogenesis and lipolysis occurs through β_2 -AR signaling (Blondin et al., 2020).

Diet-induced activation

Hypercaloric diets and/or cafeteria diets, with high carbohydrate and fat, have been widely used for activation and recruitment of BAT. In fact, several studies in humans showed that postprandial thermogenesis is increased after intake of a meal rich in polyunsaturated fatty acids compared to that rich in monosaturated and saturated fatty acids.

One of the mechanisms that can be responsible for this postprandial increase in thermogenesis is the increased plasma levels of NA and tissue NA turnover levels immediately after food intake, as it was shown in several studies in animals and humans (Glick & Raum, 1986; Schwartz et al., 1987; Tappy, 1996). This increased sympathetic activation in BAT was also already shown in mice overfed with cafeteria and high-caloric diets. Furthermore, it was also found in rats, that metabolic activation of BAT after meal was diminished with surgical resection of the sympathetic innervation to the BAT (Saito et al., 1989). All these studies suggest that diet-induced/postprandial BAT thermogenesis is mediated through sympathetic nerve activation. However, it was observed in humans that resting metabolic rate and plasma NE levels were not increased after administration of a meal by gavage (Blaak et al., 1995) and that postprandial thermogenesis was reduced after a non-palatable meal in comparison with a highly palatable meal (LeBlanc & Brondel, 1985), suggesting that part of diet-induced sympathetic activation and BAT thermogenesis are due to food palatability (LeBlanc & Brondel, 1985).

In obesity, the mechanisms involved in the diet-induced thermogenesis are still not well understood. However, several studies showed that diet-induced thermogenesis is decreased, being this decrease associated to the presence of insulin resistance and to a deregulated SNS activity (Park et al., 2020).

2. Cold exposure activation

When rodents are exposed to low temperatures, the cold is detected by the transient receptor potential (TRP) channels on sensory neurons leading to an increase in the activity of sympathetic nerves innervating the BAT (Nakamura, 2011), resulting in the release of NA that stimulates brown adipocytes via the β -AR and triggers cAMP-activated intracellular events, such as, hydrolysis of triglyceride and activation of UCP1. Sympathetic activation also results in increased release of fatty acids from WAT and increased glucose utilization (Inokuma et al., 2005). Furthermore, when animals are exposed to cold temperatures for a long time, BAT hyperplasia occurs accompanied by an increase in the amount of UCP1 (Bukowiecki et al., 1986; Okamatsu-Ogura et al., 2017). In addition to BAT hyperplasia, prolonged cold exposure gives rise to an apparent induction of UCP1-positive adipocytes in WAT, the beige adipocytes, which derive from Myf5-positive myoblastic cells (Harms & Seale, 2013; Kajimura & Saito, 2014).

Brown adipose tissue in obesity

The activity and prevalence of BAT substantially decrease with age (Alcalá et al., 2019; Pfannenberg et al., 2010; Yoneshiro et al., 2011) However, ageing is not the only factor prompting BAT disappearance and dysfunction, with the BAT from obese and hyperglycemic mice showing higher levels of inflammation, endoplasmic reticulum stress, oxidative damage, and enhanced mitochondrial respiration activity (Alcalá et al., 2017; Calderon-Dominguez et al., 2017). The mechanisms by which obesity leads to these deleterious effects on BAT are not completely understood, although some mechanisms were already studied. Such mechanisms include: 1) catecholamine resistance characterized by decreased synthesis of NE and expression of β -AR and by defective intracellular signaling, which avoid PKA-mediated cell proliferation (Villarroya et al., 2018); 2) the infiltration of M1 macrophages that participate in NE clearance and contribute to the synthesis of proinflammatory cytokines, promoting a decline in UCP1 expression (Sakamoto et al., 2016); 3) NF-κB-mediated signaling inhibiting the PKA proliferation pathway and repressing PPARγ and C/EBPs gene expression, which inhibits differentiation of the brown adipocytes (Bae et al., 2015) and 4) inflammation signals

that also promote cellular apoptosis and consequently restrain BAT expansion (Alcalá et al., 2017; Miranda et al., 2010; Valladares et al., 2000).

The SNS in obesity

The autonomic nervous system is part of the peripheral nervous system and contains three anatomically distinct divisions: sympathetic, parasympathetic and enteric.

The SNS and the parasympathetic nervous system (PNS) contain both afferent and efferent fibers that provide sensory input and motor output, respectively, to the central nervous system (Waxenbaum et al., 2021). The presynaptic sympathetic neurons use acetylcholine (ACh) as their neurotransmitter while the postsynaptic sympathetic neurons generally produce NE as their effector transmitter to act on target tissues (Koopman et al., 2011; Sternini, 1997).

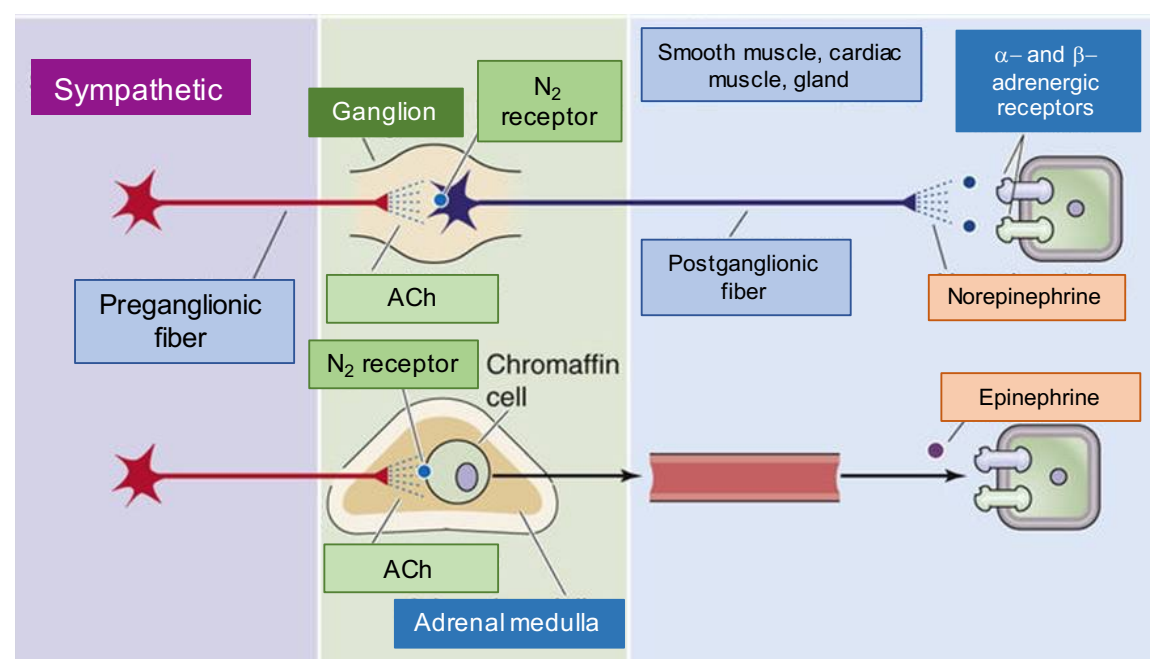


Figure 5 - Sympathetic neurons and neurotransmitters released. The preganglionic neuron releases acetylcholine (Ach), which acts at N2 receptors on the postsynaptic membrane of the postganglionic neuron. In the case of most postganglionic sympathetic neurons, the neurotransmitter is NE. The postsynaptic receptor is an adrenergic receptor (i.e., GPCR) of one of two major subtypes (α and β). Adapted from Boron & Boulpaep (2012).

As already mentioned in this manuscript, the physiological response to a meal is an increase in the sympathetic nerve activity, as indicated by a rise in plasma NA concentrations and by an increase in muscle sympathetic nerve activity. This is

important to promote thermogenesis and also to induce compensatory peripheral vasoconstriction, to maintain blood pressure following splanchnic vasodilatation (Fagius, 2003). However, there is solid evidence that the SNS becomes overactive in obesity, with the degree of sympathetic activity appearing to be dependent on body fat distribution and with central obesity showing to be associated with greater sympathetic nerve activation (Alvarez et al., 2002; Straznicky et al., 2008). When compared to lean individuals, obese adults have increased urinary NA and metabolite levels (Lee et al., 2001), elevated levels of NA in the plasma (Vaz et al., 1997) and increased resting sympathetic outflow to skeletal muscle (Grassi et al., 1995, 2004). Furthermore, obese insulin-resistant individuals display blunted sympathetic neuronal responses to physiological hyperinsulinemia, glucose consumption and changes in energy states (Grassi et al., 1995). Several mechanisms are proposed to be involved in this overactivation of SNS in obesity, including hyperinsulinemia (Lembo et al., 1992; Vollenweider et al., 1993), overeating (Arone et al., 1995; O'Dea et al., 1982) and hyperleptinemia, increased visceral adiposity (Alvarez et al., 2002) and activation of the Hypothalamic-Pituitary-Adrenal Axis, (Brunner et al., 2002; Grassi et al., 2001) among others. However, there is still a debate whether SNS overactivation is a consequence or a cause of obesity (Thorp & Schlaich, 2015). Also, there is also discussion on whether there is a regional or an overall sympathetic activation. In fact, the first studies regarding SNS activity on obesity led to disagreement since some showed low overall activity of the SNS while others reported a normal or an elevated activity, which could be related with the methods used to evaluate SNS activity. Nowadays is consensual that obese subjects (Kalil & Haynes, 2012) exhibit an overactivation of the SNS, although evidences indicate that SNS activity is typically regionalized (E. A. Lambert et al., 2013) and that there are variations in the sympathetic tone among vascular beds, in human obesity (Vaz et al., 1997). It was showed that normotensive obese have elevated sympathetic nervous activity in the kidneys, reduced sympathetic activity in the heart (Esler et al., 2001) and increased muscle sympathetic nerve activity (Alvarez et al., 2004; Grassi et al., 1995), when compared with age-matched lean controls (Straznicky et al., 2008).

Knowing that CB activation promotes an increase in the SNS activity and taking into account its role as a metabolic sensor, the CB could be a new player to explain the link between obesity and SNS overactivity.

Carotid body

The CBs are paired chemoreceptor organs, located in the bifurcation of the common carotid arteries. The CB is morphologically organized in glomeruli, composed of neuron-like glomus cells (type I), which are derived from the neural crest and that are synaptically connected with the sensory nerve endings of the carotid sinus nerve (CSN), the CB sensitive nerve, and glia-like cells (type II) (Gonzalez et al., 1994). Type I cells are chemoreceptor cells that have the ability to sense changes in arterial blood gases such as hypoxia, hypercapnia, and pH levels(Ortega-Sáenz & López-Barneo, 2020). On the other hand, type II cells were first described as elements of support of the CB glomeruli but more recently it was shown that these cells are also involved in the chemosensory response and in the plasticity of the CB (Nurse, 2014; Ortega-Sáenz & López-Barneo, 2020; Platero-Luengo et al., 2014). It was already proposed that type II cells exhibit properties of stem cells that in response to hypoxia can proliferate and differentiate into new type I cells (Pardal et al., 2007) (Fig. 6).

Briefly, hypoxia, hypercapnia and acidosis activate the CB leading to the release of neurotransmitters that act on the CSN to generate action potentials to activate or to inhibit its activity (Gonzalez et al., 1994). The action potentials generated postsynaptically are integrated in the brainstem to induce cardiorespiratory responses, to normalize blood gases via hyperventilation and to regulate blood pressure and cardiac performance via activation of the sympathetic nervous system (Gonzalez et al., 1994; Marshall, 1994).

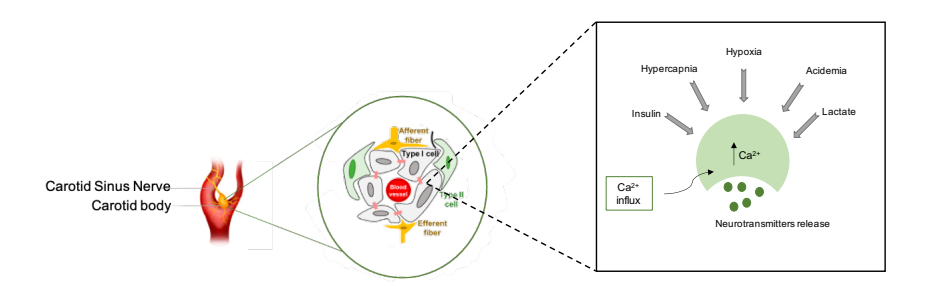


Figure 6 - Carotid Body (CB) morphology. The CB is organized in glomeruli, composed of neuron-like glomus cells (type I), that are synaptically connected with sensory nerve endings of the carotid sinus nerve (CSN) and the glia-like cells (type II). Type I cells release neurotransmitters when exposed to stimuli, such as hypoxia or hypercapnia/acidosis, among others, in order to activate afferent fibers of the glossopharyngeal nerve terminating at the brainstem respiratory and autonomic centers. Adapted from Ortega-Sáenz & López-Barneo (2020).

1. Physiology of the CB

Type I/glomus cells release neurotransmitters during exposure to hypoxia and other stimuli such as hypercapnia/acidosis, hyperthermia, hyperkalemia, hypotension and osmolarity (Kumar & Bin-Jaliah, 2007), in order to activate afferent fibers of the glossopharyngeal nerve terminating at the brainstem respiratory and autonomic centers.

Classically, the oxygen transduction cascade on CB involves a decrease in arterial PO₂ followed by oxygen sensing and closure of K⁺ channels that will lead to cell depolarization and activation of voltage-dependent Ca²⁺ channels. This will culminate in an increase in intracellular Ca²⁺ and consequent release of neurotransmitters that act post-synaptically on their receptors leading to an increase in ventilation (Gonzalez et al., 2010) and SNS activity.

The molecular mechanisms of oxygen sensing by glomus cells are still unknown. However, several hypotheses have been postulated and among them are a) the involvement of a specific nicotinamide adenine dinucleotide phosphate (NADPH) oxidase, b) activation of AMP kinase, c) the reversible fast regulation of ion channels by gasotransmitters or d) the expression of an atypical olfactory receptor (Ortega-Sáenz et al., 2020). All these processes can influence glomus cells function, although it seems that none of them is essential for acute oxygen sensing, since various animal models with

ablation of genes coding for the relevant enzymes or receptors did not promote alterations in the normal responsiveness of CB to hypoxia (He et al., 2002; Mahmoud et al., 2016; Ortega-Sáenz et al., 2006, 2020). Recently, new studies have provided support for a model of acute oxygen sensing which is the "mitochondrial-to-membrane signaling" model that combines the membrane hypothesis (cell depolarization and activation of voltage-dependent Ca²⁺ channels) and the mitochondrial hypothesis, in which is proposed the existence of a mitochondrial O₂ sensor (Ortega-Sáenz et al., 2020). This mitochondrial hypothesis is supported by studies showing that the CB is highly sensitive to mitochondrial poisoning and that mitochondrial inhibitors are powerful CB stimulants (Ortega-Sáenz et al., 2020).

The CB has been classically associated with the peripheral control of respiration, although this view has changed in the last decades since the CB is now considered as a multimodal sensory organ that is also activated alterations in plasma levels of hormones, such as insulin and leptin, as well as glucose and lactate, and in blood temperature, osmolality and flow.

2. Role of carotid body as a metabolic sensor

The role of the CB as a glucose sensor has been subject of much debate in the last decades. In fact, several studies have tried to clarify the role of the CB as a glucose sensor and while the initial results supported the idea of the CB as low-glucose sensors (Pardal & López-Barneo, 2002), others have reinforced the hypothesis that low glucose levels do not modify CSN activity (Conde et al., 2014).

Several authors described that adult CB glomus cells, from several species including humans, can be activated by low levels of glucose leading to the release of neurotransmitters in an external Ca²⁺-dependent manner (Fitzgerald et al., 2009; Pardal & López-Barneo, 2002; Zhang et al., 2007). Furthermore, animal studies have also demonstrated that CB activity is inhibited by intravascular administration of glucose (Koyama et al., 2000; Ortega-Sáenz & López-Barneo, 2020). In contrast, it was shown, using freshly isolated intact rat CB preparations, that the release of catecholamines from

type I cells was identical in the presence of low or physiological glucose concentrations. Also, the authors described that both the release of ATP from the CB and the CSN action potential frequency were unaffected by low glucose. These results support the notion that low glucose is not a direct stimulus for rat CB chemoreceptors, as previously suggested by others studies (Conde et al., 2014).

Recent evidence in animal models (Bin-Jaliah et al., 2004; Ribeiro et al., 2013) and in humans (Barbosa et al., 2018; Vidal et al., 2019) proposes that insulin may directly activate the CB independently of glycemia. Bin-Jaliah et al. showed, in rats, that insulininduced hypoglycemia increased spontaneous ventilation, an effect that was abolished by CNS resection, and that hypoglycemia per se did not alter CSN frequency (Bin-Jaliah et al., 2004). This effect was supported by the study of Ribeiro et al., in rats that showed that insulin, during an euglycemic clamp, increased ventilation in a dose-dependent manner, an effect that was abolished after CSN resection (Ribeiro et al., 2013). In humans, Barbosa et al. showed that hyperinsulinemia, during an euglycemic clamp, increased minute ventilation independently of alterations in glucose levels (Barbosa et al., 2018). The effect of insulin on the CB was consolidated by the presence of insulin receptors at the CB and its phosphorylation in response to insulin and by the fact that insulin, in physiological concentrations, evoked a neurosecretory response from CB type I cells (Ribeiro et al., 2013). Moreover, when evaluating the effect of insulin, perfused intravenously, in the output of the CB, it was possible to observe that insulin increased CSN and SNS electrophysiological activity in vivo. The effect of insulin on SNS electrophysiological activity was abolished by CSN resection (Cracchiolo et al., 2019a, 2019b).

As already mentioned, leptin is a hormone generated by adipose tissue that acts on the hypothalamus to regulate food intake and energy consumption, promoting lipolysis by the activation of sympathetic inputs to adipose tissue (Poher et al., 2015). Furthermore, it is well known that plasma leptin levels are increased in obesity and metabolic diseases, generating a state called leptin resistance (Phillips et al., 2000; Sanner et al., 2004; Schmidt et al., 2006). Leptin is also involved in the central control of breathing (O'Donnell et al., 1999; Tankersley et al., 1998) and its role in the control of

breathing is highlighted by the fact that the administration of the hormone reverses hypoxia and hypercapnia commonly encountered in leptin-deficient animal models (O'Donnell et al., 1999; Tankersley et al., 1998). Also, Groeben et al. showed that hyperoxia decreased the respiratory rate in wild-type mice but not in leptin receptor deficient (ob/ob) mice, an effect that was restored by leptin replacement in ob/ob mice (Harald et al., 2004). However, leptin effects on the control of breathing are mediated not only by central structures but also at a peripheral level. Messenger et al. described that rat CB expresses the leptin receptors and that these colocalize with cells expressing tyrosine hydroxylase (Messenger et al., 2012). Furthermore, an increase in basal ventilation and in ventilation in response to ischemic hypoxia was observed after intravenous (Olea et al., 2015; Ribeiro et al., 2018) and intracarotid (Ribeiro et al., 2018) administration of leptin. More recently, it was shown that leptin increases CSN activity, in vivo, at baseline and in response to physiological levels of hypoxia (Caballero-Eraso et al., 2019) and that CSN resection decreases the spontaneous ventilation induced by acute leptin intracarotid administration (Sacramento et al., 2020). Taken together, all these studies confirm that the CB contributes to the effects of leptin on basal ventilation and in response to acute hypoxia.

3. Carotid body and the sympathetic-mediated diseases

The CB has been implicated in several diseases and diseases comorbidities associated with higher SNS activity, which include heart failure, obstructive sleep apnea, hypertension and metabolic syndrome, among others. In heart failure development and progression, the contribution of an increased CB chemoreflex drive and sympathetic overactivity has been demonstrated in both humans and animal models (Ahmed et al., 2010; Del Rio et al., 2013a; Schultz & Sun, 2000). In fact, it is already known that increased CB chemoreflex drive has an essential role in the progression of cardiorespiratory disorders in this disease (Ponikowski et al., 2001; Rio, 2015), strongly correlating with high mortality risk and poor prognosis (Giannoni et al., 2009). On the other hand, it was shown that CB ablation reduces, not only hyperventilation and

oscillatory breathing, but also the tonic sympathetic outflow in animal models of heart failure, leading to an improvement in cardiac function and survival (Del Rio et al., 2013b). The OSA is characterized by repeated total or partial occlusions of the upper airway, which produce cyclic intermittent hypoxia and hypercapnia, and studies have demonstrated that OSA, and consequent chronic intermittent hypoxia, is an independent risk factor for the development and progression of systemic hypertension (Iturriaga et al., 2005; Marin et al., 2005; Peppard et al., 2000; Streijger et al., 2009) Studies demonstrated that patients recently diagnosed with OSA present increased ventilatory responses to acute hypoxemia and sympathetic overactivity (Narkiewicz, Montano, et al., 1998; Narkiewicz, van de Borne, Cooley, et al., 1998; Narkiewicz, van de Borne, Montano, et al., 1998). Similarly, rodents exposed to chronic intermittent hypoxia have enhanced cardiorespiratory and sympathetic responses to hypoxia, with development of systemic hypertension (Dick et al., 2007; Greenberg et al., 1999; Reeves et al., 2003).

Essential hypertension is another condition that has been recently associated with CB dysfunction and increased CB-mediated sympathetic drive. It is well known that the sympathetic activity responses evoked by the CB chemoreflex are increased both in humans and in animal models (Abdala et al., 2012; Somers et al., 1988) and that hyperoxia, which abolishes CB activity, reduces both arterial pressure and sympathetic activity in hypertensive patients (Siński et al., 2012). Further studies, where the effects of unilateral versus bilateral CSN denervation were evaluated in spontaneously hypertensive rats, demonstrated that unilateral CSN denervation does not promote reductions on blood pressure while bilateral denervation is effective in reducing blood pressure (McBryde et al., 2013). On the other side, unilateral CB resection in patients with drug-resistant hypertension produced reductions in ambulatory blood pressure coincident with decreases in sympathetic activity (Narkiewicz et al., 2016).

Among the pathological conditions associated with an increased CB-mediated sympathetic drive are metabolic syndrome and T2D. In fact, in 2013, Ribeiro et al. described that CB activity is increased in animal models of insulin resistance and hypertension, showed by an increase in ventilatory parameters (respiratory frequency,

tidal volume and minute ventilation), in the release of dopamine from the CB, induced by hypoxia, and in CB weight. CSN resection abolished the effect of hypercaloric diet on the ventilatory parameters and prevented the development of insulin resistance and hypertension in these animals. Furthermore, it was demonstrated that the IR is present in the CB and that insulin triggers the peripheral chemoreceptors located in the CBs, suggesting that hyperinsulinemia may play a role in the CB-induced sympathoadrenal overactivity associated with metabolic disturbances (Ribeiro et al., 2013). After, in 2017, Sacramento et al. found that CSN resection normalized, not only, systemic SNS activity, insulin sensitivity and glucose tolerance but also lipid profile, arterial pressure and endothelial function and also decreased weight gain induced by hypercaloric diets in prediabetes and early T2D animal models, by improving glucose uptake by the liver and perienteric adipose tissue (Sacramento et al., 2017). Next, it was showed that employing a bioelectrical approach, by the use of bilateral kilohertz frequency alternating current modulation to inhibit CSN activity, it was possible to restore metabolic homeostasis, with an improvement in insulin sensitivity and glucose tolerance, in animal models of T2D (Sacramento et al., 2018). Finally, it is important to note that these mechanisms are also present in humans since it was showed that patients with T2D exhibit CBs with a larger size than control volunteers (Cramer et al., 2014) and more recently it was described that prediabetes patients exhibit increased CB activity measured by the double-breath Dejours test, that evaluates CB chemosensitivity in patients while breathing 100%O₂ (Cunha-Guimaraes et al., 2020).

All these findings demonstrated that CB dysfunction is involved in the development of metabolic diseases through SNS activity modulation making the CB a relevant target to develop new therapeutic strategies to these disorders.

Therapeutic options for the treatment of obesity

The management of overweight and obesity usually starts with lifestyle modifications as caloric restriction and/or portion control, physical activity and behavioral changes. However, these approaches are insufficient for long-term weight loss maintenance in

the majority of patients, with one-third to two-thirds of the lost weight being regained within the one-year following end of treatment (Foster, 2006). To add to life changes for weight management, several pharmacological therapeutics were developed, both for short or long-term use. All medications, except or listat, act centrally to promote weight control. As examples of short-term use therapeutics are Phentermine, which remains available today and is a sympathomimetic anorexigenic agent and Diethylpropion, which is another sympathomimetic and derivative of bupropion. In a study from 1968, 64 patients were randomized to placebo, phentermine 30 mg daily, or intermittent phentermine 30 mg daily with both phentermine groups showing a loss of approximately 13% of their initial weight (Cercato et al., 2009). Regarding Diethylpropion usage, it achieved an average weight loss of 9.8% at 6 months (Munro et al., 1968). These drugs have several side effects, related to their sympathomimetic properties, such as elevation in blood pressure and pulse, insomnia, constipation, and dry mouth («Diethylpropion», 2012; Zhi et al., 1994) and are contraindicated in individuals with uncontrolled hypertension, cardiovascular disease, hyperthyroidism or glaucoma, among others. As examples of long-term consumption drugs are Orlistat, Bupropion-naltrexone, Liraglutide, Dulaglutide and Exenatide, among others. Orlistat promotes weight loss by inhibiting gastrointestinal lipases and consequently decreasing the absorption of fat from the gastrointestinal tract (Drent & van der Veen, 1995). On the other side, Bupropion-naltrexone is a combination of bupropion, which is a reuptake inhibitor of dopamine and norepinephrine that promotes activation of the central melanocortin pathways (Greenway et al., 2009), and naltrexone which is an opioid receptor antagonist that diminishes the mu-opioid receptor auto-inhibitory feedback loop on anorexigenic hypothalamic neurons (Billes et al., 2014). Finally, Liraglutide, Dulaglutide and Exenatide are glucagon-like peptide-1 (GLP-1) analogues that improve glycemic control and stimulate satiety, leading to decreases in food intake (Garvey et al., 2020; Kanoski et al., 2016).

These therapeutic options have a relatively low efficacy, between 5-10% of weight loss, with high rates of weight regain. Furthermore, side effects to the treatment with these drugs are fatty/oily stool, fecal urgency, oily spotting, increased defectation, fecal

incontinence, nausea/vomiting, constipation, headache, dizziness and insomnia, among others (Drent & van der Veen, 1995; Tchang et al., 2000). There are several medications prescribed for conditions other than obesity that have also been found to be effective weight loss drugs in patients with obesity (Metformin, Semaglutide and Sodium-Glucose Transporter-2 Inhibitors) however also with low efficacy (between 2-6% of weight loss) (Tchang et al., 2000).

Bariatric surgery, on the other hand, has been the most effective treatment for severe obesity in terms of long-term weight loss, comorbidities and quality of life improvements, being laparoscopic sleeve gastrectomy the most common procedure. However, it is associated with acute and chronic postoperative complications, such as bleeding, leakage, gastric fistulae (Kheirvari et al., 2020), nutrient deficiencies and postoperative alterations in the pharmacokinetics of medications (Padwal et al., 2010; Xanthakos, 2009), which sometimes discourage patients and make it less desirable to them. Furthermore, in most cases it requires weight loss before the surgery which can lead to delays and dropouts throughout the process. Taking all these into account, new therapeutic options are still necessary in order to fight obesity and its comorbidities.

Chapter I
chapter .

General and specific aims

General and specific aims

The therapeutic approaches currently available for obesity are clearly ineffective and therefore it is imperative to identify prevention strategies and treatment interventions that help to stop this epidemic. In the last years, it was demonstrated that the CB is a metabolic sensor and that CB dysfunction is involved in the development of dysmetabolic states. Additionally, it was found that CSN resection or electrical modulation reverse dysmetabolism highlighting the CSN neuromodulation as a possible therapeutic target for metabolic diseases. However, the therapeutic efficacy of CB abolishment on obesity is not clear, neither the mechanisms involved in the beneficial effects on weight gain or in metabolism. Therefore, the general aim of this work was to unravel the role of CB in the development of obesity, by studying the impact of CSN resection on weight gain, adipose tissue amount/metabolism and glucose metabolism, and the mechanisms by which CSN resection promotes these effects.

Therefore, the specific aims of this work were:

- 1. Identify the most appropriate rodent model to study obesity and its comorbidities
- 2. Investigate the impact of CSN surgical resection on weight and fat mass loss and glucose metabolism, in animals with established obesity;
- 3. Investigate if these effects on weight and fat loss, are due to altered adipose tissue metabolism and/or conversion of white to beige adipocytes;
- 4. Investigate the impact of CSN resection on sympathetic integration in white and brown adipose tissues.

The clarification of the role of CB in the development of obesity and the effects of CSN resection on weight and fat mass changes in obesity models as well as the interpretation of weight loss-associated mechanisms will open new doors for the treatment of obesity.

Chapter	Ш
---------	---

This chapter is based on the following manuscript:

Evaluating the Impact of Different Hypercaloric Diets on Weight Gain, Insulin Resistance, Glucose Intolerance, and its Comorbidities in Rats

Bernardete F. Melo†, Joana F. Sacramento†, Maria J. Ribeiro, Cláudia S. Prego,
Miguel C. Correia, Joana C. Coelho, João P. Cunha-Guimaraes, Tiago Rodrigues,
Ines B. Martins, Maria P. Guarino, Raquel M. Seiça, Paulo Matafome and
Silvia V. Conde. (2019) *Nutrients*, May 28;11(6):1197

Abstract

Aims/hypothesis: Animal experimentation has a long history in the study of metabolic syndrome-related disorders. However, no consensus exists on the best models to study these syndromes. Knowing that different diets can precipitate different metabolic disease phenotypes, herein we characterized several hypercaloric rat models of obesity and type 2 diabetes, comparing each with a genetic model, with the aim of identifying the most appropriate model of metabolic disease.

Methods: The effect of hypercaloric diets (high fat (HF), high sucrose (HSu), high fat plus high sucrose (HFHSu) and high fat plus streptozotocin (HF+STZ) during different exposure times (HF 3 weeks, HF 19 weeks, HSu 4 weeks, HSu 16 weeks, HFHSu 25 weeks, HF3 weeks + STZ) were compared with the Zucker fatty rat. Each model was evaluated for weight gain, fat mass, fasting plasma glucose, insulin and C-peptide, insulin sensitivity, glucose tolerance, lipid profile and liver lipid deposition, blood pressure, and autonomic nervous system function.

Results: All animal models presented with insulin resistance and dyslipidemia except the HF+STZ and HSu 4 weeks, which argues against the use of these models as metabolic syndrome models. Of the remaining animal models, a higher weight gain was exhibited by the Zucker fatty rat and wild type rats submitted to a HF diet for 19 weeks.

Conclusions/interpretation: We conclude that the latter model presents a phenotype most consistent with that observed in humans with metabolic disease, exhibiting the majority of the phenotypic features and comorbidities associated with type 2 diabetes in humans.

Introduction

Over the last few years, the incidence and prevalence of metabolic diseases such as obesity, type 2 diabetes (T2D) and metabolic syndrome has increased dramatically, recently being highlighted as a worldwide epidemic, with a high socioeconomic impact (Sah et al., 2016). This increase emphasizes the urgent need to understand the causes and mechanisms underlying the onset and progression of these metabolic disorders,

aiming to develop new therapeutic strategies to prevent or halt the progressive rise in incidence of these disorders. This growing epidemic highlights the need for further experimental research, enabled by the availability of animal models that closely mimic the metabolic and cardiovascular phenotype exhibited by humans.

Pathological weight gain is the major cause of both metabolic and cardiovascular diseases (Sah et al., 2016; *World Health Organization - Obesity and overweight*, 2021), with 1 in 5 deaths in the world today associated with obesity (*World Health Organization - Obesity and overweight*, 2021). In fact, in 2016, more than 1.9 billion adults were overweight and from these, more than 650 million were obese (*World Health Organization - Obesity and overweight*, 2021). Obesity is defined by the World Health Organization (WHO) as an excessive adipose tissue accumulation sufficient to impair health (Goossens, 2008; *World Health Organization - Obesity and overweight*, 2021). It is characterized by excessive central visceral adiposity that contributes to a chronic increase in circulating free fatty acids and the resulting metabolites that will activate various signaling cascades, interfering with insulin signaling and β -cell function and increasing circulatory disease and cancer risk (Goossens, 2008; Lai et al., 2014).

Type 2 diabetes (T2D) accounts for over 90–95% of all diabetes, being a complex multifactorial metabolic disorder influenced by lifestyle, environmental, and genetic risk factors. In 2017, 425 million people worldwide had diabetes, a number that continues to increase and which, by 2045, is anticipated to affect 629 million people (*IDF Diabetes Atlas 8th Edition 2017*; Pérez-Hernández et al., 2014). T2D is characterized by impaired glucose homeostasis with insulin resistance and β -cell dysfunction, the primary trait induced by obesity being insulin resistance in metabolic tissues (adipose, hepatic, and muscular tissues). This peripheral insulin resistance induces pancreatic β cells to secrete more insulin, leading to hyperinsulinemia, which often leads to β cell depletion and sustained hyperglycemia in T2D (*IDF Diabetes Atlas 8th Edition 2017*).

Metabolic syndrome is defined by a cluster of metabolic abnormalities that increase the risk of coronary heart disease, other forms of cardiovascular diseases, and T2D. Its main pathological characteristics are obesity, insulin resistance, raised fasting plasma glucose, hypertension, and atherogenic dyslipidemia (elevated serum triacylglycerols and

apolipoprotein B, increased small low-density lipoprotein (LDL) particles, and a reduced level of high-density lipoprotein (HDL)) (Kassi et al., 2011; Moreira et al., 2014).

One of the mechanisms involved in the pathogenesis of metabolic diseases and its comorbidities is autonomic dysfunction. Obesity, T2D, and metabolic syndrome are all associated with an increased sympathetic and decreased parasympathetic drive (E. Lambert et al., 2007; Triggiani et al., 2017), with previous studies showing an increase of serum noradrenaline, noradrenaline excretion, renal and heart and muscle sympathetic nervous system activity, and heart rate variability indexes (Indumathy et al., 2015; E. A. Lambert et al., 2015; G. W. Lambert et al., 2010; Straznicky et al., 2010). Autonomic dysfunction has been linked to target organ damage, such as diastolic dysfunction, ventricular hypertrophy or cardiac remodeling, as well as with insulin resistance, hyperinsulinemia, and dyslipidemia (G. W. Lambert et al., 2010; Straznicky et al., 2010). It has been postulated that prevention of autonomic dysfunction could be a strategy for reducing these comorbidities and that the assessment of autonomic function could be used as an early biomarker for metabolic diseases (Sun et al., 2012; Zhu et al., 2016).

Several rodent models have been developed to study metabolic disturbances, particularly obesity and T2D. In general, T2D is induced by surgical, chemical, dietary or genetic manipulations, or by a combination of these and other techniques. However, the pathophysiological conditions of these types of models are far from the human characteristics of disease. Thus, hypercaloric, hyperlipidemic diets or the combination of both have been used to induce obesity and T2D as well as metabolic syndrome in animals (Burchfield et al., 2018; Rasool et al., 2018; Rosini et al., 2012; Sun et al., 2012). However, a lack of consensus exists on the best diets and time of exposure to these diets used to promote alterations in metabolic parameters, such as insulin resistance, hyperinsulinemia, and glucose intolerance, among others, as well as associated metabolic comorbidities, such as hypertension and non-alcoholic fatty liver disease.

The present investigation evaluates the impact of different hypercaloric diets and different times of exposure to diets on weight gain, insulin resistance, glucose intolerance, as well as autonomic dysfunction and consequences hypertension, and lipid

deposition in the liver as an indication of non-alcoholic fatty liver disease. Additionally, we compared these models with a genetic model, the Zucker fatty diabetic rat, which is a reference model for obesity and T2D. Moreover, we discuss the outcomes for these different animal models, with the aim of identifying the most appropriate model(s) to investigate physiopathological mechanisms and therapeutic strategies for metabolic diseases.

Methods

Diets and animal care

Experiments were performed in 8-9-weeks-old male Wistar rats (200-300 g) obtained from the animal house of NOVA Medical School, Faculty of Medical Sciences, New University of LisbonUniversidade Nova de Lisboa, Lisbon, Portugal, except for the male Zucker diabetic fatty (ZDF) animals and their respective controls Zucker lean that were acquired with 6-weeks-old from Charles River (Paris, France) and maintained for 2 weeks in quarantine. After randomization, the hypercaloric diet animals were assigned to one of six groups: (1) The 3 weeks high-fat diet-fed (HF) group, fed with a 45% fat diet (45% fat + 35% carbohydrate + 20% protein; for detailed composition, see Table S1 of Supplementary Data; Mucedola, Milan, Italy); (2) the 19 weeks HF group, fed with 60% fat diet (61.6% fat + 20.3% carbohydrate + 19.1% protein; for detailed composition see Table S2 of Supplementary Data; Test Diets, Missouri, USA); (3) the 4 weeks HF group, fed with a 45% fat diet (45% fat + 35% carbohydrate + 20% protein; Mucedola, Milan, Italy) and submitted to an injection of streptozotocin (25 mg/kg, i.p.), an antibiotic derived from Streptomyces achromogenes that causes β-cell damage (Gheibi et al., 2017), in the beginning of the 4th week of diet (HF+STZ group); (4) the high-sucrose dietfed (HSu) group, fed with 35% (wt/vol.) sucrose (PanReac, Madrid, Spain) in drinking water for 4 weeks; (5) the HSu group fed with 35% (wt/vol.) sucrose (PanReac, Madrid, Spain) in drinking water for 16 weeks; and (6) a combined model of HF (61.6% fat + 20.3% carbohydrate + 19.1% protein; Test Diets, Missouri, USA) and HSu (35% (wt/vol.)) diet for 25 weeks. ZDF animals were fed with Purina 5008 (Formulab Diet 5008 and Formulab Diet 5008C33, for detailed composition, see Table S3 of Supplementary Data; Purina) that consisted of a mix of 23.6% protein, 14.8% lipid, 50.3% carbohydrates, 3.3% fiber, and the remaining minerals and vitamins. All control animals were fed a control diet (7.4% lipid and 75% carbohydrates, of which 4% were sugars and 17% protein; for detailed composition, see Table S4 of Supplementary Data; SDS RM3). All groups of hypercaloric diet animals and its aged-matched controls as well as Zucker diabetic rat and its lean controls of 17 weeks included 6–8 animals per group; Zucker diabetic rat of 23 weeks included 3 animals per group, and its lean control only one animal.

Animals were kept under temperature and humidity control (21 ± 1 °C; $55\pm10\%$ humidity) with a 12 h light/12 h dark cycle and were given ad libitum access to food and water. Body weight was monitored weekly, and energy and liquid intake were monitored daily. Insulin sensitivity and glucose tolerance were also evaluated over the experimental period.

At a terminal experiment, animals were anesthetized with sodium pentobarbitone (60 mg/kg, i.p), and catheters were placed in the femoral artery for arterial blood pressure measurement. Afterwards, blood was collected by heart puncture for serum and plasma quantification of mediators and the liver, soleus, and gastrocnemius and the adipose tissue pads as the visceral, perinephric, epididymal, and subcutaneous fat were then rapidly collected, weighted, and stored at –80 °C for further analysis. Laboratory care was in accordance with the European Union Directive for Protection of Vertebrates Used for Experimental and Other Scientific Ends (2010/63/EU). Experimental protocols were approved by the NOVA Medical School/Faculdade de Ciências Médicas Ethics Committee and by Portuguese DGAV.

Insulin Tolerance Test

Insulin sensitivity was evaluated using insulin tolerance test (ITT) after overnight fasting as previously described (Conde et al., 2012). Briefly, fasting blood glucose was measured and immediately followed by an insulin bolus (100 mU/kg), administered via the tail vein. Subsequently, the decline in plasma glucose concentration was measured over a 15 min period.

Oral Glucose Tolerance Test

Glucose tolerance was evaluated using oral glucose tolerance test (OGTT) after overnight fasting as described by Sacramento et al. (Sacramento et al., 2017). Briefly, fasting blood glucose was measured and immediately followed by administration of a saline solution of glucose (2 g/kg, VWR Chemicals, Leuven, Belgium), by gavage. Blood glucose levels were measured at 15, 30, 60, 120, and 180 min.

Quantification of Biomarkers: Plasma Insulin, C-Peptide, Lipid Profile, and Catecholamines

Insulin and C-peptide concentrations were determined with an enzyme-linked immunosorbent assay kit (Mercodia Ultrasensitive Rat Insulin ELISA Kit and Mercodia Rat C-peptide ELISA Kit, respectively, Mercodia AB, Uppsala, Sweden). Catecholamines were measured in plasma and in homogenized adrenal medulla samples as previously described (Sacramento et al., 2017). The lipid profile was assessed using a RANDOX kit (RANDOX, Irlandox, Porto, Portugal) as described by Sacramento et al. (Sacramento et al., 2017).

Blood Pressure Evaluation

Mean arterial pressure (MAP) was determined by catheterization of the femoral artery. The catheter was connected to a pressure transducer (–50, +300 mmHg) and amplifier (Emka Technologies, Paris, France). MAP was calculated using the values of systolic blood pressure (SBP) and diastolic blood pressure (DBP) by the lox 2.9.5.73 software (Emka Technologies, Paris, France). To calculate a mean arterial pressure, double the diastolic blood pressure and add the sum to the systolic blood pressure. Then divide by 3. MAP = (SBP + 2 (DBP))/3.

Lipid Deposition in the Liver

Lipid deposition in the liver was quantified by an extraction method described by Folch (Folch et al., 1957). Briefly, 0.5 g of liver samples were homogenized in 3 ml of Folch solution. The samples were shaken and filtered to a test tube and the process repeated twice. After, 2 ml of NaCl 0.73% were added to the filtered samples and samples were

left in rest overnight. Afterwards, the organic phase was collected and transferred to a petri dish. To the other phase was added 2.5 mL of Folch solution: NaCl 0.58% (80:20). The process was repeated, and all the organic phase collected was left to dry for 24 h before weighing the petri dish, for determination of total lipids in the sample. The results were expressed as a percentage of lipids per total weight of homogenized liver.

Western Blot Analysis

Visceral adipose tissue (100 mg) was homogenized in Zurich (10 mM Tris-HCl, 1 mM EDTA, 150 mM NaCl, 1% Triton X-100, 1% sodium cholate, 1% SDS) with a cocktail of protease inhibitors (trypsin, pepstatin, leupeptin, aprotinin, sodium orthovanadate, phenylmethylsulfonyl fluoride (PMSF)), and samples were centrifuged (Eppendorf, Madrid, Spain) and supernatant was collected and frozen at -80 °C until further use. Samples of the homogenates (50 µg) and the prestained molecular weight markers (Precision, BioRad, Madrid, Spain) were separated by sodium dodecyl sulfate polyacrylamide gel electrophoresis (10% with a 5% concentrating gel) under reducing conditions and electrotransferred to polyvinylidene difluoride membranes (0.45 µM, Millipore, Spain). After blocking for 1 h at room temperature with 5% nonfat milk in Trisbuffered saline, pH 7.4 containing 0.1% Tween 20 (TTBS) (BioRad, Spain), the membranes were incubated overnight at 4 °C with the primary antibodies against glucose transporter type 4 (GLUT4; 1:200, Abcam, Cambridge, UK), insulin receptor (IR; 1:200, Santa Cruz Biotechnology, Madrid, Spain), phosphorylated insulin receptor (p-Tyr1361, 1:500, Abcam, Cambridge, UK), Protein Kinase B (Akt; 1:1000, Cell Signaling, Leiden, The Netherlands) and phosphorylated Akt (p-Ser473, 1:1000, Cell Signaling, Leiden, The Netherlands). The membranes were washed with Tris-buffered saline with Tween (TBST) (0.1%) and incubated with mouse anti-goat (1:2000) or goat anti-mouse (1:2000) in TBS and developed with enhanced chemiluminescence reagents in accordance with the manufacturer's instructions (ClarityTM Western ECL substrate, Hercules, CA, USA). Intensity of the signals was detected in a Chemidoc Molecular Imager (Chemidoc; BioRad, Madrid, Spain) and quantified using Image Lab software (BioRad). The membranes were re-probed and tested for Calnexin (1:1000, SICGEN,

Cantanhede, Portugal) immunoreactivity (bands in the 85 kDa region) to compare and normalize the expression of proteins with the amount of protein loaded.

Evaluation of Autonomic Nervous System

The balance between the sympathetic and parasympathetic components of the autonomic nervous system was made by calculating the sympathetic nervous system (SNS) and parasympathetic nervous system (PNS) indexes computed in Kubios HRV software (www.kubios.com). The SNS index in Kubios is based on Mean heart rate, Baevsky's stress index, and low frequency power expressed in normalized units and the PNS index which is based on the mean intervals between successive heartbeats (RR intervals), the root mean square of successive RR interval differences (RMSSD) and high frequency power expressed in normalized units. Heart rate and RR intervals were obtained using lox 2.9.5.73 software (Emka Technologies, Paris, France), with an acquisition frequency of 500 Hz.

Statistical Analysis

Data were evaluated using GraphPad Prism Software, version 6 (GraphPad Software Inc., San Diego, CA, USA) and presented as mean values with SEM. The significance of the differences between the mean values was calculated by one- and two-way ANOVA with Bonferroni multiple comparison test. Differences were considered significant at p < 0.05.

Results

Weight Gain, Fat Mass Depots, and Lipid Profile in Animal Models of Type 2 Diabetes and Obesity

In Figure 1A, we depict the growth curves of the animal models of obesity and T2D studies and their corresponding age-matched controls and in which a clear increase can be noted in weight gain in almost all disease models. When the data are plotted as the increase in grams per day, the disease models presented an increased weight gain when compared to their correspondent age-matched controls (Figure 1B, HF 3 weeks = 1.43 ± 0.28 ; HF 19 weeks = 4.10 ± 0.30 ; HF+STZ = 3.45 ± 0.17 ; HSu 4 weeks = 1.31 ± 0.10 ; HSu

16 weeks = 0.68 ± 0.13 ; HFHSu 25 weeks = 2.60 ± 0.19 ; Zucker 17 weeks = 26.23 ± 1.27 Zucker 23 weeks = 19.12 ± 3.83 ; CTL 3 weeks = 0.82 ± 0.17 ; CTL 19 weeks = 2.66 ± 0.16 ; CTL for HF+STZ group = 1.12 ± 0.33 ; CTL 4 weeks = 0.82 ± 0.17 ; CTL 16 weeks = 0.54 ± 0.10 ; CTL 25 weeks = 1.43 ± 0.07 ; lean 17 weeks = 16.21 ± 0.81 ; lean 23 weeks = 13.18 ± 0.00 g/day). Only the sucrose-rich diet for 16 weeks did not produce a significant increase in weight gain in comparison to the controls. When comparing HF 19 weeks with all the disease models, induced by hypercaloric diets, it was observed that this group presented a more pronounced weight gain that was only exceeded by the genetic model, the Zucker rat, with 17 and 23 weeks (Figure 1B).

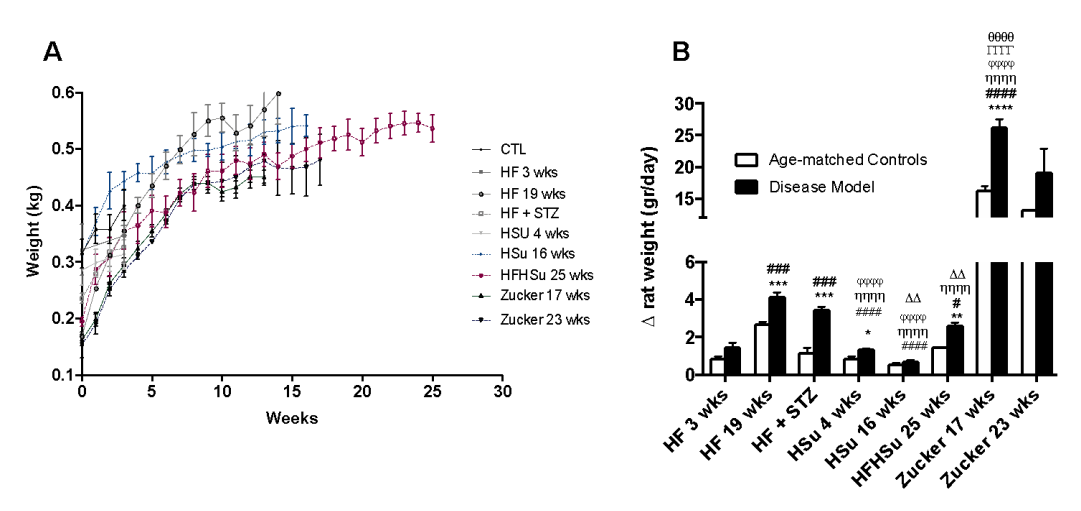


Figure 1 - Weight gain in animal models of type 2 diabetes and obesity. (A) Growth curves. (B) Weight increase in animal groups expressed as g/day. All groups of hypercaloric diet animals and their aged-matched controls as well as Zucker diabetic rat and its lean controls of 17 weeks included 6–8 animals per group; Zucker diabetic rat of 23 weeks included 3 animals per group, and its lean control only one animal. Bars represent means \pm SEM. Two-way ANOVA with Bonferroni's multiple comparisons test: *p < 0.05, **p < 0.01, ***p < 0.001, and ****p < 0.0001 comparing age-matched controls with disease models; #p < 0.05, ###p < 0.001, and ####p < 0.0001 comparing HF3 weeks with HF19 weeks, HF+STZ, HSu 4 weeks, HSu 4 weeks, HFHSu 25 weeks, and Zucker 17 weeks, respectively; ηηηηρ < 0.0001 comparing HF19 weeks with HSu 4 weeks, HSu 16 weeks, HFHSu 25 weeks, and Zucker 17 weeks; $\phi\phi\phi\phi$ p < 0.0001 comparing HSu 4 weeks with HSu 16 weeks and Zucker 17 weeks; $\theta\theta\theta\theta$ p < 0.0001 comparing HFHSu 25 weeks with Zucker 17 weeks; $\Gamma\Gamma\Gamma\Gamma$ p < 0.0001 comparing HSu 16 weeks with Zucker 17 weeks.

Table 1 depicts the amount of fat mass of the animal models of obesity and T2D studied and their corresponding age-matched controls. All disease models, except the HF+STZ

and HSu 4 weeks, exhibited a significant increase in the total amount of fat when compared to age-matched controls. Furthermore, an increase was also observed in the amount of perienteric, epididymal, and perinephric depots, except for the models described above, HF+STZ and HSu 4 weeks (Table 1). As can be seen in Table 1, when comparing all disease models, the HF 19 weeks group was the animal model that exhibited a higher amount of total fat as well as higher amount of all adipose tissue depots (Table 1).

When comparing the levels of cholesterol, HDL, LDL, and triglycerides, it was possible to identify the disease models that presented alterations in lipid profile, in comparison to their corresponding age-matched controls (Table 1). HF 19 weeks, HSu 4 weeks, and Zucker 17 weeks groups showed increased levels of total cholesterol and HF 3 weeks, HF 19 weeks, Hsu 4 weeks, HSu 16 weeks, HFHSu 25 weeks, and Zucker 17 weeks showed increased levels of triglycerides. Further, HDL levels were decreased in HF 3 weeks, HF 19 weeks, HSu 16 weeks, and Zucker 17 weeks, and LDL levels were increased in the HF 19 weeks, HSu 16 weeks, HFHsu 25 weeks, and Zucker 17 weeks groups. The HF 19 weeks and Zucker 17 weeks groups exhibited dysfunctional levels in all the parameters of the lipid profile evaluated.

Animals were randomly allocated to the HSu and HF groups, submitted to the respective diet protocol and then randomly allocated to CSN transection or sham surgery in which the CSN was left intact. The sham procedure did not alter body weight and energy intake in comparison with the respective controls (data not shown). Bilateral CSN resection was confirmed by the absence of increased ventilatory responses to ischaemic-hypoxia during common carotid artery occlusion (data not shown). Bilateral CSN resection and the sham procedure did not significantly modify animal behaviour or energy intake, measured as the average energy intake per day during the 3 weeks after CSN denervation (data not shown).

Table 1 - Adipose tissue depots and lipid profile (total cholesterol, triacylglycerols, high-density lipoprotein (HDL)—cholesterol and low-density lipoprotein (LDL)—cholesterol) in animal models of obesity and type 2 diabetes.

		Total Fat (g/kg Body Weight)	Perienteric Fat (g/kg Body Weight)	Epidydymal Fat (g/kg Body Weight)	Perinephric Fat (g/kg Body Weight)	Cholesterol (mmol/L)	HDL-Cholesterol (mmol/L)	LDL- Cholesterol (mmol/L)	Triglycerides (mmol/L)
HF 3	age-matched control	48.72 ± 2.21	9.56 ± 0.43	19.81 ± 2.06	17.80 ± 1.72	1.77 ± 0.09	0.72 ± 0.03	0.13 ± 0.01	0.35 ± 0.04
weeks	disease model	70.05 ± 3.62 ***	13.82 ± 0.79 ***	38.47 ± 0.97 **	30.18 ± 1.97 **	1.83 ± 0.08	0.53 ± 0.03 ***	0.11 ± 0.02	0.51 ± 0.04 **
HF 19	age-matched control	91.23 ± 7.63	13.76 ± 1.60	29.66 ± 1.98	29.01 ± 2.04	1.69 ± 0.08	0.80 ± 0.05	0.12 ± 0.01	1.14 ± 0.09
weeks	disease model	223.37 ± 2.58 ****,####	32.12 ± 2.23****,####	61.58 ± 2.08 ****,##,ΔΔΔΔ	75.21 ± 2.17 ****,####	2.48 ± 0.15 ***,###	0.55 ± 0.03 **,###	0.23 ± 0.01 ****,###	1.66 ± 0.27 *,###
HF+	age-matched control	54.23 ± 2.81	11.00 ± 0.88	18.66 ± 1.15	25.27 ± 1.42	-	-	-	-
STZ	disease model	61.37 ± 2.50 nnnn	$13.21 \pm 0.62^{\eta\eta\eta\eta}$	21.83 ± 0.88 *,###,nnnn	26.33 ± 1.89 nnnn	-	-	-	-
HSu 4	age-matched control	48.72 ± 2.21	9.56 ± 0.43	19.81 ± 2.06	17.80 ± 1.72	1.77 ± 0.09	0.72 ± 0.03	0.13 ± 0.01	0.35 ± 0.04
Weeks	disease model	52.46 ± 2.28 ###-ողող-φφ	$10.17\pm0.52^{ ext{#\#-nnnn-pp}}$	20.62 ± 2.34	$23.37\pm0.95~^*$	2.13 ± 0.11 *,#	0.69 ± 0.05 ##	0.14 ± 0.02 ⁿⁿ	0.61 ± 0.07 **,###,ηη
HSu 16	age-matched control	59.83 ± 1.74	13.58 ± 0.31	25.98 ± 1.35	20.27 ± 2.11	1.80 ± 0.10	0.79 ± 0.04	0.10 ± 0.01	0.48 ± 0.06
weeks	disease model	80.44 ± 2.34****,nnnn	$17.93 \pm 0.75^{\text{***}}.\text{nnn}$	31.43 ± 2.40 hhan-fraga.	31.08 ± 2.66 *-nnnn	1.98 ± 0.11 ⁿ	$0.60\pm0.04^{~**,\#\#\#}$	0.12 ± 0.01 nnn	0.79 ± 0.05 **, $\eta\eta$

HFHSu 25	age-matched control	66.44 ± 3.93	15.58 ± 0.82	25.08 ± 1.52	25.78 ± 1.75	1.90 ± 0.25	0.63 ± 0.04	0.24 ± 0.03	0.90 ± 0.14
weeks	disease model	113.91 ± 9.72 ***,###.nnnn	$24.44 \pm 2.84^{**,\#\#,\phi\phi\phi}$	$36.90 \pm 2.83^{**,\eta\eta\eta\eta,\varphi\varphi\varphi}$	$52.57 \pm 4.45^{****,\#,\eta\eta}$	2.26 ± 0.16	0.59 ± 0.04 ⁿ	0.37 ± 0.05 ###,ΔΔ	1.53 ± 0.13 **,####
Zucker 17	age-matched control	42.83 ± 4.15	6.55 ± 0.65	8.82 ± 0.71	11.37 ± 0.92	2.27 ± 0.07	1.64 ± 0.13	0.10 ± 0.02	1.16 ± 0.21
weeks	disease model	151.77 ± 7.58****,####,nnnn	15.11 ± 1.25 ***, $\eta \eta \eta \cdot \Delta \Delta$	22.75 ± 3.15 **,#,ŋnnŋ.θθ	$35.05 \pm 1.80^{****}$, nnnn	4.51 ± 0.29***	0.87 ± 0.03 ***,####	0.70 ± 0.07 ****,####	8.72 ± 1.21***,####
Zucker 23 weeks	age-matched control	30.44 ± 0.00	3.19 ± 0.00	7.45 ± 0.00	6.33 ± 0.00	-	-	-	-
	disease model	168.3 ± 34.94	12.27 ± 2.47	26.33 ± 4.21	45.64 ± 6.59	-	-	-	-

All groups of hypercaloric diet animals and its aged-matched controls as well as Zucker diabetic rat and its lean controls of 17 weeks included 6–8 animals per group; Zucker diabetic rat of 23 weeks included 3 animals per group, and its lean control only one animal. Values represent means \pm SEM; one- and two-way ANOVA with Bonferroni's multiple comparisons test: *p < 0.05, **p < 0.01, **** p < 0.001, and ***** p < 0.0001 comparing age-matched controls with disease models; *p < 0.05, **p < 0.001, and **p < 0.001, and

Effect of Hypercaloric Diets and Genetic Deletion of Leptin Receptors on Glucose Metabolism in Animal Models of Obesity and Type 2 Diabetes

Figure 2A represents the effect of hypercaloric diets and genetic deletion of leptin receptors on fasting glycemia in animal models of obesity and T2D and their corresponding age-matched controls. All the disease groups, except the HSu 16 weeks, presented a significant increase in fasting glycemia (% increase glycemia: 15% HF 3 weeks, 13% HF 19 weeks, 33% HF+STZ, 25% HSu 4 weeks, 17% HF+HSu 25 weeks, 154% Zucker 17 weeks, 201% Zucker 23 weeks). Note, however, that even though fasting glycemia levels increased in all models, only the genetic model presented values above 126 mg/dl, the reference value for diabetes diagnosis.

As depicted in Figure 2B, insulin resistance was observed in all disease models, as the constant rate for glucose disappearance (KITT) significantly decreased when compared to their correspondent age-matched controls, except for the HF+STZ group, (HF 3 weeks = 2.07 ± 0.19 ; HF 19 weeks = 1.97 ± 0.29 ; HF+STZ = 5.01 ± 0.18 ; HSu 4 weeks = 2.45 ± 0.25 ; HSu 16 weeks = 1.79 ± 0.19 ; HFHSu 25 weeks = 1.82 ± 0.13 ; Zucker 17 weeks = 1.55 ± 0.47 Zucker 23 weeks = 1.59 ± 0.33 ; CTL 3 weeks = 4.56 ± 0.41 ; CTL 19 weeks = 4.32 ± 0.26 ; CTL for HF+STZ group = 4.17 ± 0.31 ; CTL 4 weeks = 4.56 ± 0.41 ; CTL 16 weeks = 5.29 ± 0.51 ; CTL 25 weeks = 4.73 ± 0.30 ; lean 17 weeks = 4.46 ± 0.49 ; lean 23 weeks = $4.22 \pm 0.00\%$ glucose/min). It can be clearly seen that a more pronounced insulin resistance was obtained with longer exposures to hypercaloric diets as well as with the genetic deletion of leptin receptors.

In agreement with these characteristics, Figure 2C represents the glucose tolerance depicted as glucose excursion curves (left panel) and as the area under the curve (AUC) obtained from the glucose excursion curves (right panel). Comparing the AUC of glucose excursion curves in the disease animal models with the AUC of their correspondent agematched controls, it was observed that the groups HF 19 weeks, HF+STZ, HSu 16 weeks, HF+HSu 25 weeks, and Zucker 17 and 23 weeks presented glucose intolerance (HF 19 weeks = 24406.29 ± 393.89 ; HF+STZ = 31330.83 ± 1625.33 ; HSu 16 weeks = 21502.75 ± 720.46 ; HF+HSu 25 weeks = 24969.63 ± 635.89 ; Zucker 17 weeks = 56526.00 ± 5115.70 ; Zucker 23 weeks = 69514 ± 1414 ; CTL 19 weeks = 19668 ± 380.34 ; CTL for HF+STZ =

 23427.83 ± 567.41 ; CTL 16 weeks = 20689.80 ± 836.43 ; CTL 25 weeks = 21986 ± 368.85 ; lean 17 weeks = 16849 ± 616.37 ; lean 23 weeks = 16208 ± 0.00 mg/dl*min). As expected, Zucker animals were the animal model that showed a more pronounced increase in fasting glycemia, higher insulin resistance, and higher glucose intolerance, followed by the diet-induced glucose dysmetabolism models, HF19 weeks and HFHSu 25 weeks groups, which also showed increases in all these characteristics, although with a lower magnitude.

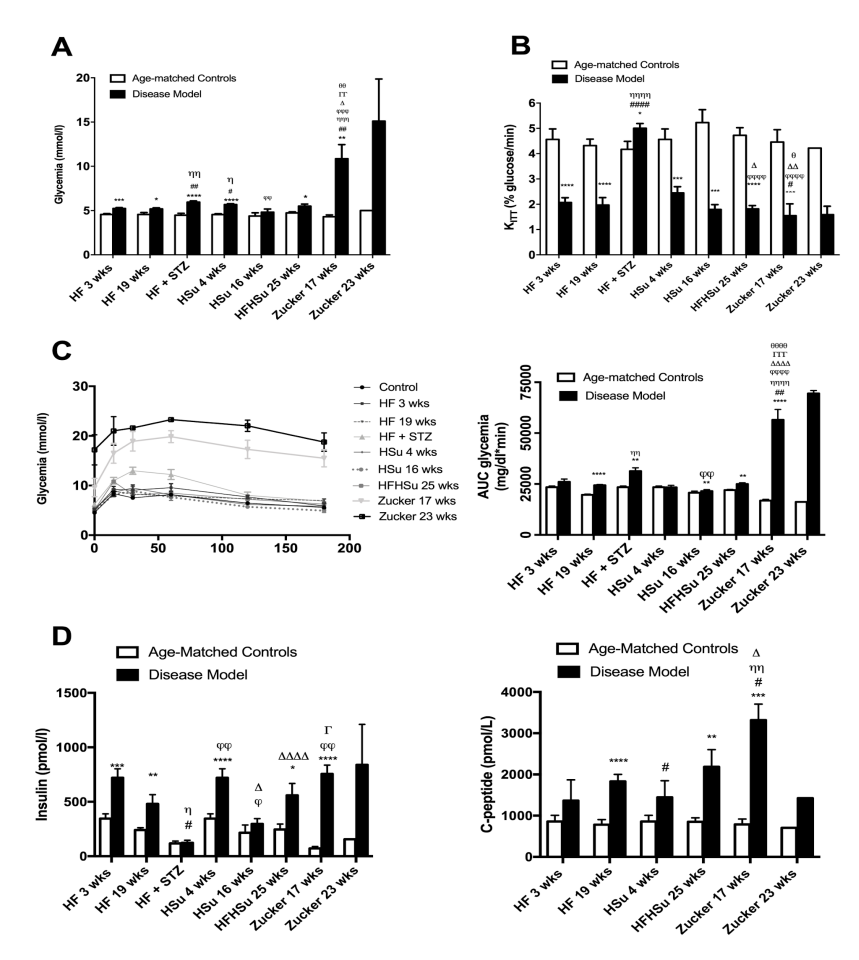


Figure 2 - Glucose metabolism and insulin action and secretion in animal models of type 2 diabetes and obesity. (A) Fasting glycemia levels; (B) insulin sensitivity expressed as the constant of insulin tolerance test (KITT); (C) glucose tolerance depicted as glucose excursion curves (left panel) and as the area under the curve (AUC) obtained from the glucose excursion curves (right panel); (D) fasting insulin (left panel) and C-peptide (right panel) levels in animal models of obesity and type 2 diabetes. All groups of hypercaloric diet animals and its aged-matched controls as well as Zucker diabetic rat and its lean controls of 17 weeks included 6–8 animals per group; Zucker diabetic rat of 23 weeks included 3 animals per group, and its lean control only one animal. Bars represent means \pm SEM; two-way ANOVA with Bonferroni's multiple comparisons test: *p < 0.05, **p < 0.01, ***p < 0.001, and ****p < 0.0001 comparing agematched controls with disease models; #p< 0.05, ##p < 0.01, and ####p < 0.0001 comparing HF 3 weeks group with HF 19 weeks, HF+STZ, HSu 4 weeks, and Zucker 17 weeks; $\eta p < 0.05$, $\eta p < 0.01$, $\eta \eta p < 0.001$, and $\eta \eta \eta \eta p < 0.0001$ comparing HF 19 weeks with HF+STZ, HSu 4 weeks, HFHSu 25 weeks, and

Zucker 17 weeks; $\phi p < 0.05$, $\phi \phi p < 0.01$, $\phi \phi \phi p < 0.001$, and $\phi \phi \phi \phi p < 0.0001$ comparing HF+STZ with HSu 16 weeks, HFHSu 25 weeks, and Zucker 17 weeks; $\Delta p < 0.05$; $\Delta \Delta p < 0.01$, and $\Delta \Delta \Delta \Delta p < 0.0001$ comparing HSu 4 weeks with HFHSu 25 weeks and Zucker 17 weeks; $\Gamma p < 0.05$, $\Gamma \Gamma p < 0.01$, and $\Gamma \Gamma \Gamma p < 0.001$ comparing HSu 16 weeks group with Zucker 17 weeks; $\theta p < 0.05$, $\theta \phi p < 0.01$, and $\theta \theta \theta \phi p < 0.0001$ comparing HFHSu 25 weeks with Zucker 17 weeks.

In accordance with the whole-body insulin resistance, it was observed that all the disease animal models, except the HF+STZ model, exhibited increased fasting insulin values (Figure 2D). Insulin values increased significantly by 82%, 142%, 116%, 38%, 128%, 946%, and 441% in HF 3 weeks, HF 19 weeks, Hsu 4 weeks, Hsu 16 weeks, HFHSu 25 weeks, Zucker 17 weeks, and Zucker 23 weeks, respectively. The values of C-peptide, which measures endogenous insulin secretion, also significantly increased by 59%, 134%, 69%, 157%, 321%, and 102% in HF 3 weeks, HF 19 weeks, Hsu 4 weeks, HFHSu 25 weeks, Zucker 17 weeks, and Zucker 23 weeks, respectively. The absence of increase in insulin levels in the HF+STZ model is consistent with the lack of insulin resistance in this group. Note also that the Zucker animals were the groups that showed higher insulin and C-peptide levels, followed by HF 19 weeks and HFHSu 25 weeks, which agrees with the more profound alterations in glucose tolerance and whole-body insulin sensitivity.

In agreement with the alterations observed in glucose tolerance and whole-body insulin sensitivity, we observed profound alterations in the expression of proteins involved in insulin signaling on white adipose tissue from the HF 3, HSu 4, and HSu 16 weeks groups (Figure 3, please see supplemental data for complete Western blot gels (Figure S1)). The disease models tested showed decreased expression of the insulin receptor and its phosphorylated form by 26%, 18%, and 23% (for IR) and 34%, 33%, and 8% (for IR phosphorylated form) for HF 3, HSu 4 and HSu 16 weeks respectively. Further, the expression of Akt and its phosphorylated form decreased by 35% and 42% (for Akt) in HF 3 weeks and HSu 4 weeks, respectively, and by 26%, 43%, and 22% (for Akt phosphorylated form) in HF 3, HSu 4, and HSu 16 weeks respectively. As a glucose transporter, GLUT4 expression also decreased by 17%, 20%, and 22% in HF 3, HSu 4, and HSu 16 weeks, respectively. Note that the effects of diet on the expression of these

proteins were higher for 4 weeks of HSu than for the 16 weeks, suggesting compensatory mechanisms to maintain cellular insulin sensitivity.

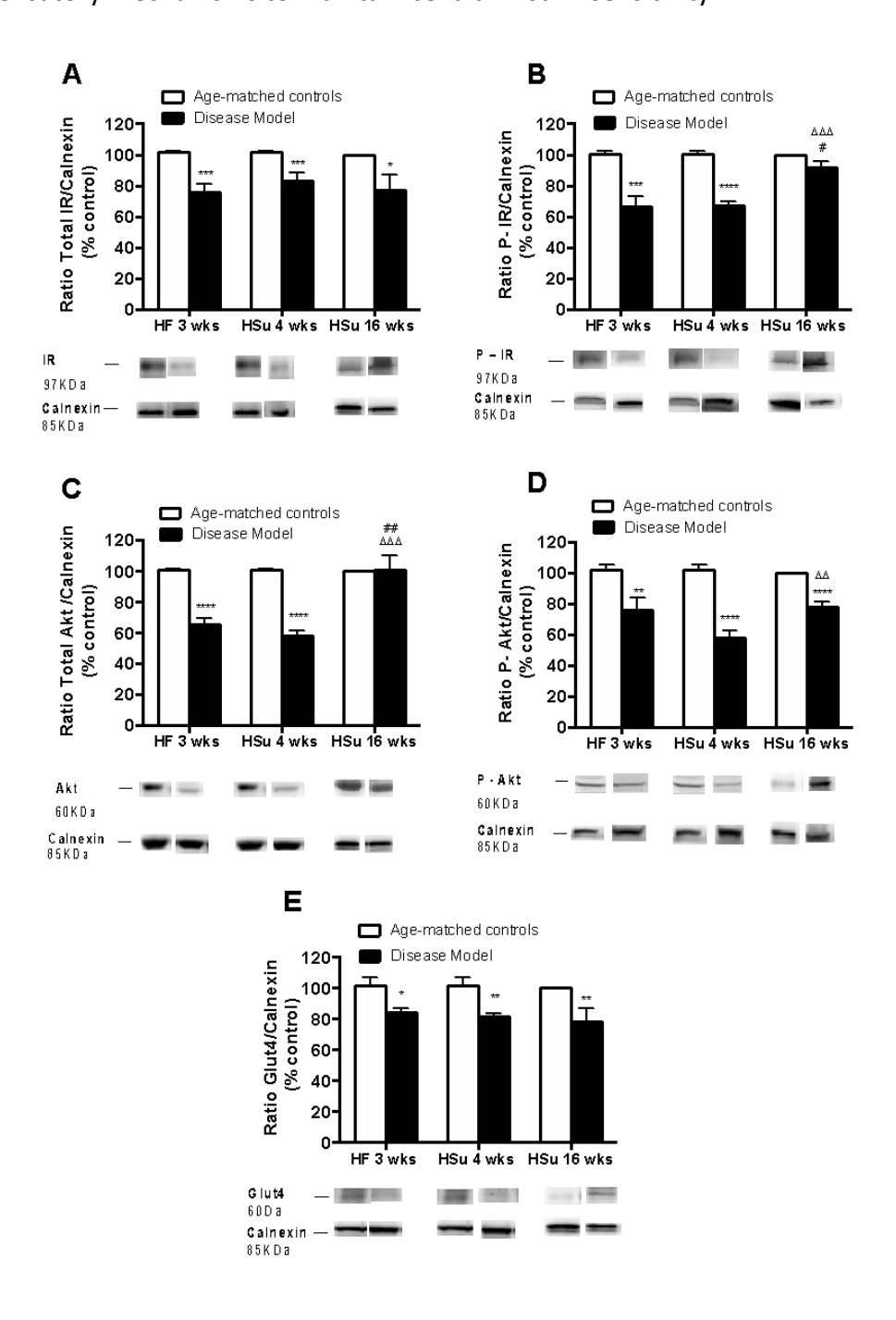


Figure 3 - Alterations in the expression of proteins involved in insulin signaling in insulin-sensitive tissues in animal models of obesity and type 2 diabetes. (A) Total insulin receptor (IR) expression (B) phosphorylated IR expression; (C) total AKT expression; (D) phosphorylated AKT expression; (E) Glu4 expression. Below the graphs, representative bands from the Western blots for the correspondent proteins are shown. Bars represent means \pm SEM; one- and two-way ANOVA with Bonferroni's multiple comparisons test: *p < 0.05, **p < 0.01, ***p < 0.001, and ****p < 0.0001 comparing age-matched

controls with disease models; #p < 0.05 and ##p < 0.01 comparing HF 3 weeks with HSu 16 weeks; $\Delta\Delta p$ < 0.01 and $\Delta\Delta\Delta p$ < 0.001 comparing HSu 4 weeks with HSu 16 weeks.

Comorbidities in the Distinct Models of Obesity and Type 2 Diabetes

Hypertension is one of the main illnesses associated with obesity and T2D (1-3). Figure 4 depicts mean arterial pressure levels for the animal models of obesity and T2D studied and their corresponding age-matched controls. All disease models exhibit increased levels of blood pressure when compared to their age-matched controls (HF 3 weeks = 127.30 ± 1.60; HF 19 weeks = 127.84 ± 6.81; HF+STZ = 119.08 ± 6.08; HSu 4 weeks = 127.04 ± 3.98 ; HFHSu 25 weeks = 121.74 ± 5.37 ; Zucker 17 weeks = 124.07 ± 6.34 ; Zucker 23 weeks = 129.80 ± 0.00 ; CTL 3 weeks = 98.36 ± 4.29 ; CTL 19 weeks = 95.38 ± 6.80 ; CTL for HF+STZ group = 89.62 ± 3.94 ; CTL 4 weeks = 98.36 ± 4.29 ; CTL 25 weeks = 82.89 ± 4.2 5.62; lean 17 weeks = 104.58 ± 3.92 ; lean 23 weeks = 115.10 ± 0.00 mmHg), HF 19 weeks (34%) and HFHSu 25 weeks (47%) being the animal models that exhibit higher increases. Another common comorbidity of obesity and T2D is non-alcoholic fatty liver disease, which is characterized by increased lipid deposition in the liver. Figure 5A shows hematoxicilin and eosin images obtained from HF 19 weeks, HFHSu 25 weeks, and Zucker 23 weeks animals and their correspondent controls. All animals present an increase in lipid deposition with a marked hepatocellular micro and macrovesicular (black arrowhead) vacuolization, and presence of fibrosis (white arrowhead) However, it can be noted that lipid deposition in HF19 weeks and Zucker diabetic it is more representative at a microvesicular level, while HFHSu animals 25 weeks animals exhibit a higher percentage of macrovesicular vacuolization. Note also some degree of fibrosis in HF 19 weeks animals as well as in Zucker diabetic fatty 23 weeks. Figure 5B represents the percentage of lipids in the liver quantified by the Folch method, and it can be observed that all disease models showed higher lipid deposition when compared to their correspondent age-matched controls (% increase in lipid deposition HF 3 weeks = 88%; HF 19 weeks = 136%; HF+STZ = 86%; HSu 4 weeks = 33%; HSu 16 weeks = 31%; HFHSu 25 weeks = 48%; Zucker 17 weeks = 147%; Zucker 23 weeks = 123%)). All animals submitted to high fat diet (HF 3 weeks, HF 19 weeks, HF+STZ) and the Zucker animals were the groups that exhibited higher lipid deposition in the liver, with HSu animals showing a lower liver

Age-matched controls lipid deposition.

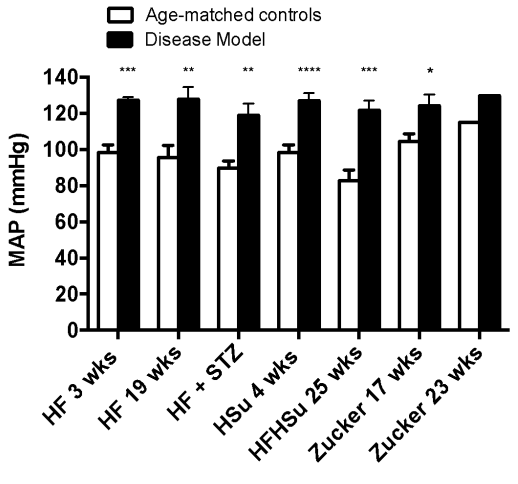


Figure 4 - Mean arterial pressure levels in the distinct models of obesity and type 2 diabetes. All groups of hypercaloric diet animals and its aged-matched controls as well as Zucker diabetic rat and its lean controls of 17 weeks included 6–8 animals per group; Zucker diabetic rat of 23 weeks included 3 animals per group, and its lean control only one animal. Bars represent means \pm SEM; two-way ANOVA with Bonferroni's multiple comparisons test: *p < 0.05, **p < 0.01, ***p < 0.001, and ****p < 0.0001 comparing age-matched controls with disease models.

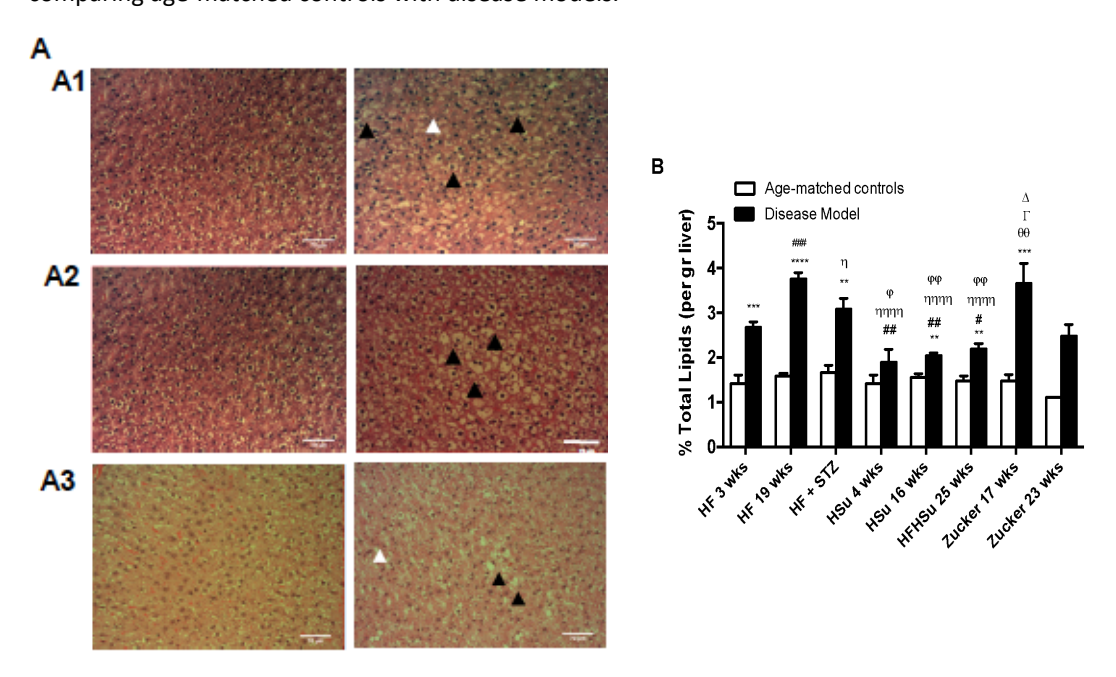


Figure 5 - Lipid deposition in the liver in the distinct models of obesity and type 2 diabetes. (A) Hematoxicilin and eosin images of liver slices from HF 19 weeks (A1), HFHSu 25 weeks (A2), and Zucker 23 weeks (A3) and their respective controls. (B) Percentage of lipid deposition in the liver quantified by the Folch method [26]. All groups of hypercaloric diet animals and its age-matched controls as well as Zucker diabetic rat and its lean controls of 17 weeks included 6–8 animals per group; Zucker diabetic rat

of 23 weeks included 3 animals per group, and its lean control only one animal. Bars represent means \pm SEM; two-way ANOVA with Bonferroni's multiple comparisons test: **p < 0.01, ***p < 0.001, and ****p < 0.0001 comparing age-matched controls with disease models; #p < 0.05, ##p < 0.01, and ###p < 0.001 comparing HF 3 weeks with HF 19 weeks, HSu 4 weeks, and HFHSu 25 weeks; ηp < 0.05 and $\eta \eta \eta \eta p$ < 0.0001 comparing HF 19 weeks with HF+STZ, HSu 4 weeks, and HFHSu 25 weeks; ϕp < 0.05, $\phi \phi p$ < 0.01 comparing HF+STZ with HSu 4 weeks and HFHSu 25 weeks; Δp < 0.05 comparing HSu 4 weeks with Zucker 17 weeks; θp < 0.01 comparing HFHSu 25 weeks with Zucker 17 weeks. Black arrowheads represent lipidosis and white arrowheads fibrosis. Scale bar, 100 µm; original magnification, 20×.

Autonomic Function in Obesity and Type 2 Diabetes

Sympathetic nervous system activation has been pointed out as one of the mechanisms contributing to cardiometabolic dysfunction in obesity and T2D. Herein, we have evaluated sympathetic and parasympathetic nervous activity using different methodologies: Through the evaluation of the SNS and PNS indexes (see Methods section) (Figure 6) and through the measurement of both circulating and adrenal medulla catecholamines (Table 2) in animal models of obesity and T2D studied. We have previously described that 3 weeks of HF diet and 4 weeks of HSu induced an overactivation of the sympathetic nervous system assessed by heart rate variability (Sacramento et al., 2017). Herein we showed that hypercaloric diet disease models tested (HF 19 weeks and HFHSu 25 weeks), but not the genetic model, showed an increased SNS index in comparison to age-matched controls, suggesting an increased sympathetic activation (Figure 6B), without any alteration of the PNS. The absence of SNS activation in Zucker 17 weeks might be explained by the absence of the effect of leptin, a powerful sympathetic activator, in this animal model. In agreement with this increased sympathetic activation, hypercaloric disease models exhibited increased plasma catecholamine levels as well as increased catecholamines in adrenal medulla content when compared to their age-matched controls [Table 2 and Sacramento et al.] (Sacramento et al., 2017).

Table 2 - Catecholamine (epinephrine and norepinephrine) levels in plasma and in adrenal medulla in animal models of obesity and type 2 diabetes.

		Plasma NE + Epi (pmol/mL)	Adrenal Medulla NE+Epi (pmol/mg Tissue)
HF 3 weeks	age-matched control	52.01 ± 6.54	36038.33 ± 2300.22
III 5 WEEKS	disease model	107.45 ± 8.17 ****	50954.94 ± 4604.37 **
UF 40	age-matched control	80.50 ± 13.75	39048.39 ± 3164.09
HF 19 weeks	disease model	161.10 ± 36.80 *	51395.94 ± 2612.16 **
	age-matched control	52.01 ± 6.54	36038.33 ± 2300.22
HSu 4 weeks	disease model	142.48 ± 18.21 ****	57081.27 ± 5877.55 **
IS., 46al.a	age-matched control	130.40 ± 29.74	-
Su 16 weeks	disease model	159.88 ± 51.57	-

Values represent means \pm SEM; one- and two-way ANOVA with Bonferroni's multiple comparisons test: *p < 0.05, **p < 0.01, and ****p < 0.0001 comparing age-matched controls with disease models.

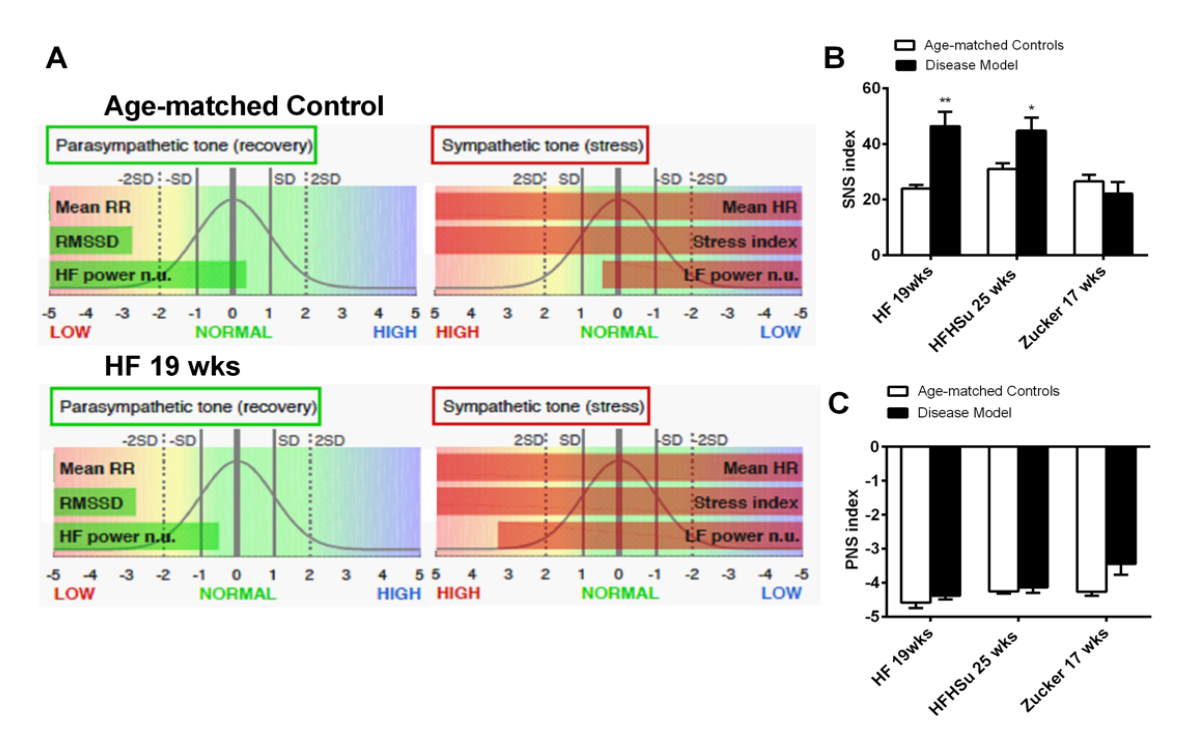


Figure 6 - Effect of hypercaloric diets and genetic deletion of leptin receptors on sympathetic activity evaluated by spectral analysis of the heart rate. (A) shows representative experiments of power spectral density (PSD) calculated in control, in HF 3 weeks, and in HF+ STZ animals. (B) Autonomic function assessed by the ratio between the percentage of low frequencies (LF) that represents the sympathetic component of the autonomic nervous system and the percentage of high frequencies (HF) that represents the

parasympathetic component of the autonomic nervous system. Frequencies are presented in normalized units. All groups of hypercaloric diet animals and their aged-matched controls as well as Zucker diabetic rat and its lean controls of 17 weeks included 6–8 animals per group; Zucker diabetic rat of 23 weeks included 3 animals per group, and its lean control only one animal. Bars represent means \pm SEM; two-way ANOVA with Bonferroni's multiple comparisons test: *p < 0.05 and **p < 0.01 comparing age-matched controls with disease models.

Discussion

In this study, we evaluated the effect of different hypercaloric diets and different exposure times to obesogenic diets as well as the genetic deletion of leptin receptors in terms of the key pathological characteristics of obesity and T2D, with the aim of identifying the most appropriate model(s) for the study dysmetabolism. We observed that all the disease models exhibited: (1) Increased weight gain; (2) increased amount of white adipose tissue, namely, perienteric, perinephric and epididymal depots; (3) deregulation of glucose metabolism, characterized by increased glucose intolerance and fasting glycemia, and also alterations in insulin secretion, sensitivity, and signaling; (4) dyslipidemia characterized by changes on lipid profile; (5) increased deposition of lipids in the liver; (6) hypertension; and finally, (7) alterations in sympathetic nervous system activation (Table 3)

Comparison of the aforementioned disease models identified HF 19 weeks and the Zucker fatty rat (at 17 and 23 weeks) as presenting more alterations related to weight, fat and lipid metabolism, and blood pressure. Zucker 17 and 23 weeks also presented higher alterations in glucose metabolism and insulin secretion. Due to its highly disrupted lipid and glucose metabolism and a fasting glycemia levels above 126 mg/dl, the Zucker diabetic rat exhibits a phenotype that has been chosen by several research groups and pharmaceutical companies as an obesity and T2D model (Davis & O'Donnell, 2013).

Table 3 - Summary of the main pathological features of animal models of dysmetabolism.

	Obesit y	Increased Fasting Glycemia	Insulin Resistance	Glucose Intolerance	Hyperinsulinemi a	Hyper Cholesterolemi a	Hyper Triglyceridem ia	Lipid Deposition in the Liver	Alterations in Insulin Signaling, in White Adipose Tissue	Increased Catecholamine Levels/SNS Activity
HF 3 weeks	X	1	✓	x	✓	X	✓	✓	1	✓
HF 19 weeks	✓	1	✓	1	1	✓	✓	✓	-	1
HF + STZ	✓	1	x	1	x	-	-	✓	-	-
HSu 4 weeks	✓	1	✓	x	X	✓	✓	x	1	1
HSu 16 weeks	X	x	✓	x	x	X	✓	-	1	-
HFHSu 25 weeks	X	1	1	1	√	x	✓	✓	-	1
Zucker 17 weeks	1	1	✓	1	1	✓	✓	1	-	-
Zucker 23 weeks	1	1	1	1	√	-	-	✓	-	-

It is also notable that this genetic animal model of obesity and T2D is used as a sleep apnea model (Davis & O'Donnell, 2013). It is our view that the widespread use of this model should be questioned, given that: (1) The Zucker diabetic rat lacks functional leptin receptors (fa/fa genotype), because leptin receptor deficiency is infrequently seen in obese and T2D humans since leptin receptor mutations are relatively rare (Farooqi et al., 2007); (2) we have shown here that Zucker diabetic rats do not exhibit an overactivation of the sympathetic nervous system, probably due to the absence of leptin receptors, which is generally accepted to be a principle driver of obesity and metabolic-related illness (E. A. Lambert et al., 2015; G. W. Lambert et al., 2010; Thorp & Schlaich, 2015). In short, this animal model does not reflect the phenotype and the pathophysiological mechanisms behind the metabolic dysfunction widely presented in humans.

In the last few years, an alternative path to the induction of obesity and/or T2D in animal models has been through dietary manipulation. However, in this respect, there is no consensus about the most appropriate diet (HF, HSu, HFHSu, HF plus low sucrose, low fat plus HSu, among others) and time of exposure to it. Herein, we showed that when compared to all other models studied, rats exposed to an HF diet for 19 weeks presented a phenotype most consistent with the human condition, inclusive of alterations in weight, fat amount, lipid metabolism, in insulin sensitivity and glucose tolerance, elevated sympathetic activity and blood pressure, and lipid deposition in the liver (Figures 1–6). The only alterations that were more pronounced in another model (HFHSu 25 weeks) were insulin levels and C-peptide levels (Figure 2D), which are associated with endogenous pancreatic insulin secretion, suggesting that the "sugar" component of this diet likely has a higher impact on the pancreatic secretion of insulin. This is in agreement with the data observed in minipigs, where the long-term high fat-high sugar diet increased the expression levels of caspase-3, Bax, and insulin and decreased the expression levels of proliferating cell nuclear antigen and Bcl-2, indicating increased βcell apoptosis (Zhao et al., 2015).

That the HF19 weeks model is the model that exhibits more phenotypic characteristics similar to humans is in agreement with other studies, which have shown that the long-

term administration of diets containing 40% to 60% of lipids promotes metabolic disorders and induces insulin resistance, arterial hypertension, and obesity in animal models and humans (Flanagan et al., 2008), T2D and hypertriglyceridemia (Fraulob et al., 2010), among others. In addition, we showed that with this HF 19 weeks rat model, it is possible to obtain the typical comorbidities of type 2 diabetes (Figures 4 and 5), such as hypertension and increased lipid deposition typical of NAFLD (Sah et al., 2016). In fact, although almost all hypercaloric regimens were able to induce a similar degree of hypertension, the HF19 weeks model was one of the animal models that presented with a high percentage of lipid deposition in the liver similar to the Zucker fatty animal. However, since the Zucker diabetic fatty rats lack the overactivity of the sympathetic nervous system, we propose that the HF 19 weeks represents more closely the human condition.

Another common T2D model frequently used is the chemical induction with low doses of STZ together with dietary manipulation, which aims to achieve a high fasting glycemia due to the mild impairment of insulin secretion (Reed et al., 2000; Zhang et al., 2008). We showed that the HF+STZ group exhibits several metabolic characteristics of human obesity and T2D, such as increased weight gain, glucose intolerance, increased fasting glycemia, and hypertension (Figures 1, 2, and 4). However, we demonstrated for the first time that this model failed to develop insulin resistance, in agreement with the observed lack of hyperinsulinemia (Figure 2D), which is now known to be a major cause of this pathological feature. For many years, insulin resistance was considered the cause of hyperinsulinemia. However, it is now generally accepted that hyperinsulinemia can itself trigger insulin resistance, leading to a vicious cycle of hyperinsulinemia-insulin resistance (for a review, see (Shanik et al., 2008)). In fact, several animal and human studies have supported the view that increased insulin levels, even in the presence of normal weight, induce insulin resistance, by producing insulin receptor desensitization (Gavin et al., 1974; Marchand et al., 1977; Rizza et al., 1985). Further, it was recently found in rat hepatoma cells that persistent high insulin levels are associated with a persistent alteration at the insulin receptor tyrosine kinase domain, which may act to initiate or progressively worsen insulin resistance (Catalano et al., 2014). Therefore, our

data are in agreement with the fact that hyperinsulinemia can cause insulin resistance, given that the HF+STZ model studied here lacks increased insulin secretion (Figure 2D) and does not exhibit insulin resistance, despite the fact that other dysmetabolic features are present.

Chapter I	IV

This chapter is based on the following manuscript:

Carotid body and adipose tissue in obesity and type 2 diabetes: an intricate

link involving browning and sympathetic integration modulation

Bernardete F. Melo, Joana F. Sacramento, Cláudia S. Prego, Julien Lavergne, Daniela

Rosendo-Silva, Aidan Falvey, Paulo Matafome, Fátima O. Martins, Miguel C. Correia,

Elena Olea, Phillipe Blancou, Silvia V. Conde (in preparation for submission)

Abstract

Obesity is a major public health concern, with increased morbidity and mortality however the therapeutic options to treat this epidemic are usually unsuccessful and therefore there is an urgent need for novel approaches that would help to find more effective therapeutic interventions for obesity.

Currently, the carotid bodies (CBs) are considered metabolic sensors, being consensual that these organs control sympathetic activity. Moreover, the overactivation of these organs, via an increase in the whole-body sympathetic nervous system, have been shown in several metabolic diseases that are strongly associated with obesity. Furthermore, it was described that the resection of carotid sinus nerve (CSN) prevented weight gain and improved glucose homeostasis by positively impacting insulin signaling and glucose uptake in the liver and adipose tissue. Herein we tested if the CBs are key players in the neural sympathetic circuit controlling white and brown adipose tissues metabolism and if the abolishment of its activity will have an anti-obesity effect. To test this hypothesis, we resected CSN in control and obese animals, achieved by submitting Wistar rats and C57/BL6 mice to 60% lipid-rich diet during 10 and 12 weeks. We found that CSN resection decreased weight gain, adipose tissue deposition and adipocytes perimeter, as well as reversed metabolic dysfunction. Also, it restored basal visceral WAT metabolism, mitochondrial activity, UCP1 expression, glucose uptake, the expression of PGC1 alpha and PPAR gamma and AMPK phosphorylation. In addition, CSN resection did not modify basal activity of BAT but increased its thermogenic activity, in response to norepinephrine, increasing also the mitochondrial activity, UCP1 expression, glucose uptake and AMPK phosphorylation. No alterations were observed in the expression of IL-6 or IL-1 β receptors in the adipose tissue either in circulating TNF α levels or IL-10 (anti-inflammatory marker) levels. Also, CSN resection did not impact HIF1α or HIF2α expression. Moreover CSN resection restored catecholaminergic signaling and integration in the WAT of HF animals, shown by the restoration of the decreased levels of catecholamines within the WAT and decreased intensity of TH expression by light-sheet microscopy and western blot induced by HF diet.

Therefore, we can conclude that the CB plays an important role in development of obesity and in the control of adipose tissue metabolism being a new player in the neurocircuitry sympathetic nervous system-adipose tissue connection, introducing a new therapeutic target for obesity management.

Introduction

Obesity, the epidemic of XXI century, is a major public health concern. According to the World Health Organization, one third of worldwide population is overweight or obese (*World Health Organization - Obesity and overweight*, 2021). Moreover, these conditions contribute significantly to morbidity and mortality due to the associated comorbidities, which are estimated to be responsible for 1 in 5 deaths in the world today (Jarolimova et al., 2013). Obesity comorbidities include cardiovascular disease (CVD), type 2 diabetes (T2D), hypertension (HT), obstructive sleep apnea (OSA) and some cancers. However, with the pandemic of COVID-19 the morbidity and the number of comorbidities will rise since obesity increases the risk of severe illness from this viral infection and may triple the risk of hospitalization, even in young adults (Yang et al., 2020)

Obesity management has been a challenge because the therapeutics available are often inadequate and require significant efforts in lifestyle modifications, which can be difficult to implement and, most of the times, only transiently successful. Thus, there is a compelling need for the discovery of novel mechanistic approaches that could lead to more effective and personalized therapeutic interventions for obesity.

Carotid bodies (CB) are peripheral chemoreceptors that respond to hypoxia by increasing chemosensory activity in the carotid sinus nerve (CSN), causing hyperventilation and activation of the sympathoadrenal system (Ribeiro et al., 2013). Currently CBs are also considered metabolic sensors implicated in the regulation of peripheral insulin sensitivity, glucose homeostasis and lipid metabolism: 1) CB chemosensory activity is increased in prediabetes and type 2 diabetes animal models and overweight prediabetes patients (Cunha-Guimaraes et al., 2020; Ribeiro et al., 2013); 2) abolishment of CB activity via resection or electrical modulation of the CSN

prevented and reversed the metabolic alterations induced by the hypercaloric diet in rats (Sacramento et al., 2017); 3) hyperbaric oxygen therapy, used to treat diabetic foot and that dramatically reduces CB activity (Lahiri & DeLaney, 1975), improves glucose homeostasis in T2D patients (Vera-Cruz et al., 2015). Moreover we showed that the restoration of metabolism induced by CSN-resection in hypercaloric animal models involves the improvement of insulin signaling and glucose uptake in the liver and adipose tissue being associated also with a decrease in fat deposition and weight gain induced by the diet. Therefore, our animal and human data strongly support a role for the CB in the control of adipose tissue metabolism and in the development of obesity, suggesting that the modulation of CB activity can be a therapeutic strategy to handle overweight and obesity.

Additionally, it is consensual that CB controls sympathetic activity (Marshall, 1994; McBryde et al., 2013; Pijacka et al., 2016) and its overactivation has been experimentally shown to be in the basis of metabolic deregulation via an increase in whole-body sympathetic nervous system (Conde et al., 2014, 2017; Ribeiro et al., 2013; Sacramento et al., 2017). On the other hand adipose tissue sympathetic innervation is responsible for the modulation of lipolysis and/or thermogenesis via norepinephrine (NE) (Bartness et al., 2014) and dopamine release (Larabee et al., 2020). Therefore, in the search of the mechanistic pathways involved on CB modulation of obesity-related dysfunctions the circuit CB-adipose tissue-sympathetic nervous system surges with high relevance. In agreement, activation of CB chemoreceptors inhibits the elevated levels of BAT sympathetic nerve activity evoked by hypothermia (Madden and Morrison 2005). Herein, we tested the innovative hypothesis that CB is a key player in neural sympathetic circuits controlling the white and brown adipose tissue metabolism. We also predict that CB/CSN blockade will have an anti-obesity effect that is associated with increased function of the adipose tissues and the recovery of sympathetic integration. To address this, we have abolished CB activity by chronically resecting CSN in control and obese animals, and used a plentitude of biochemical and immunohistochemical techniques to study the adipose tissue metabolism and its sympathetic activation. We demonstrated that the CB is a key intervenient in the neurocircuitry sympathetic nervous systemadipose tissue connection, which therefore introduces a completely new therapeutic approach for obesity management.

Methods

Diets and Animal Care

Experiments were performed in 8–9-weeks-old male Wistar rats (200–300 g) obtained from the animal house of NOVA Medical School, Faculty of Medical Sciences, New University of Lisbon, Lisbon, Portugal and 4 week-old male C75BL/6 J mice purchased from Charles River (Massachusetts, EUA). After randomization, the animals were assigned to the HF group, fed with 60% fat diet (61.6% fat + 20.3% carbohydrate + 19.1% protein; Test Diets, Missouri, USA) for 10 weeks (Wistar rats) or 12 weeks (C75BL/6 J mice); or to an aged-matched control group fed with a standard diet (7.4% lipid and 75% carbohydrates, of which 4% were sugars and 17% protein). After 10 and 12 weeks of diet, respectively, both HF and control groups were randomly divided and half of the group was submitted to carotid sinus nerve (CSN) resection and the other half submitted to sham procedure.

For the CSN resection procedure the carotid artery bifurcations, located bilaterally, and the CSN were identified and sectioned bilaterally or left intact (sham groups). These procedures were performed in aseptic conditions under either ketamine [75mg/kg body weight (i.p.), Nimatek, Dechra, Northwich, UK]/medetomidin [0.5mg/kg body weight (i.p.), Sedator®, Dechra, Northwich, UK), for Wistar rats, and Isoflurane (Piramal, CSP, France) mixed with air at 2.5%, for C75BL/6 J mice. Before CSN resection the animals were injected intraperitoneally with carprofen [5mg/kg/ml (sc), Rymadil ™, Pfizer, New York, USA) and saline.

After CSN resection, the groups were maintained in the diets for 9 weeks or 3 weeks, for rats and mice respectively, and at a terminal experiment, animals Wistar rats were anesthetized with sodium pentobarbitone (60 mg/kg, i.p), and catheters were placed in the femoral artery for arterial blood pressure measurement. In both species, blood was collected by heart puncture for serum and plasma quantification of mediators (such as

insulin and c-peptide levels and inflammatory markers) and the adipose tissue pads (visceral, perinephric, epididymal, subcutaneous depots and interscapular brown adipose tissue depot) were then rapidly collected, weighted, and stored at either –80 °C or transferred to 4% PFA or collected and maintained in Tyrode medium (140 mM NaCl, 5 mM KCl, 2 mM CaCl2, 1.1 mM MgCl2, 10 mM Hepes and 5.5 mM glucose; pH 7.4) for O₂ consumption rate analysis.

During all the experimental period animals were kept under temperature and humidity control (21 ± 1 °C; $55 \pm 10\%$ humidity) with a 12 h light/12 h dark cycle and were given ad libitum access to food and water, except in the night prior to insulin sensitivity and glucose tolerance evaluation. Body weight was monitored weekly, and energy and liquid intake were monitored daily. Insulin sensitivity and glucose tolerance were also evaluated over the experimental period and CSN resection was confirmed by the abolishment of responses to hypoxia, through pletismographic analysis.

Laboratory care was in accordance with the European Union Directive for Protection of Vertebrates Used for Experimental and Other Scientific Ends (2010/63/EU). Experimental protocols were approved by the NOVA Medical School/Faculdade de Ciências Médicas Ethics Committee (nº08/2015/CEFCM and 41/2021/CEFCM), by Portuguese Direção-Geral de Alimentação e Veterinária (DGAV) and by the National Ethical Committee of France (CIEPAL #2018082016528754).

Insulin sensitivity evaluation

Insulin sensitivity was evaluated using an insulin tolerance test (ITT) after overnight fasting (Wistar rats) or 5 hours fasting (C75BL/6 J mice) as previously described (Sacramento et al., 2018). Fasting blood glucose was measured and immediately followed by an insulin bolus (100 mU/kg for Wistar rats or 0.5U/Kg for C75BL/6 J mice), administered via the tail vein, for Wistar rats or intraperitoneally, for C75BL/6 J mice. Subsequently, the decline in plasma glucose concentration was measured over a 15 min period with 1 min interval in the rats or at minutes 5, 10, 20, 30, 45, 60, 90 e 120, after insulin administration, in the mice, after insulin administration. Blood was collected via

tail tipping and glucose levels were measured with a glucometer (Precision Xtra Meter, Abbott Diabetes Care, Portugal) and test strips (Abbott Diabetes Care, Portugal). The constant rate for plasma glucose decline ($K_{\rm ITT}$) was calculated by the formula $0.693/t_{1/2}$. Glucose half-time ($t_{1/2}$) was calculated from the slope of the least square analysis of plasma glucose concentrations during the linear decay phase.

Glucose Tolerance evaluation

Glucose tolerance was evaluated using oral glucose tolerance test (OGTT) after overnight fasting as described (Sacramento et al., 2018). Briefly, fasting blood glucose was measured and immediately followed by administration of a saline solution of glucose (2 g/kg or 1.5g/kg, for rats or mice, respectively; VWR Chemicals, Leuven, Belgium), by gavage. Blood samples were collected by tail tipping before (0 min) and 15, 30, 60, 120, 180 minutes after glucose administration. The product of the area under the curve (AUC) was used to estimate the glucose tolerance.

Evaluation of Autonomic Nervous System

The balance between the sympathetic and parasympathetic components of the autonomic nervous system was made by calculating the sympathetic nervous system (SNS) and parasympathetic nervous system (PNS) indexes computed in Kubios HRV software (www.kubios.com). The SNS index in Kubios is based on Mean heart rate, Baevsky's stress index, and low frequency power expressed in normalized units and the PNS index which is based on the mean intervals between successive heartbeats (RR intervals), the root mean square of successive RR interval differences (RMSSD) and high frequency power expressed in normalized units. Heart rate and RR intervals were obtained using lox 2.9.5.73 software (Emka Technologies, Paris, France), with an acquisition frequency of 500 Hz.

Quantification of Biomarkers: plasma insulin, c-Peptide, lipid profile, inflammatory markers and catecholamines

Insulin and C-peptide concentrations were determined with an enzyme-linked immunosorbent assay kit (Mercodia Ultrasensitive Rat Insulin ELISA Kit and Mercodia

Rat C-peptide ELISA Kit, respectively, Mercodia AB, Uppsala, Sweden). Catecholamines were measured in plasma and in homogenized perienteric adipose tissue samples by HPLC with electrochemical detection as previously described (González-Martín et al., 2009), while the plasma IL-10 and TNF α levels were evaluated using the chemiluminescence-based assay kit V-PLEX Proinflammatory Panel 1 Mouse Kit (Meso, Maryland, USA).

The lipid profile was assessed using a RANDOX kit (RANDOX, Irlandox, Porto, Portugal) to determine total cholesterol and triglycerides by Trinder-based colorimetric end-point assays, and high-density lipoprotein (HDL) and low-density lipoprotein (LDL) by a direct-HDL and direct-LDL clearance method, respectively.

Western Blot Analysis

Visceral adipose tissue (WAT) depot (100 mg) or BAT (75 mg) were homogenized in Zurich (10 mM Tris-HCl, 1 mM EDTA, 150 mM NaCl, 1% Triton X-100, 1% sodium cholate, 1% SDS) with a cocktail of protease inhibitors (trypsin, pepstatin, leupeptin, aprotinin, sodium orthovanadate, phenylmethylsulfonyl fluoride (PMSF)), and samples were centrifuged (Eppendorf, Madrid, Spain) and supernatant was collected and frozen at – 80 °C until further use.

Samples of the homogenates and the prestained molecular weight markers (Precision, BioRad, Madrid, Spain) were separated by sodium dodecyl sulfate polyacrylamide gel electrophoresis (10% with a 5% concentrating gel) under reducing conditions and electrotransferred to polyvinylidene difluoride membranes (0.45 μ M, Millipore, Spain). After blocking for 1 h at room temperature with 5% nonfat milk in Tris-buffered saline, pH 7.4 containing 0.1% Tween 20 (TTBS) (BioRad, Spain), the membranes were incubated overnight at 4 °C with the primary antibodies against PGC-1 α (1:1000; 92kDa; Santa Cruz Biotechnology INC, Texas, EUA), PPAR γ (1:1000; 53-57kDa, Cell Signaling Technology, Massachusetts, EUA), phospho-AMPK α (Thr172) (1:1000; 60kDa; Cell Signaling Technology, Massachusetts, EUA), TH (1:1000; 60kDa; Abcam, Cambridge, Reino Unido), IL-1 β RI (1:500; 80kDa; Santa Cruz Biotechnology INC, Texas, EUA), HIF1a (1:500; 120kDa;

SICGEN, Cantanhede, Portugal), HIF2 α (1:500; 100kDa; Abcam, Cambridge, Reino Unido). The membranes were washed with Tris-buffered saline with Tween (TBST) (0.1%) and incubated with rabbit anti-goat (1:5000; Thermofisher Scientific, Massachusetts, EUA), goat anti-mouse (1:5000; Bio-Rad Laboratories, Califórnia, EUA) or goat anti-rabbit (1:5000; Bio-Rad Laboratories, Califórnia, EUA) in TBS and developed with enhanced chemiluminescence reagents (ClarityTM Western ECL substrate, Hercules, CA, USA). Intensity of the signals was detected in a Chemidoc Molecular Imager (Chemidoc; BioRad, Madrid, Spain) and quantified using Image Lab software (BioRad). The membranes were re-probed and tested for Calnexin (1:1000, SICGEN, Cantanhede, Portugal) immunoreactivity (bands in the 90 kDa region) to compare and normalize the expression of proteins with the amount of protein loaded.

Histological and immunohistochemical evaluation

WAT and BAT depot were collected, dissected and immersion-fixed in PFA 4%. Samples were then embedded into paraffin (Sakura Finetek Europe B.V., Zoeterwoude, Netherlands) and longitudinal serial sections of 8 or 10µm thick were obtained with a Microtome Microm HM200 (MICROM Laborgeräte GmbH, ZEISS Group, Walldorf, Germany).

Evaluation of adipocytes perimeter in WAT and BAT depots

After sectioning, the samples were transferred into slides and stained with hematoxylin and eosin, for staining of the nuclei, extracellular matrix and cytoplasm. Representative photographs were acquired using NDP.view2 software (Hamamatsu, Japan) in slides digitally scanned in the Hamamatsu NanoZoomerSQ (Hamamatsu, Japan). Adipocytes perimeter was visualized with software Fiji app for Image J (https://imagej.nih.gov/ij/).

Evaluation of UCP1 protein and mitochondrial density in WAT and BAT depots

After sectioning, the samples were transferred into slides. Immunohistochemistry was performed on multiple slides from the collected samples from several different animals. Paraffin sections were deparaffinized and rehydrated followed by antigen retrieval and blocking, performed with a 5% bovine serum albumin solution for 60min. Sections were

then incubated with primary antibody rabbit anti-UCP1 (1:1000 for WAT and BAT; Santa Cruz Biotechnology INC, Texas, EUA) and MitotrackerTM Red CMXRos [15nM] for WAT and [1nM] for BAT (Termofisher Scientific, Massachusetts, EUA), overnight at 4°C. Next, sections were incubated with anti-rabbit secondary antibody Alexa 488 (1:4000 for WAT and 1:6000 for BAT; Termofisher Scientific, Massachusetts, EUA)) and DAPI (1ug/ml; Santa Cruz Biotechnology INC, Texas, EUA) for 90min. Finally, sections slides were mounted with Dako mounting medium (Agilent, Califórnia, EUA), visualized at the widefield Z2 Zeiss Microscope (ZEISS Group, Walldorf, Germany) and analyzed with software Fiji app for Image J (https://imagej.nih.gov/ij/) to count the number of UCP1 and Mitotracker Red CMXRos -immunoreactive cells.

Evaluation of oxygen consumption

Three weeks after the CSN resection, mice were sacrificed by cervical dislocation and brown adipose tissue and brown adipose tissue were collected for the evaluation of oxygen consumption rate (OCR) by using the Seahorse XF24 (Seahorse Bioscience, North Billerica, MA). Tissue samples were placed in an XF24 Islet Capture Microplate (Seahorse Bioscience, North Billerica, MA) and once in position, were rinsed twice with Seahorse XF DMEM assay media (Seahorse Bioscience, North Billerica, MA) supplemented with 10mM glucose, 1mM pyruvate and 2mM L-glutamine. Finally, 575µl of assay media was added to all the samples and control wells. Before the measurement of the OCR, the microplate was incubated at 37°C without CO2 for 45 min. Each OCR measurement consisted of 3min of mixing, 2min of wait time and 3 min of continuous measuring of O2 levels. To evaluate adrenergic stimulation, OCR was measured after norepinephrine [15µM] or dopamine [100nM] application. OCR was calculated by plotting the O2 tension of the media as a function of time (pmol/min).

In vivo tissue-specific glucose uptake evaluation

An intravenous glucose tolerance test (IVGTT) was performed in sham versus CSN - transected control and HF animals. For that, the animals were fasted overnight and a bolus of 2-deoxy-D-[1,2-3H]-glucose (1mC/ml; specific activity: 20Ci/mmol; PerkinElmer, Madrid, Spain) mixed with glucose (100µCi/kg body weight; 0.5g/kg body weight) was

administered in the tail vein. Blood samples were taken from the tail vein at regular intervals (0, 2, 5, 10, 15, 30 and 60 minutes).

To determine glucose-specific activity, 20µl plasma was deproteinized with 200µl ice-cold perchloric acid (0.4N), centrifuged and radioactivity was measured in a scintillation counter (Tri-Carb 2800TR, Perkin-Elmer, Madrid, Spain). At 60 minutes, animals were euthanized and the tissues (white and brown adipose tissue depots) were rapidly excised. 2-deoxy-D-[3H]glucose incorporation was investigated in 50-200mg tissue homogenized in 1ml ice cold perchloric acid (0.4 N) (Sacramento et al., 2017). The samples were centrifuged and the radioactivity in the supernatant was measured in a scintillation counter.

Light-sheet based fluorescent microscopy

After perfusion, the excised brown or white adipose tissues were washed with PBS and clarified using the iDisco+ method (https://idisco.info/). Briefly, samples were dehydrated at room temperature in successive washes of 20% Metanol (MetOH) for 1h, 40% MetOH for 1h, 60% MetOH for 1h, 80% MetOH for 1h, 100% MetOH for 1h and 100% MetOH overnight. After, the samples were incubated in a solution of 33% MetOH and 66% Di-ChloroMethan (DCM, Sigma) overnight and washed twice with 100% methanol for 1h. Samples were then bleached in chilled fresh 5% H₂O₂ in methanol overnight, at 4°C, before being rehydrate with methanol/H₂O series (80%, 60%, 40%, 20% and PBS, 1 h each at room temperature). Samples were them immunolabeled for 24 h with anti-TH (AB152, Merck) after overnight permeabilization at 37°C and overnight blocking with 1,7% TritonX- 100, 6% donkey serum and 10% DMSO in PBS. After 3 washes in PBS/ 0.2%Tween-20, samples were incubated with the secondary antibody donkey anti-goat (Jackson Immunoresearch) for 24h. Samples were then dehydrated at room temperature in successive baths of 20% MetOH for 1h, 40% MetOH for 1h, 60% MetOH for 1h, 80% MetOH for 1h, 100% MetOH for 1h and 100% MetOH overnight, and then incubated in a solution of 33% MetOH and 66% Di-ChloroMethan (DCM, Sigma) for 3h at RT, then in 100% DCM twice for 15 min twice and transferred overnight into the clearing medium 100% DiBenzylEther 98% (DBE, Sigma).

Imaging was performed using a home-made light-sheet ultramacroscope. The specimen was placed into a cubic cuvette filled with DBE placed on the Z-stage of the bench. It was illuminated with planar sheets of light, formed by cylinder lenses. The light coming from a multi-wavelength (561 nm) laser bench (LBX-4C, Oxxius) was coupled via two single mode optical fibers into the setup, allowing illumination from one or two sides. Two-sided illumination was used. The specimen was imaged from above with a MVX10 macroscope, through a PlanApo 2X/0.5 NA objective (Olympus) with an additional zoom of the macroscope of 1.6, which was oriented perpendicular to the 561nm light sheet. Images were captured using a sCMOS Camera (Orca-Flash4.0) synchronized with the z-stage moving the sample through the light sheet. The ultramicroscope is managed by Micro-manager software and z-stacks of images were taken every 2 µm. The images stacks were fused using the alpha-blending method with a home-made ImageJ macro (Rasband, W.S., ImageJ, U. S. National Institutes of Health, Bethesda, Maryland, USA, http://imagej.nih.gov/ij/, 1997e2012).

Statistical Analysis

Data were evaluated using GraphPad Prism Software, version 6 (GraphPad Software Inc., San Diego, CA, USA) and presented as mean values with SEM. The significance of the differences between the mean values was calculated by one- and two-way ANOVA with Bonferroni multiple comparison test. Differences were considered significant at p < 0.05.

Results

CSN resection decreases weight gain and adipose tissue deposition in obese rodents

Submitting rodents to hypercaloric diets promotes alterations on body weight, SNS activity, blood pressure and glucose metabolism, that are very similar with the human condition (Landsberg & Young, 1978). Therefore, in order to investigate the effects of the abolishment of CB activity on weight gain and body fat mass, we used a diet-induced obesity model, by submitting Wistar rats and C75BL/6 J mice to 10 and 12 weeks, respectively, of a lipid-rich diet. Both rats and mice submitted to this hypercaloric diet exhibit a higher growth curve (Fig. 1A left and right panels, respectively) and increased weight gain (Fig. 1B) and total fat amount (Fig. 1C) than the control animals, fed with a standard diet. The increase in fat amount was accompanied by an increase in all the WAT depots studied (Fig. 1D). Furthermore, and as previously demonstrated, HF diet promoted a dysmetabolic state, characterized by insulin resistance, glucose intolerance, dyslipidemia, hyperinsulinemia and increased c-peptide levels (Table 1). Additionally, and confirming previous data by Ribeiro et al. (2013), obese rats showed increased respiratory responses to hypoxia (Fig. 2) without alterations in the responses to hypercapnia. To evaluate the link role of CB in the development of obesity, we abolished CB activity, through CSN resection. The resection of CSN was confirmed by the abolishment of responses to hypoxia (Fig. 2). We found that bilateral CSN chronic resection decreased weight gain in the HF animals of both species (Fig. 1A-B). This effect was clearer when the weight corresponding to the growing period of the animals and the week after the surgery was excluded (Fig. 1B). CSN resection decreased weight gain in both normal chow and HF diet animals. Note that rats and mice submitted to HF diet and to CSN resection decreased by 31% and 39% weight gain, in comparison with HF sham animals (Fig. 1B), respectively.

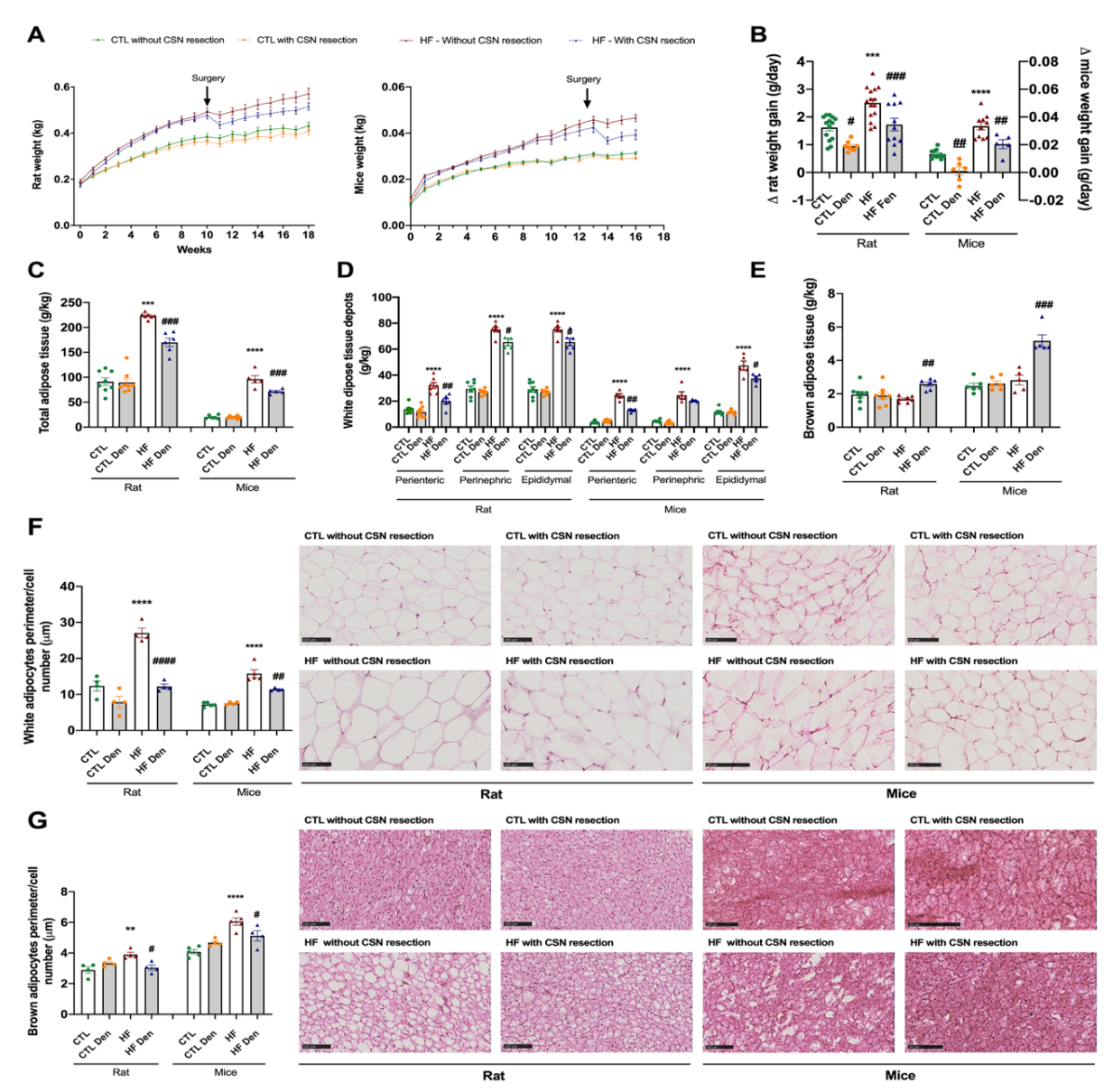


Figure 1- Carotid sinus nerve (CSN) resection decreases weight gain and adipose tissue deposition in obese rodents. Effect of high fat (HF) diet and of CSN resection on: A) growth curves of Wistar rats (n=9-15, corresponding to two cohorts of animals that were used for different sets of experiments) (left panel) and C75BL/6 J mice (n=5-11) (right panel); B) average weight gain (g/day) in rats and mice; C) total white adipose tissue (WAT) weight (g/kg) (n=5-8); D) white adipose tissue (WAT) depots weight (g/kg) in rats and mice (n=5-8); E) brown adipose tissue (BAT) weight (g/kg) (n=5-8); F) visceral WAT adipocytes perimeter per cell number (μ m) – left panel shows average adipocytes perimeter, right panel shows representative H&E histological images of visceral fat in rat and mice (n=4-5); G) Brown adipocytes perimeter per cell number (μ m) in the BAT depot in rats and mice (n=4-5) - left panel shows average

adipocytes perimeter, Right panel representative H&E histological images of BAT in rat and mice (n=4-5). Bars represent mean values ± SEM. Two-Way ANOVA with Bonferroni multicomparison test. **p<0.01,

This decrease in weight gain in HF animals was accompanied by a decrease in the total amount of fat (24% for both species) (Fig. 1C) and by a decrease in all WAT depots, namely 38% in perienteric depot for rats and 40% for mice, 13% in perinephric depot for both species, 13% in epididymal depot for rats and 21% for mice (Fig. 1D). As expected, and previously described, CSN resection also reverses dysmetabolism, with an improvement of glucose tolerance and a reversion of insulin resistance, hyperinsulinemia and dyslipidemia (Table 1).

Α

Basal Respiratory Frequecy (bpm)		Before Surgery	1 week after surgery	3 weeks after surgery	5 weeks after surgery	7 weeks after surgery	9 weeks after surgery
CTL	Sham	69.80±10.11	71.22±15.51	75.87±10.97	66.10±9.21	72.46±16.88	72.09±9.40
CIL	Denervated	76.27±12.57	82.10±20.62	70.26±7.52	73.59±9.21	75.64±11.96	74.59±12.26
HF	Sham	76.18±13.06	71.96±12.60	83.45±14.59	80.96±15.12	79.84±7.58	80.08±12.66
nr	Denervated	88.44±14.38	70.05±20.55	76.45±11.60	81.12±16.55	81.35±14.42	87.37±13.74
Basal Tidal Volume (ml/kg)							
CTL	Sham	4.48±0.72	4.84±1.47	4.61±0.99	5.00±0.84	4.50±1.80	4.59±0.55
CIL	Denervated	4.50±1.79	4.83±0.89	5.00±0.51	5.04±1.49	5.37±0.97	4.76±2.53
HF	Sham	4.04±0.68	4.08±1.60	4.38±1.93	4.21±0.68	3.93±1.40	3.76±0.95
nr	Denervated	4.13±1.73	4.14±1.17	3.86±0.77	4.22±1.54	3.38±1.06	3.44±0.86
Basal Minute Volume (ml/minute*kg)							
CTL	Sham	312.08±65.15	335.91±94.54	347.34±75.29	327.46±65.46	338.31±180.02	331.48±60.94
CIL	Denervated	348.48±166.12	392.86±102.14	352.85±63.41	377.13±139.85	403.19±81.65	341.77±161.19
HF	Sham	307.98±58.10	284.67±120.06	373.59±195.27	321.87±51.92	314.83±121.67	303.69±111.11
ПF	Denervated	381.58±235.07	294.99±118.56	299.33±91.63	343.12±136.18	280.96±123.44	300.99±89.09

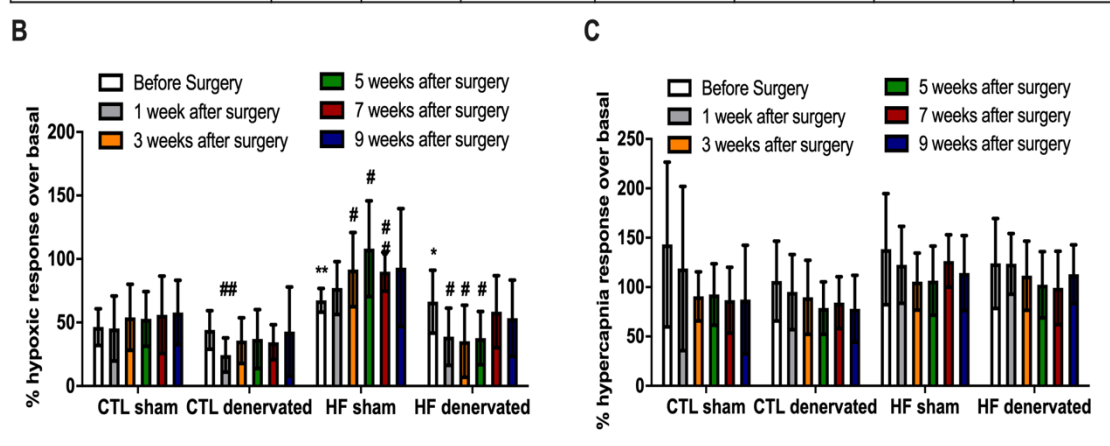


Figure 2 – Carotid Sinus Nerve (CSN) resection decreases respiratory responses to hypoxia: A) basal respiratory parameters, namely respiratory frequency, tidal volume and minute ventilation (n=9-15, corresponding to two cohorts of animals used for different set of experiments); values represent mean \pm SEM. B) respiratory responses to hypoxia; bars represent means \pm SEM (n=9-15); Two-Way ANOVA with Bonferroni multicomparison test. *p<0.05, comparing CTL -normal chow - and HF animals without CSN resection; *p<0.05 comparing groups before and after CSN resection. C) respiratory responses to hypercapnia; bars represent means \pm SEM (n=9-15).

Coincident with the increase in total WAT amount and depots, both rats and mice presented increased adipocytes perimeter in their perienteric adipose tissue (Fig. 1F) and CSN resection was able to decrease it by 55% and 28%, for rats and mice respectively.

 Table 1 - Effect of CSN resection on metabolism and lipid profile on obese rats and mice

Wistar Rats							
Caloric intake (Kcal/day/kg)		Before diet	Before surgery	9 weeks after surgery			
Normal chow	Sham	-	197.63±27.37	218.77±74.00			
Normal Chow	Denervated	-	215.15±20.21	217.22±56.31			
HF	Sham	-	280.08±98.69*	301.63±51.54*			
	Denervated	-	274.63±85.21*	248.45±60.37			
Glycemia (mg/dl)							
Normal chow	Sham	95.22±15.80	75.11±10.43	82.90±10.80			
	Denervated	85.66±11.31	84.44±13.13	85.22±11.12			
HF	Sham	78.22±9.47	95.11±15.19*	92.90±6.60 ^{§§}			
	Denervated	81.56±6.35	98.78±12.31**	81.5±6.02##			
Kitt (%glucose/min)							
Normal chow	Sham	4.43±0,72	4.24±0.73	4.78±0.89			
	Denervated	5.03±0.98	4.50±0.75	4.85±0.87			
HF	Sham	4.1±0.62	1.76±0.99***,####	1.84±0.65 ^{555,####}			
	Denervated	4.7±1.05	1.92±1.13***	4.24±0.60###			
AUC OGTT (mg/dl*min)							
Normal chow	Sham	20747.55±2077.68	18439.55±2430.23	19966.89±1347.82			
	Denervated	19286±1496.96	18160.22±2311.44	20813.45±1986.42			
HF	Sham	21028.67±2277.72	25359.45±2476.79***,##	24504.63±1004.12 ^{§§}			
	Denervated	20116.11±2240.22	25415.33±2067.99***,####	23264.29±1147.66#			
Insulin (pmol/l)							
Normal chow	Sham	5.24±3.80	170.39±26.02	240.55±45.26			
	Denervated	19.43±5.83	146.68±43.65	227.78±48.54			
HF	Sham	22.98±10.74	415.58±93.50****,####	584.21±121.57 ^{§§§§} ,##			
	Denervated	25.87±4.39	506.94±55.07****,####	420.92±53.13 ^{§§§§,#}			

C-peptide (nmol/l)				
Normal chow	Sham	0.90±0.09	0.68±0.16	0.59±0.16
rtermarene w	Denervated	0.58±0.16	0.72±0.14	0.78±0.17
HF	Sham	0.45±0.22	1.23±0.12****,####	1.75±0.29 ^{§§§§} ,###
	Denervated	0.37±0.08	1.58±0.17****,####	1.45±0.26
			9 weeks afte	r surgery
Cholesterol (mg/dl)			Sham	Denervated
Normal chow			61.20±11.83	63.84±4.06
HF			95.65±11.18****	77.33±10.14#
Triglycerides (mg/dl)			Sham	Denervated
Normal chow			90.65±27.17	91.96±21.77
HF			147.05±48.15*	108.12±24.72
c-LDL (mg/dl)			Sham	Denervated
Normal chew			4.08±1.53	4.32±0.55
HF			7.97±2.36***	5.87±1.32
NEFA (mg/dl)			Sham	Denervated
Normal chow			1.06±0.34	1.10±0.22
HF			1.19±0.13	0.70±0.39#
		Mice		
Caloric intake (Kcal/day/kg)		Before diet	Before surgery	3 weeks after surgery
Normal chow	Sham	-	0.38±0.01	0.40±0.00
	Denervated	-	0.38±0.00	0.41±0.00
HF	Sham	-	0.82±0.13*	0.83±0.16*
	Denervated	-	1.07±0.22**	1.08±0.48
Glycemia (mg/dl)				
Normal chow	Sham	-	80.60±5.41	86.40±6.23
	Denervated	-	79.00±9.44	80.33±3.78
HF	Sham	-	124.50±10.75***	144.75±20.12
	Denervated	-	112.40±17.33**	94.75±23.67
AUC ITT (mg/dI*min)				
Normal chow	Sham	-	10641.20±1934.06	9276.60±1391.94
	Denervated	-	11135.83±1432.41	10477.50±1764.23

HF	Sham	-	21645.75±3369.78***	23392.00±1391.94
	Denervated	-	22336.20±4626.50****	15251.80±4465.69 ^{#, §}
OGTT (mg/dl*min)				
Normal chow	Sham	-	23194.80±1517.46	19657.60±2173.46
	Denervated	-	20851.33±3452.07	18667.83±1311.51
HF	Sham	-	32773.25±2311.63***	30596.35±2222.85
	Denervated	-	33064.60±6223.05**	26894.00±2665.08

Values represent means \pm SEM; Two-Way ANOVA with Bonferroni multicomparison test. *p<0.05, **p<0.01, ***p<0.001 and ****p<0.0001 comparing normal chow animals and HF values; *p<0.05, **p<0.01, ***p<0.001 and ****p<0.0001 comparing values without and with CSN resection; \$p<0.05, \$\$p<0.01, \$\$\$p<0.001, \$\$\$\$p<0.001, \$\$\$\$p<0.0001 comparing values 9 weeks after CSN with values 9 weeks after sham. AUC- area under the curve; c-LDL – low density lipoproteins cholesterol; HF – high fat; Kitt – constant of the insulin tolerance test; OGTT – oral glucose tolerance test; NEFA- non-esterified free fatty acids.

HF diet also promoted alterations in the BAT in rats and mice, shown by an increase in adipocytes perimeter (Fig. 1G). Interestingly, CSN resection increased the amount of BAT by 53% and 84% in rats and mice (Fig. 1E), contributing to a decrease in adipocytes perimeter of 22% and 15%, respectively (Fig. 1G).

CSN resection ameliorates visceral white adipose tissue function in rodents by promoting the beiging of adipose tissue and its metabolism

We assessed visceral WAT metabolism by measuring basal oxygen consumption rate (OCR) and sympathetic-evoked OCR (NE [15 μ M] or Dopamine [100nM]) using Seahorse technology in mice (Fig. 3A, left and right panels). It is well established that mitochondrial morphology, mass and function are impaired in multiple adipose tissue depots in obese rodents (de Mello et al., 2018). In agreement here we observed that the visceral WAT basal OCR of mice submitted to HF diet was decreased by 51% in comparison with normal chow diet animals (Fig. 3B). Interestingly, CSN resection, in HF animals, promoted an increase of 77% in basal OCR, therefore restoring WAT OCR (Fig. 3B). Sympathetic mediators such as NE (Straznicky et al., 2008; Zeng et al., 2015) or dopamine (Tavares et al., 2021) are known to activate WAT. Herein, NE and dopamine-

evoked OCR in WAT of HF mice were reduced by 57 and 44%, respectively, in comparison with normal chow animals. NE and dopamine evoked-OCR showed a tendency to increase in normal chow CSN-resected animals and increased by 156 and 77%, respectively, in HF animals submitted to CSN resection, thereby restoring completely the catecholaminergic responses (Fig. 3C).

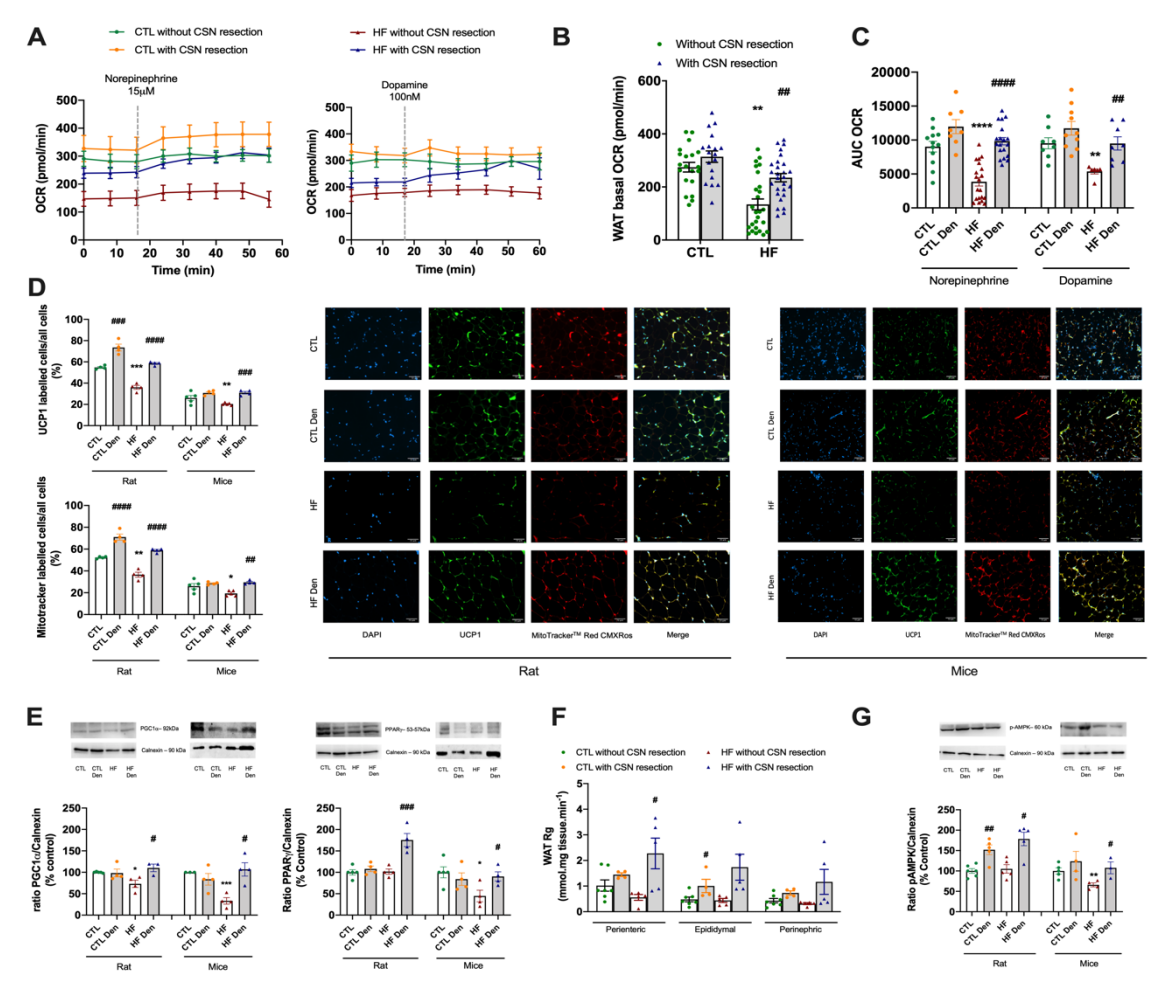


Figure 3 - Carotid sinus nerve (CSN) resection ameliorates visceral white adipose tissue (WAT) metabolism in obese rodents. Effect of high fat (HF) diet and of CSN resection on the: A) curves of oxygen consumption rate (OCR) per minute, before and after stimulation with norepinephrine [15μM] (left panel) or Dopamine [100nM] (right panel) in mice (n=15-27 pieces of tissue from 4-6 animals); B) average basal OCR in mice (n=15-27 pieces of tissue from 4-6 animals); C) average OCR after stimulation with [15μM] or Dopamine [100nM] (n=4-17 pieces of tissue from 4-6 animals); D) percentage of UCP1 protein labeled cells (top panels) and mitotrackerTM Red CMXRos labelled cells (bottom panels) in the perienteric depot (n=4-5) in rats and mice – left panels show average; Right panels show representative images of UCP1 and MitotrackerTM Red CMXRos labelled cells Green- UCP1 labelled adipocytes; Red- MitotrackerTM Red CMXRos labelled adipocytes; Blue – DAPI labelled nuclei of the adipocytes; Yellow – Merge of UCP1 and MitotrackerTM Red CMXRos labelled cells; E) average expression of PGC1α (92kDa, left panel) and PPARγ (53-57kDa, right panel) on visceral fat of rats and mice (n=3-5) – representative western blots are shown on the top of the graphs; F) Rg′ values, reflecting glucose uptake in WAT depots in rats; and on G)

average AMPK phosphorylation [phospho-AMPKa (Thr172), 60kDa] - representative western blots are shown on the top of the graph. Bars represent mean values \pm SEM. Two-Way ANOVA with Bonferroni multicomparison test. *p<0.05, **p<0.01, ***p<0.001 and ****p<0.0001 comparing CTL vs HF groups; #p<0.05, ##p<0.01 and ###p<0.001 comparing values with and without CSN resection.

To confirm the thermogenic-mediated effect of CSN resection on obesity and adipose tissue, we evaluated mitochondrial density and UCP1 expression in the visceral WAT. HF diet decreases by 34 and 22% UCP1 protein expression in perienteric adipose tissue depot, respectively in rats and mice (Fig. 3D, top panel). In agreement, mitochondrial density decreases by 30 and 25%, respectively, in rats and mice submitted to the HF diet (Fig. 3D, bottom panel). Bilateral CSN resection increased UCP1 protein expression and mitochondrial density in both species, with an increase of 39 and 52% in UCP1 expression, respectively in HF rats and mice, and an increase in mitochondrial density of 61 and 52%, respectively, suggesting a restoration of WAT metabolism through increased thermogenesis and acquisition of a beiging phenotype.

We therefore evaluated by western blot the expression of PGC1 α and PPARy proteins, key mediators of lipid metabolism and markers of brown fat phenotype. HF diet decreased PGC1α expression by 27 and 67%, respectively for rat and mice, effects completely reversed by CSN resection (Fig. 3E, left panel). Interestingly, HF diet did not alter the expression of PPARy in visceral WAT of rats while decreased by 55% in the WAT of mice. CSN resection increased PPARy expression by 73% in the HF rats and restored completely its expression in mice (Fig. 3E, right panel). Glucose uptake has been widely used as a surrogate marker for thermogenesis, being glucose one of the substrates for adipocytes metabolism (Carpentier et al., 2018). Here we evaluated glucose uptake, in vivo, in WAT depots and the phosphorylated AMPK protein expression by Western Blot. HF diet decreased non-significantly perienteric fat. The CSN resection increased glucose uptake in all fat depots in normal chow and HF animals, an effect significantly different in the perienteric depot of the HF animals (Fig. 3F). Finally, we found no alterations with HF diet in phosphorylated AMPK of rats but a decrease of 34% in obese mice. CSN resection increased AMPK phosphorylation by 52 and 70%, respectively, in the CTL and HF Wistar rats, and restored the phosphorylation of AMPK in obese mice (Fig. 3G).

CSN resection improves brown adipose tissue metabolism

It is consensual that obesity leads to BAT dysfunction with accumulation of enlarged lipid droplets and mitochondrial dysfunction (Lefranc et al., 2018). To study BAT mitochondrial function, we evaluated basal OCR as well as the OCR in response to NE [15µM] or Dopamine [100nM] in mice (Fig. 4A, left and right panels). HF diet or with CSN resection did not change significantly basal OCR (Fig. 4A-B). As expected, NE increased OCR in BAT (Fig. 4A, left panel), an effect that was decreased by 20% in obese mice (Fig. 4C). CSN resection augmented NE activation of BAT by 23 and 42%, respectively in the normal chow and obese mice (Fig. 4C). Dopamine is described to directly activate thermogenesis and to increase mitochondrial mass in brown adipocytes (Kohlie et al., 2017). Herein, we were unable to see an increase in OCR evoked by dopamine both in normal chow and obese mice (Fig. 4A right panel). However, in CSN-resected animals dopamine increased OCR by 37% in mice fed with a standard diet and showed a tendency to increase in obese mice (Fig. 4A-C). Aiming a correlation of OCR with increased thermogenesis, we evaluated mitochondrial density and expression of proteins involved in the thermogenic process by immunohistochenistry and Western blot. HF diet promoted a decrease of 21% in UCP1 labeled cells, on both species (Fig. 4D,

top panel). In agreement, mitochondrial density decreased by 30 and 23%, respectively, in rats and mice submitted to the HF diet (Fig. 4D, bottom panel). Bilateral CSN resection increased UCP1 protein expression and mitochondrial density in normal chow animals and reversed the impact of HF diet in these parameters in both species. In contrast with what happen in visceral WAT, no alterations were observe in PGC1 α and PPAR γ protein levels with HF diet or CSN resection apart from the increase of 48% in PGC1 α expression with CSN resection in mice (Fig. 4E, left panel). In agreement with a high metabolic activity, CSN-resected normal chow and obese animals exhibited an increased BAT glucose uptake, measured *in vivo* (Fig. 4F). Finally, and as it was observed in visceral WAT we found no alterations with HF diet in phosphorylated AMPK in rats but a decrease of

48% in obese mice. CSN resection restored phosphorylation of AMPK in mice, with an increase of 81% compared to the HF mice (Fig. 4G).

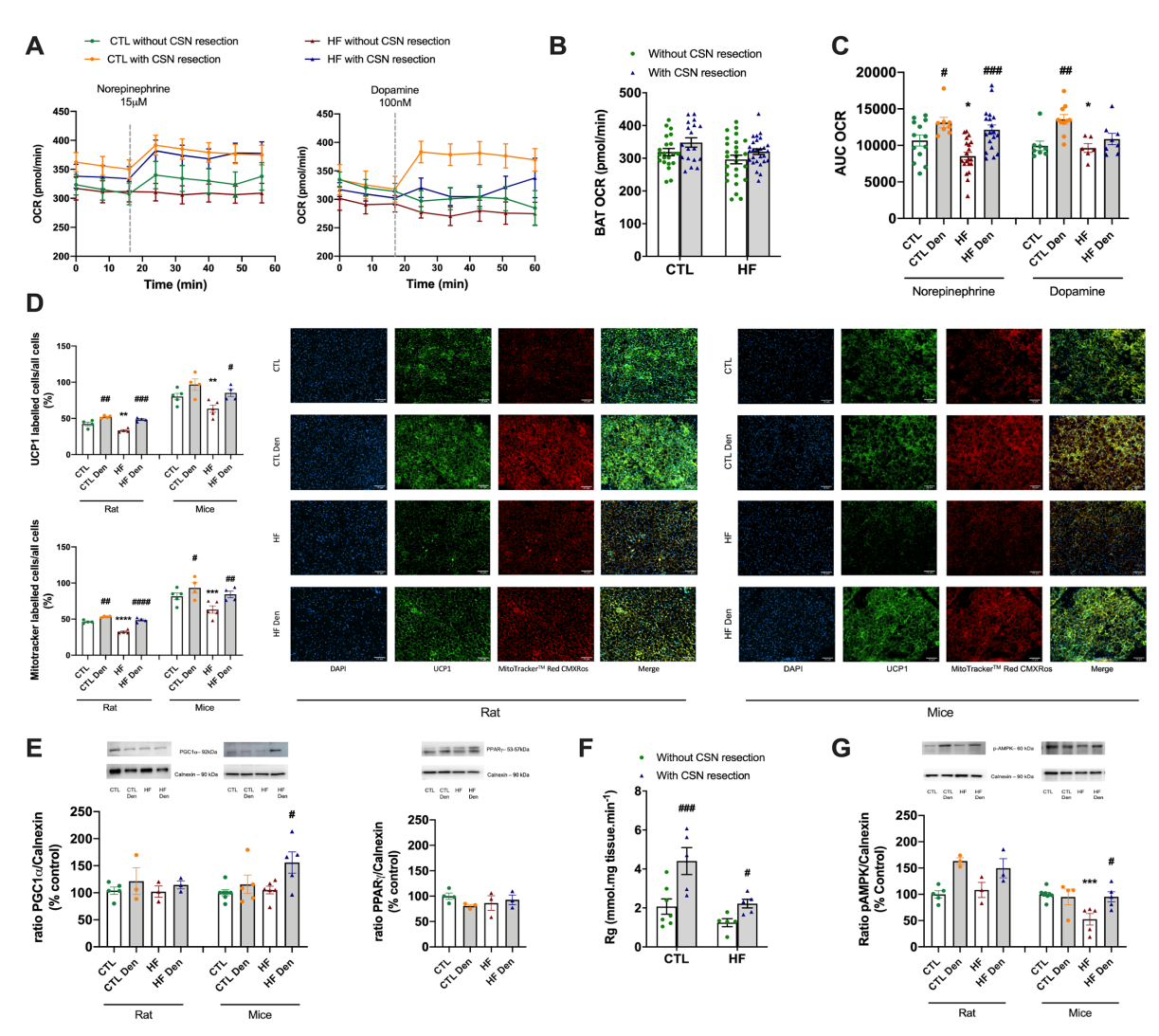


Figure 4 - Carotid sinus nerve (CSN) resection improves brown adipose tissue metabolism and reestablish sympathetic integration in rodents. Effect of high fat (HF) diet and of CSN resection on the: A) Curves of oxygen consumption rate (OCR) per minute, before and after stimulation with norepinephrine [15μ M] (left panel) or Dopamine [100nM] (right panel) in the BAT of mice (n=18-27 pieces of tissue from 6-8 animals). B) Average basal OCR, evaluated in the perienteric depot in mice (n=18-27 pieces of tissue from 6-8 animals); C) Average OCR after stimulation with [15μ M] or Dopamine [100nM] (n=6-20 pieces of tissue from 6-8 animals); D) percentage of UCP1 protein labeled cells (top panels) and mitotrackerTM Red CMXRos labelled cells (bottom panels) in the BAT depot (n=4-5) in rats and mice – left panels show average; Right panels show representative images of UCP1 and MitotrackerTM Red CMXRos labelled cells Green- UCP1 labelled adipocytes; Red- MitotrackerTM Red CMXRos labelled adipocytes; Blue – DAPI labelled nuclei of the adipocytes; Yellow – Merge of UCP1 and MitotrackerTM Red CMXRos labelled cells; E) average expression of PGC1 α (92kDa, left panel) and PPAR γ (53-57kDa, right panel) on BAT of rats and mice (n=3-5) – representative western blots are shown on the top of the graphs; F) Rg' values, reflecting glucose uptake in BAT in rats; and on G) average AMPK phosphorylation [phospho-AMPKa (Thr172),

60kDa] - representative western blots are shown on the top of the graph. Bars represent mean values \pm SEM. Two-Way ANOVA with Bonferroni multicomparison test. *p<0.05, **p<0.01 and ***p<0.001 and ***p<0.001 comparing CTL vs HF groups; #p<0.05, ##p<0.01, ###p<0.001 and ####p<0.0001 comparing values with and without CSN resection.

CSN resection impacts obesity associated-adipose tissue inflammation and hypoxia

Inflammation and hypoxia are two hallmarks of obesity that contribute to the dysfunction of adipose tissue and consequently to metabolic dysfunction. Here we evaluate some plasma inflammatory mediators and the expression of pro-inflammatory mediator receptors by Western Blot. HF diet or CSN resection did not modify TNF α , a major proinflammatory mediator or IL-10, an anti-inflammatory cytokine in plasma in the mice (Fig. 5A, left panel). In contrast, HF diet increased the expression of Il-6 receptors by 35% in visceral WAT, suggesting a pro-inflammatory status within the adipose tissue in mice, although without altering IL-1 β receptor expression (Fig. 5A, right panel). CSN decreased IL-6 receptor expression by 53 and 68% in normal chow and HF mice (Fig. 5A, right panel). In agreement with the idea that BAT is generally more resistant to inflammation (Omran & Christian, 2020) no alterations were found in the expression of IL-6 and IL-1 β receptors in obese mice and rats (Fig. 5B, left and right panel respectively). As well, CSN denervation did not change the expression of these receptors within the BAT. Surprisingly HF diet did not change HIF1 α and HIF2 α expression in visceral WAT of obese mice and rat, but CSN resection decreased by 51% $HIF2\alpha$ expression in obese mice (Fig. 5C, right panel). In contrast, HF diet increased HIF2 α expression by 89% in BAT of rats, without changing HIF1 α in rats or mice and HIF2 α in mice. CSN reversed this effect (Fig. 5C and D) and promoted a decrease of 31% in the BAT of rats (Fig. 5D, right panel).

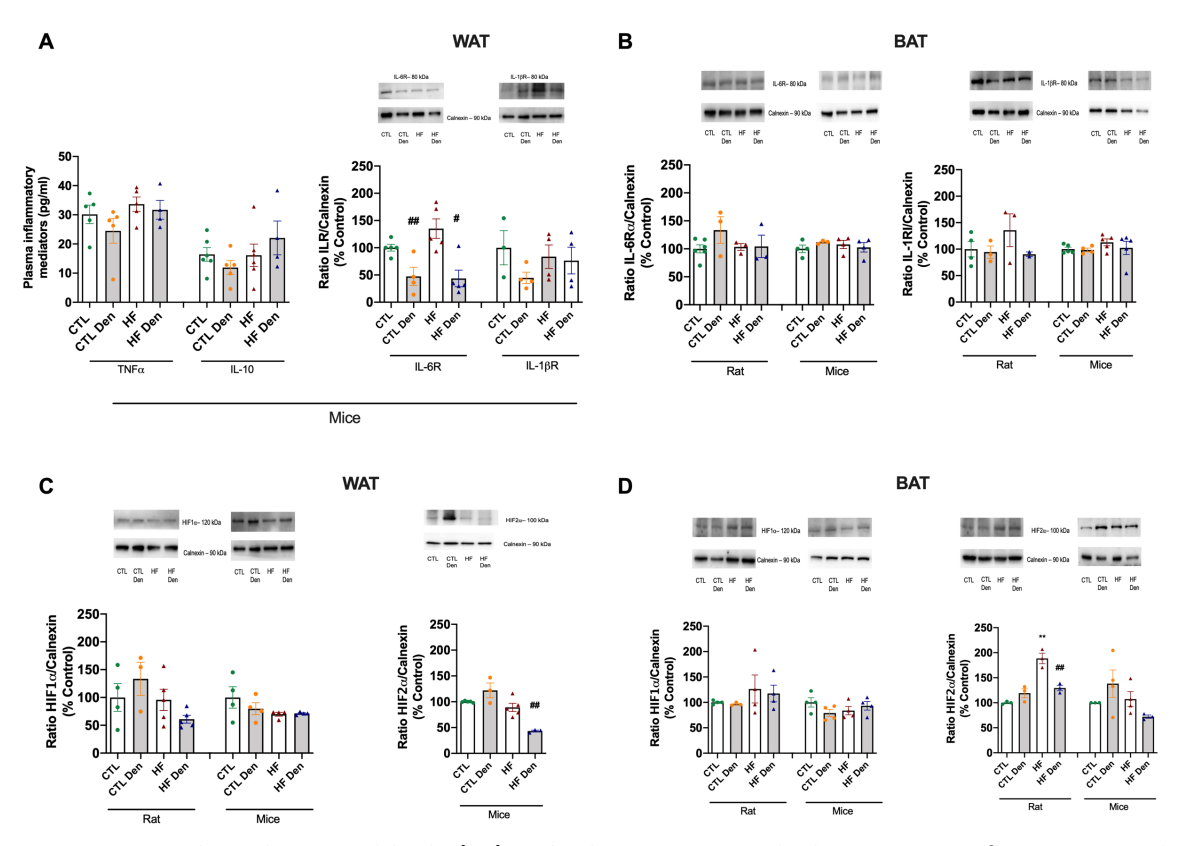


Figure 5 - Linking the carotid body (CB) with obesity associated-adipose tissue inflammation and hypoxia. Effect of high fat (HF) diet and of CSN resection on the: A) Average plasma levels of TNF α and IL-10 (n=4-6) (left panel); Average IL-6 and IL-1b receptors expression (80kDa) in the WAT (n=3-5) - representative western blots are shown on the top of the graphs; B) Average HIF1 α (120kDa; left panel) and HIF2 α (100kDa; right panel) expression in the WAT (n=3-5) - representative western blots are shown on the top of the graphs; C) Average IL-6 receptors (80kDa; left panel) and IL-1 β receptors (80kDa; right panel) expression in the BAT (n=3-5) - representative western blots are shown on the top of the graphs; D) Average HIF1 α (120kDa; left panel) and HIF2 α (100kDa; right panel) expression in the BAT (n=3-5) - representative western blots are shown on the top of the graphs; Bars represent mean values \pm SEM. Two-Way ANOVA with Bonferroni multicomparison test. **p<0.01 comparing CTL vs HF groups; #p<0.05 and ##p<0.01 comparing values with and without CSN resection.

CB modulates catecholaminergic and sympathetic integration in visceral white and brown adipose tissues

Obesity and dysmetabolic states have been linked to a whole-body overactivation of the SNS (Conde et al., 2020). In agreement, we show herein that obese rats exhibit an

overactivation of SNS, reflected by an increase in 23 and 65%, respectively, in plasma NE and epinephrine levels (Fig. 6A) and by an increase of 46% in the SNS index evaluated by heart rate variability analysis (Fig. 6B). As expected and in agreement with the findings that CB activation leads to an overactivation of the SNS (Conde et al., 2017; Iturriaga et al., 2016), CSN resection reverted the effects of HF diet on plasma epinephrine and attenuated NE plasma levels and restored SNS index (Fig. 6A-B). In contrast with the whole-body overactivation of the SNS (Fig. 6B) and in line with the idea that sympathetic activation increases adipose tissue metabolism (Rayner, 2001), catecholamines levels within the visceral adipose tissue, namely NE, epinephrine and dopamine were decreased by 59, 60 and 70%, respectively (Fig. 6A), effects attenuated by CSN resection. The decreased catecholamines content within the visceral WAT in obese animals was coincident with a decrease by 34% in the expression of TH in HF mice, evaluated by Western Blot (Fig. 6C, left panel), and by a decrease of 82% in the intensity of TH innervation measured by light-sheet microscopy in the HF rats, with no significant alterations in the volume of fibers (Fig. 6D, left panel). Establishing a direct link between the CB and adipose tissue catecholaminergic signaling, CSN resection increased TH expression by 93% and 30% in obese rats and in mice, respectively (Fig. 6C) and increased enormously the intensity of TH immunostaining, evaluated by light-sheeting microscopy, without changing the volume of sympathetic fibers innervating visceral WAT (Fig. 6D, left panel). BAT followed the same tendency observed in visceral WAT, with the BAT of obese mice showing a decrease of 44% in TH expression (Fig. 6C, right panel) and a decrease of 73% in the intensity of TH immunostaining in rat BAT. Interestingly, HF diet induced a decrease of 73% in the volume of sympathetic fibers innervating the BAT (Fig. 6E, left panel). CSN resection in obese mice restored BAT TH expression to control levels. In rats, CSN resection increased BAT TH expression and the intensity of TH immunostaining, by 34% and 187% in normal chow rats and TH immunostaining by 182% in HF animals, without changing the volume of sympathetic fibers innervating the BAT (Fig. 6E, left panel). These results indicate that the CB controls sympathetic innervation to the adipose tissue and that CSN resection restores catecholaminergic integration.

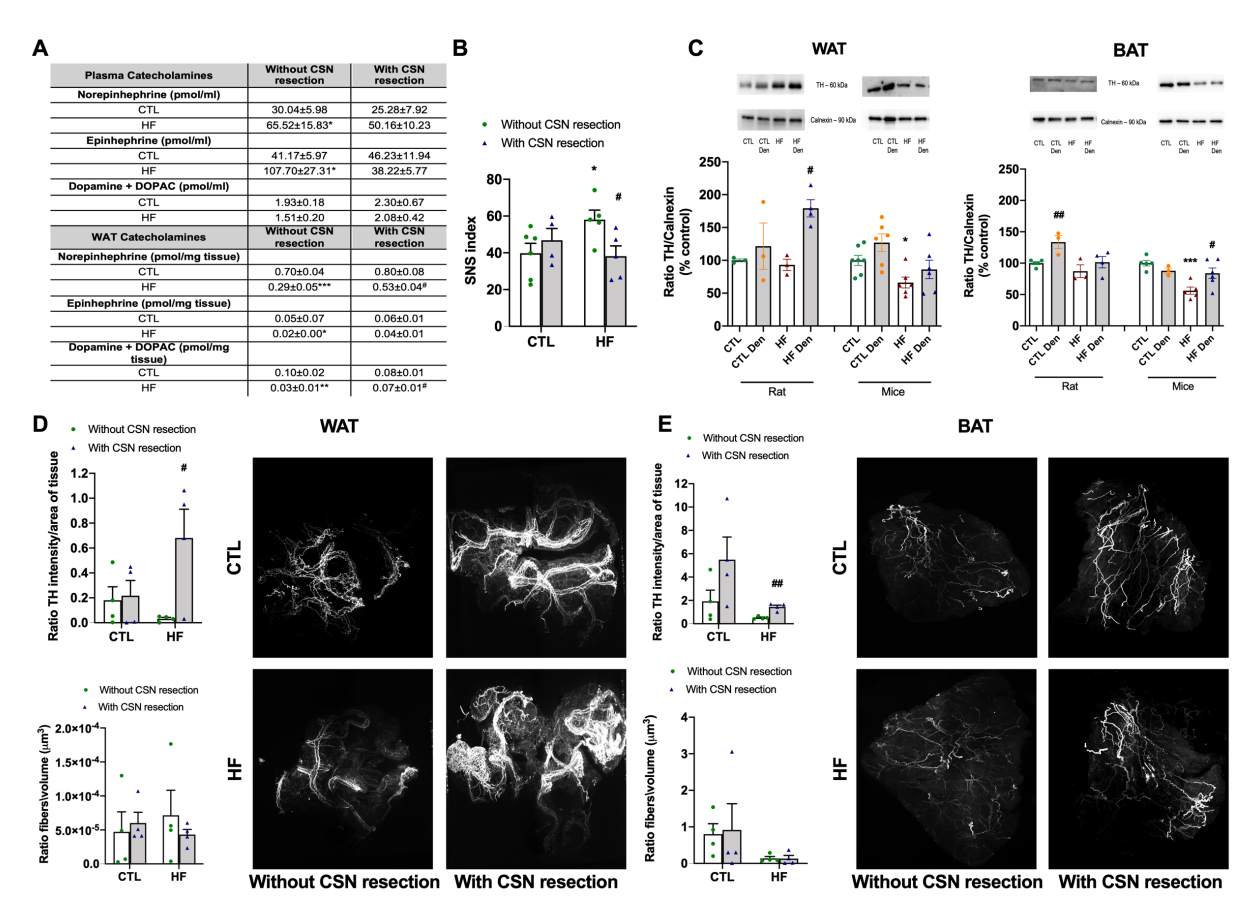


Figure 6 - CSN resection restores sympathetic integration in visceral white and brown adipose tissues. A) Wistar rats plasma and WAT catecholamines levels measured by HPLC with electrochemical detection (n=4-5); B) Wistar rats whole body SNS index (n=4-5); C) average TH expression (60 kDa) on the WAT (left panel) and on the BAT (right panel) of both species - representative western blots are shown on the top of the graph (n=3-7); D) Sympathetic innervation in the WAT of Wistar rats, presented by the intensity (left, top panel) and fibers volume (left, bottom panel) of TH immunolabeling (n=4) – representative images are shown at the right panel; E) Sympathetic innervation in the BAT of Wistar rats, presented by the intensity (left, top panel) and fibers volume (left, bottom panel) of TH immunolabeling (n=4) – representative images are shown at the right panel. Bars represent mean values \pm SEM. Two-Way ANOVA with Bonferroni multicomparison test. *p<0.05, **p<0.01 and ***p<0.001 comparing CTL vs HF groups; #p<0.05 and ##p<0.01 comparing values with and without CSN resection.

Discussion

Herein we described for the first time the CB controls white and brown adipose tissue metabolism via the modulation of catecholaminergic signaling. Moreover, we show that

this organ is a key player in the development of obesity since the abolishment of its activity via the resection of the CSN, decreases weight gain and adipose tissue deposition in obese rodents by ameliorating baseline visceral WAT metabolism through the promotion of a beiging phenotype, and by improving BAT sympathetic activation. We demonstrate that CSN resection restores catecholaminergic action and sympathetic integration in visceral WAT and BAT in obese animals, therefore concluding that the CB is a key intervenient in the neurocircuitry SNS-adipose tissue connection.

In the previous chapter we showed that the best rat model to study obesity and its comorbidities is the HF model. Consistently, here we showed that Wistar rats and C57BL/6 mice submitted to 19 or 15 weeks of 60% lipid-rich diet, respectively, presented a phenotype consistent with the phenotype observed in obese humans, presenting a marked increase in weight gain accompanied by increased fat deposition, coincident with an increase in adipocytes perimeter both in WAT and BAT, and by the development dysmetabolism characterized by insulin resistance, glucose intolerance, hyperinsulinemia, reduction on phosphorylated AMPK expression and dyslipidaemia.

As expected, 19 weeks of HF diet contributed to a decrease in both WAT and BAT metabolism (Choi et al., 2015; Heinonen et al., 2020), displayed by decreased basal OCR and OCR in response to catecholaminergic mediators as NE or dopamine, as well as a decrease in thermogenesis markers, as UCP1 protein and mitochondrial density and a reduction on the expression of PGC1 α and PPARy (Crunkhorn et al., 2007; Semple et al., 2004).

We also showed that in agreement with the increased weight gain and body fat mass in HF rodents, the increase in white adipose tissue depots was accompanied by increased adipocytes perimeter in the perienteric depot, as described in the literature in rodents (Choi et al., 2015; DeClercq et al., 2016; Hageman et al., 2010; Paglialunga et al., 2015; Roberts-Toler et al., 2015) and in humans (McLaughlin et al., 2016).

Consistently with the metabolic dysfunction in HF animals, HF diet decreased BAT amount and contributed to increased lipid deposition within this tissue, characterized by large lipid droplets accumulated within brown adipocytes and increased adipocyte

perimeter. The decrease in the BAT amount is not consensual with some studies using C57BL/6 mice and with different times of exposure to HF diet showing an increase in BAT weight(Kuipers et al., 2019; Roberts-Toler et al., 2015). Nevertheless, the increase in adipocytes perimeter and the accumulation of lipid droplets within the brown adipocytes, that we observed, is consensual between several studies (Kuipers et al., 2019; Roberts-Toler et al., 2015). These different results can be explained by differences in tissue collection and processing: in our work, the WAT around the BAT depot was dissected and weighed separately from the BAT depot, and in fact it was increased (data not shown), a detail that is not mentioned in these studies.

Here we observed that WAT exhibits lower oxygen consumption rates than the BAT in lean animals, which is in line with the idea that AT oxygen consumption is relatively low in lean healthy subjects, accounting for approximately 5% of whole-body oxygen consumption (Lempesis et al., 2020). As expected, HF diet decreased WAT basal OCR of the WAT, and reduced NE and dopamine-evoked OCR, suggesting that HF diet is not only affecting the mitochondrial activity of the adipocytes but also affecting adipocytes response to SNS stimuli and consequently affecting lipolysis (Lempesis et al., 2020).

These results on the effects of HF diet on WAT metabolism are in accordance with the general idea that HF diet leads to a decreased WAT metabolism. However, the majority of the studies dedicated to evaluate basal OCR in WAT in mice under HF diet did not found alterations on basal adipocytes oxygen consumption, measured with high-resolution respirometry or seahorse technology (Schöttl et al., 2015). However, they did found that HF animals exhibited lower maximal cellular respiration rates in the adipocytes. All these results indicate that, beside the absence of alterations on basal OCR, HF diet affects mitochondrial activity in the WAT. In agreement, we found that UCP1 and mitotracker immuno-labeling, as well as PGC1 α and PPAR γ proteins were decreased in HF animals.

In contrast with what we found in WAT, HF diet did not alter either BAT basal OCR or dopamine-stimulated OCR in obese mice but decreased the NE-evoked OCR in the BAT. In agreement, rats and mice under HF diet exhibited decreased UCP1 protein expression and mitochondrial density in BAT.

The effect of HF diets on increasing or decreasing UCP1 protein expression or UCP1 mRNA levels in the WAT has been debated for years, with studies showing increases in UCP1 mRNA levels in the WAT (Chiang et al., 2009; Collins et al., 1997; Margareto et al., 2001) while others reported no changes (Prpic et al., 2002) or decreased levels (Collins et al., 1997; Prpic et al., 2002; Rong et al., 2007). Indeed, some studies found that in both C57BL/6 mice (Shirkhani et al., 2018) submitted to 12 weeks of HF diet (45% energy from fat) and Sprague-Dawley rats submitted to 8 weeks of HF diet (50% of lipids), UCP1 mRNA levels were decreased or even absent in the subcutaneous WAT and also in the BAT (Zhang et al., 2010). In contrast, other studies also in C57BL/6 mice submitted to HF diet (60% Kcal from fat), found no alterations in UCP1 mRNA expression in the BAT (Roberts-Toler et al., 2015). In 2011, a meta-analysis performed by Fromme and Klingenspor (Fromme & Klingenspor, 2011) dedicated to evaluate UCP1 alterations promoted by HF diet concluded that HF diet feeding in the WAT consistently leads to decreased Ucp1 mRNA levels while in the BAT it has the opposite effect, however a huge variance of results regarding the effects of the diet in BAT UCP1, even when using the same animal species or the same diet composition.

In accordance with the decreased basal OCR activity in WAT and no effect on BAT induced by the HF diet, we also observed that HF diet decreased PGC1 α , PPAR γ and phosphorylated AMPK expression in the WAT, with no alterations in the BAT, regarding PGC1 α and PPAR γ . Some studies already demonstrated that in obese models, PGC1 α mRNA levels were decreased not only in the WAT (Semple et al., 2004) and BAT (Shirkhani et al., 2018) but also in skeletal muscle (Crunkhorn et al., 2007). Also it is known that PPAR γ is decreased in obese states (Yamauchi et al., 2001). Furthermore, the effect herein observed in phosphorylated AMPK with HF diet is consistent with studies performed in humans (Gauthier et al., 2011) and in animal models (Lindholm et al., 2013) showing that, phosphorylated AMPK was reduced in several tissues, including the BAT and the WAT.

Inflammation and hypoxia are two hallmarks of obesity, being consensual that both plasma and adipose tissue of obese animals and humans (Ferrante, 2007) present high levels of IL-6, IL1 β and TNF α exhibiting also activation of HIF-1 α and HIF-2 α subunits.

Herein, we did not find any alterations in the expression of IL-6 or IL-1 β receptors in both adipose tissue depots or in circulating TNF α levels or IL-10 levels. Studies in obese adults showed higher IL-6 mRNA expression in obese versus lean/overweight individuals (Sindhu et al., 2015), however the analysis were performed in the subcutaneous depot and evaluated mRNA levels while we evaluated visceral depot and protein expression, which could explain the differences found between our work and some literature. We also did not found any alterations in the expression of HIF1 α assessed by western blot in obese mice or rat, in both WAT and BAT. This is not consensual with the description that HIF1 α protein accumulation is restricted to adipose depots of pathologically obese and diabetic humans and mice, being HIF1 α protein higher in the adipose tissue of obese mice (Ye et al., 2007) and morbidly obese individuals (Todorčević et al., 2021), resulting in an inhibition of FFA oxidation (Krishnan et al., 2012). In addition, literature also described that HIF-2 α protein levels are increased in adipose tissue of mice fed with HFD for 4 weeks (Shimba et al., 2004), which we only observed in the BAT of rats. These differences might be due to the use of different techniques to evaluate HIF-1 α and HIF- 2α expression and also the type of adipose depots use and therefore this might involve further clarification.

Obesity is associated with a general whole-body SNS overactivity, in particular in the outflow to the kidneys (Vaz et al., 1997), with obese adults presenting increased urinary and plasmatic NA levels (Lee et al., 2001), and in the skeletal muscle vasculature (Grassi et al., 1995). Moreover, animal (Mancia, 1997) and clinical studies (Schlaich et al., 2003) demonstrated that increased SNS activity is involved in the pathophysiology of altered cardiac structure and function in essential hypertension, and that obese insulin-resistant individuals display blunted sympathetic neuronal responses to physiological hyperinsulinemia, glucose consumption and changes in energy states (Grassi et al., 2005). In concordance with these studies and as shown by our group in animal models of prediabetes and T2D (Ribeiro et al., 2013; Sacramento et al., 2017), we observed increased plasma levels of NE and epinephrine in the obese rats and whole-body SNS index, demonstrating overall SNS overactivity in our models of obesity. However, we also know that now there is some lines of evidence indicating that SNS activity is typically

regionalized and that there are variations in the sympathetic tone among tissues. Here we shown that, while whole-body sympathetic activity is increased, the sympathetic tone and catecholaminergic action within both visceral WAT and BAT are decreased in HF rodents. In agreement with the low concentrations of catecholamines present within the adipose tissue found herein in rats submitted to HF diet, we observed herein a general decrease in TH expression and TH immunostaining intensity. These results are in line with the notion that the sympathetic activation promotes lipolysis within the adipose tissue (Bartness et al., 2014) and that sympathetic activation (e.g. β -adrenoreceptors agonism) promote an increase in adipose tissue metabolism (Bartness et al., 2014) therefore having the potential to be a therapeutic for obesity.

The CB is a powerful modulator of SNS activity, as showed by previous studies on its involvement in cardiovascular responses/adjustments to its classical physiological stimuli, hypoxia (Marshall, 1994) and its involvement on the pathophysiological mechanisms of sympathetic mediated diseases, as essential hypertension (Abdala et al., 2012; McBryde et al., 2013) and chronic heart failure (Schultz et al., 2015). Moreover, the dysfunction of CB activity leading to the overactivation of the SNS has already been described to be associated with the development and maintenance of prediabetes, T2D and metabolic syndrome (Cracchiolo et al., 2019b; Ribeiro et al., 2013; Sacramento et al., 2017). In fact, CSN resection, that abolished the connection between the CB and the central nervous system, prevents and normalizes sympathetic overaction measured as plasma and adrenal medulla catecholamines content, as the increase percentage of low frequencies and on the ratio low frequency/high frequency in the power spectra of the heart rate variability (Sacramento et al., 2017) and as the increase in the electrophysiological activity measured in the cervical sympathetic chain (Cracchiolo et al., 2019b). Here we described that the CB is also a powerful modulator of catecholaminergic action/sympathetic integration to the adipose tissue, controlling adipose tissue metabolism, both white and brown. We showed that the abolishment of CB activity, by resecting the CSN, decreases weight gain and adipose tissue deposition in obese rodents, contributing to a reduction of adipocytes perimeter and reversing metabolic dysfunction. Moreover, CSN resection ameliorated visceral WAT and BAT

metabolism, increasing thermogenic markers and improving glucose metabolism, which is in line with the previous findings that CSN resection improved dysmetabolism by positively impacting glucose metabolism in visceral adipose tissue (Sacramento et al., 2017). The link between the BAT and CB chemoreceptors in not new, as Madden and Morrison (2005) previously shown that activation of CB chemoreceptors inhibits the elevated levels of BAT sympathetic nerve activity evoked by hypothermia (Madden & Morrison, 2005). However, new is this link between the restoration of metabolism and decrease weight gain by restoring WAT and increasing BAT metabolism. Also, new is the link between CB and SNS control of the WAT adipose.

We can conclude that the CB is a new player in the link SNS-adipose tissue therefore controlling adipose tissue metabolism via the modulation of catecholamines action and sympathetic integration. Moreover, we showed here that the CB is a key player in the genesis and maintenance of obesity and its dysmetabolic states and therefore the modulation if its activity is a therapeutic target for the treatment of obesity and its comorbidities.

Chapter IV

General discussion

Herein we described that CSN resection decreases weight gain and adipose tissue deposition in obese rodents, ameliorating visceral WAT metabolism, by promoting the beiging of this tissue, and improving BAT metabolism. Finally we demonstrate that the CB controls catecholaminergic action at adipose tissue depots by showing that CSN restores dopaminergic and noradrenergic integration in visceral WAT and potentiating noradrenergic action in BAT. It can be concluded that the CB is a key intervenient in the neurocircuitry SNS-adipose tissue connection.

Role of CB in obesity and its comorbidities

It is consensual that the SNS becomes overactive in obesity, with the degree of overactivation appearing to be dependent on body fat distribution and with central obesity showing to be associated with a greater sympathetic nerve activation (Schlaich et al., 2003). Several mechanisms have been proposed to be the basis of this overactivation, including overeating (Arone et al., 1995; O'Dea et al., 1982; Welle et al., 1991), increased visceral adiposity (Alvarez et al., 2002, 2004), with the consequent hyperinsulinemia (Lembo et al., 1992; Vollenweider et al., 1993) and hyperleptinemia and increased inflammation, among others. For years this increase in SNS activity was thought to be mainly promoted through the central nervous system. Insulin is known to act in the central nervous system to induce sympathoexcitation (Muntzel et al., 1995) as: 1) the intracerebroventricular administration of insulin augmented central sympathetic activity (Muntzel et al., 1994); and 2) increased levels of circulating insulin acted on neurons in the arcuate nucleus in the ventromedial hypothalamus, increasing sympathetic activity and baroreflex sensitivity (Cassaglia et al., 2011). Moreover, leptin also acts centrally in several brain regions, via melanocortin-system-dependent pathways, to increase sympathetic activity (da Silva et al., 2013) and administration of leptin in cerebral ventricles increased sympathetic nerve activity to the BAT and hindlimb, an effect that can be blocked by selective lesioning of the hypothalamic arcuate nucleus (Haynes, 2000).

However, apart from acting centrally, nowadays it is known that both insulin and leptin stimulate the CB, with both insulin and leptin receptors being present in the CB (Caballero-Eraso et al., 2019; Ribeiro et al., 2013, 2018). In addition, it is known that CB activation is involved into sympatho-excitation (Cracchiolo et al., 2019a; Marshall, 1994; McBryde et al., 2013; Ribeiro et al., 2013) and that sympathoexcitatory mediators as insulin, leptin and inflammatory cytokines that are involved in obesity and obesity related illness also act on the CB promoting its activation (Cunha-Guimaraes et al., 2020; Ribeiro et al., 2013, 2018; Sacramento et al., 2020). Therefore, it is reasonable to hypothesize that the CB, apart from having a role in the regulation on peripheral insulin sensitivity and on the SNS-hyperactivity related with type 2 diabetes, could be a new player, in the link obesity and SNS overactivity. The overactivation of the CB has been implicated in several cardiometabolic diseases, such as T2D, essential hypertension and dysmetabolism and hypertension associated with OSA (Conde et al., 2017; Narkiewicz et al., 1998; Ribeiro et al., 2013). Furthermore, it was already shown that animal models of metabolic dysfunction induced by hypercaloric diets, like the high fat (HF), which is an obese model of insulin resistance and hypertension, and the high sucrose (HSu) diet rat, which is a lean model of insulin resistance and hypertension exhibit an overactivation of the CB that is higher in HF than HSu animals. This CB overactivation was reflected by increases in basal ventilation, in the ventilatory responses to ischemic hypoxia (Ribeiro et al., 2013), in the electrophysiological activity of the CSN activity recorded in vitro (Ribeiro et al., 2018) and in vivo (Cracchiolo et al., 2019a) and in CB chemoreceptor cell activity (Ribeiro et al., 2013). Also, Dos Santos et al. (2018) showed that the CBs from animals submitted to a combined HF plus HSu diet, are bigger than control CBs, have more type 1 cells and express more tyrosine hydroxylase, the limiting enzyme in the synthesis of catecholamines, the best well-described neurotransmitter in the CB (Dos Santos et al., 2018; Ribeiro et al., 2013). In accordance Cramer et al. (2014) demonstrated that patients with T2D exhibit enlarged CBs and more recently it was described that prediabetes patients exhibit increased CB chemosensitivity, measured through a Dejour test, that consists in measuring the decrease in ventilation produced by two breaths of hyperoxia (100%O2) (Cunha-Guimaraes et al., 2020). This increased

CB chemosensitivity correlates with insulin levels, with insulin resistance and with the abdominal perimeter (Cunha-Guimaraes et al., 2020), suggesting a direct link between the CB and visceral obesity.

The proof-of-concept of the crucial role of CB on the control of metabolism and its key importance in the genesis of metabolic dysfunction was confirmed in animal experiments in where CSN resection, thereby abolishing CB activity, was able to prevent (Ribeiro et al., 2013) and reverse (Sacramento et al., 2017) dysmetabolic features, as insulin resistance, glucose intolerance and hyperinsulinemia, induced by hypercaloric diets. Also, CSN resection was able to prevent (Ribeiro et al., 2013) and reverse (Sacramento et al., 2017) sympathetic overactivity, measured as the sympathetic balance of heart rate variability analysis and by indirectly evaluating plasma and adrenal medulla catecholamines, in obesity and metabolic syndrome and avoid weight gain in animals submitted to 3 weeks of HF diet (Ribeiro et al., 2013). Importantly, were also the findings showing that SNS overactivity measured as electrophysiological recordings in the cervical sympathetic chain were normalized in CSN-resected animals, confirming the link between CB and SNS activity in metabolic dysfunction. Taking into consideration that obesity and metabolic dysfunction run with an overactivation of the SNS (Kalil & Haynes, 2012), that the CB modulates SNS activity (Cracchiolo et al., 2019a; Ribeiro et al., 2013; Sacramento et al., 2017), that several key mediators released by the adipose tissue, as leptin and inflammatory cytokines and by the pancreas, as insulin act on the CB (Ribeiro et al., 2018; Sacramento et al., 2020), and that CSN resection avoid weight gain in prediabetes (Ribeiro et al., 2013; Sacramento et al., 2017), it is reasonable to postulate that CSN resection will impact weight gain as we see herein in an animal model of manifested obesity. Indeed, we observed that CSN resection decreased weight gain and fat deposition on animals submitted to the HF diet during 19 weeks showing a marked obesity.

In the same line of reasoning, and knowing that the abolishment of CB activity normalized dysmetabolism by mechanisms that involve the improving glucose uptake in the perienteric adipose tissue (Sacramento et al., 2017) and that the SNS controls

adipose tissue metabolism (Barbatelli et al., 2010; Bartness et al., 2014), it is plausible to think that the CB might control adipose tissue metabolism. In fact, it was already shown that hypoxic activation of CB inhibits sympathetic outflow to brown adipose tissue in rats (Madden & Morrison, 2005). Herein, we showed that CSN resection not only increased BAT amount and improved its function in obesity but also decreased the amount of visceral/perienteric WAT and the size of its adipocytes with an associated amelioration of WAT function. This clearly points to a direct control of adipose tissue metabolism of both white and brown depots by the CB.

Mechanistic insights on role of CB in obesity: linking the CB with catecholaminergic activity and the metabolic activity of the adipose tissue

Here we showed that CB controls adipose tissue metabolism, both white and brown, via the modulation of catecholaminergic signalling, as the CSN resection induces a beiging phenotype in the WAT and the activation of BAT and restored sympathetic integration within these adipose tissue depots

It is consensual that the SNS directly innervates both BAT and WAT and plays a key role in the modulation of lipolysis and/or thermogenesis through NE and dopamine release (Larabee et al., 2020) and the activation of its receptors (Bartness and Song 2007; Barbatelli et al. 2010; Bartness et al. 2010; Vitali et al. 2012; Nguyen et al. 2014). For example, $\beta 2$ and $\beta 3$ agonists have been shown to induce thermogenesis in the BAT (Blondin et al., 2020; Cypess et al., 2015) and dopamine directly increases mitochondrial mass and thermogenesis in this tissue (Kolie et al. 2017). More recently, dopamine was also shown to potentiate insulin action on glucose uptake in visceral WAT and to act to promote adipose tissue metabolism (Tavares et al. 2021). Here we show that hypercaloric diet intake produce a decrease baseline metabolism in WAT, accessed by measuring oxygen consumption rate, as well decreased mitochondrial activity, UCP1 expression, PPAR γ and PGC1 α and decreased catecholaminergic activation in WAT and BAT. These results are in agreement with the decreased levels of catecholamines found in WAT and with the low intensity of TH expression in the adipose tissue measured by

light-sheet microscopy but contradict the idea that obesity and its metabolic comorbidities are associated with a SNS overactivation. However, more recently several pieces of evidence were generated supporting the idea of a regional activation/modulation of the SNS (Tchkonia et al., 2013). Our results herein clearly support that by showing an HF diet produced a decreased catecholaminergic activation to the adipose tissues while increasing whole-body SNS activity.

Here we also show that CSN restored WAT baseline metabolism, while promoting an increase in BAT thermogenic function and restored catecholaminergic signaling and activation within these tissues. This clearly makes the proof-of-concept that the CB is a key player in the neurocontrol of metabolism, particularly in the link obesity-SNS.

Targeting the CBs to treat obesity

Among the several possible targets for managing obesity, the beiging of WAT or the activation of BAT, has gained a lot of attention in the last few years. Several studies tried a pharmacological approach such as the administration of β 3-AR, GLP-1 receptor or PPAR γ agonists, among others, however, they are known to have several side effects as, for example, heart failure, edema, weight gain, hypertension, nasopharyngitis, urinary tract infections, headache, upper respiratory tract infection, diarrhea, tachycardia and fatigue, among others (Bragg et al., 2014; Tamucci et al., 2018). Other strategies to induce browning have been studied such as BAT transplantation, with cases of loss of function from the transplanted tissue, and intermittent fasting or caloric restriction which are known to have side effects such as alteration in the integrity of the brain, digestive problems and fatigue, among others (Horne et al., 2020)

So, there is still a need to find an effective therapeutic option, with low side effects and that can be effectively and safely used in humans.

The results presented herein on the role of CB in the development of obesity and on the control of adipose tissue as well as the effect of CSN resection on the decrease in weight gain and obesity comorbidities by promoting the beiging of WAT and increasing the activation of BAT, open new doors for the treatment of obesity. The abolishment of CB

activity through bilateral CSN resection or CB ablation techniques has been already employed for the treatment of asthma in the sixties and more recently for heart failure and hypertension (Del Rio et al., 2013; Marcus et al., 2014). However, these kind of approaches have several side effects, such as for example the loss of hypoxic responses and fluctuations in blood pressure (Conde, 2018). Other options were already applied, such as the unilateral CB ablation, however with low efficacy in long-term due to the compensation of the remaining CB (Narkiewicz et al., 2016), and the exposure to hyperoxia, a stimuli known to block functionally the CB (Bavis et al., 2019). In fact, it has been shown that 1 hour per day of hyperbaric oxygen therapy exposure during 1 month ameliorates glucose tolerance in type 2 diabetic patients (Vera-Cruz et al., 2015)

Another approach could be the pharmacological modulation of CB activity. For example (Pijacka et al., 2016) showed that the antagonism of P2X3 ATP receptors reduced arterial pressure and basal sympathetic activity and normalized CB hyperreflexia in conscious hypertensive rats, suggesting that the antagonism of P2X3 receptors could be a therapeutic approach to normalize CB overactivation in sympathetically-mediated diseases. However, ATP is one of the key mediators involved in CB-hypoxic responses via P2X2/P2X3 receptors and therefore by blocking these receptors one could be interfering with these responses.

More recently, the bioelectronic modulation of CB activity, by applying bilateral kilohertz frequency alternating current, was successfully used in animal models of T2D to reverse insulin resistance and glucose intolerance (Sacramento et al., 2017). Also, it was shown that this modality of electrical blocking was reversible and did not damage the nerve. Therefore, we could postulate that bilateral kilohertz frequency alternating current might be a feasible and efficacious way to achieve CSN neuromodulation to treat obesity and its related illness.

Conclusions

In conclusion this work adds to the understanding of the role of CB in the control of whole-body metabolism, its role in the genesis of metabolic dysfunction and the

pathophysiological mechanisms behind it, by testing the innovative hypothesis that the CB is involved in the genesis and maintenance of obesity and that the abolishment of its activity can decrease weight gain and ameliorate obesity-comorbidities. Also, here the innovative hypothesis that the CB controls the catecholaminergic system and sympathetic integration on the adipose tissue, inducing thermogenic pathways in the adipose tissue was tested.

We concluded that:

- 1. The animal that better mimics human obesity and comorbidities is the animal submitted to 19 weeks of an HF diet, composed by 60% of lipids, since it presents a phenotype that more closely related with human obesity and T2D, with:
 - 1.1. Increase in weight gain and fat deposition;
 - 1.2. Metabolic dysfunction, characterized by insulin resistance, glucose intolerance, hyperinsulinemia and dyslipidemia, and hypertension;
- 2. CSN resection decreases weight gain and has a beneficial impact on obesity-comorbidities in obese rodents by a mechanism that involves the acquisition of a beiging phenotype by the WAT and by improving the thermogenic function of the BAT, since it:
 - 2.1. Decreases weight gain, fat depots and adipocytes perimeter;
 - 2.2. Reverses insulin resistance, ameliorates glucose intolerance and decreases plasma insulin levels;
 - 2.3. Restores WAT and BAT function by increasing basal and/or sympathetic-induced OCR and improving thermogenic pathways (improves UCP1, PGC1 α and PPAR γ proteins expression);
 - 2.4. Improves WAT and BAT glucose uptake and AMPK;

- 3. The CB is a new intervenient in the neuronal circuitry adipose tissue metabolism, via sympathetic nervous system activity, as:
 - 3.1. CSN resection restores overall SNS activity, by decreasing plasma catecholamines and SNS index;
 - 3.2. CSN resection restores WAT adipose tissue catecholamines content, particularly the levels of norepinephrine and dopamine
 - 3.3. CSN increases TH expression in WAT and BAT
 - 3.4. CSN restores sympathetic integration in WAT and BAT, depicted by increased intensity of TH labelled sympathetic innervation
- 4. The role of CB in the genesis and maintenance of dysmetabolic states as well as the pathophysiological mechanisms behind are well conserved in different rodent species.

Final considerations and future directions

The present PhD thesis clearly states that the CB controls adipose tissue metabolism and that its dysfunction is associated with obesity and highlights the potential of the modulation of CB activity for the treatment of obesity and its associated illness.

Activation of adrenergic receptors β_2 -AR and β_3 -AR is known to be one the mechanism promoting lipolysis of the TAGs stored not only in the white but also in the brown adipocytes, increasing thermogenesis and energy consumption (Asensio et al., 2005; Collins, 2012). Furthermore, it is known that animals models of obesity present dysfunctional β -adrenergic system which translates into decreased lipolysis and thermogenesis and that genetic polymorphisms of the β -AR genes (ADRB2 and ADRB3) are related with the development of hypertension, T2D and obesity (Masuo, 2010). In addition, chronic administration of selective agonists for these receptors promotes an

anti-diabetic effect in animal models of obesity and T2D, via normalization of glycemia and insulinemia and an increase in lipolysis and energy expenditure (de Souza & Burkey, 2001). Taking all of this into consideration, it would be interesting to understand in the future if these receptors are involved in CB mediated effects on the adipose tissue. Moreover, since it is known that the chronic administration of these selective agonists of adrenergic receptors might bring several adverse effects related with the activation of the receptors in the cardiac tissue (Bhadada et al., 2011), the modulation of CSN might be one strategy to decrease obesity and improve metabolic function without adverse effects related with the activation of these receptors in other tissues. Therefore, the electric and/or pharmacological modulation of the CB/CSN for the purpose of treating obesity deserves further investigation aiming the translation of these promising results into human medicine.

Another interesting area to explore is the brain integration of these stimuli coming from the CB to the adipose tissue to achieve the completion of the neurocircuitry CB-adipose tissue. Therefore, knowing that the sensory information from the CB is transmitted to the nucleus of the tractus solitarius, that after communicates the information to nucleus from other regions of the brain (Zera et al., 2019) such as the hypothalamus, in which are specific regions where hormones interact regulating appetite and satiety, as a future work it will also be important to study the integration of CSN signals to understand the brain regions involved in the CB-dependent metabolic control. The unraveling of the complete circuit CB-SNS-adipose tissue will contribute to establish a new paradigm on the physiological and pathophysiological mechanisms involving this tiny organ, the CB, our mini brain of the periphery.

Chapter IV

References

- Abdala, A. P., McBryde, F. D., Marina, N., Hendy, E. B., Engelman, Z. J., Fudim, M., Sobotka, P. A., Gourine, A. V., & Paton, J. F. R. (2012). Hypertension is critically dependent on the carotid body input in the spontaneously hypertensive rat. *The Journal of Physiology*, 590(Pt 17), 4269–4277.
- Ahmed, K., Tunaru, S., Tang, C., Müller, M., Gille, A., Sassmann, A., Hanson, J., & Offermanns, S. (2010). An Autocrine Lactate Loop Mediates Insulin-Dependent Inhibition of Lipolysis through GPR81. *Cell Metabolism*, *11*(4), 311–319.
- Alcalá, M., Calderon-Dominguez, M., Bustos, E., Ramos, P., Casals, N., Serra, D., Viana, M., & Herrero, L. (2017). Increased inflammation, oxidative stress and mitochondrial respiration in brown adipose tissue from obese mice. *Scientific Reports*, 7(1), 16082.
- Alcalá, M., Calderon-Dominguez, M., Serra, D., Herrero, L., & Viana, M. (2019). Mechanisms of Impaired Brown Adipose Tissue Recruitment in Obesity. *Frontiers in Physiology*, *10*, 94.
- Alvarez, G. E., Ballard, T. P., Beske, S. D., & Davy, K. P. (2004). Subcutaneous obesity is not associated with sympathetic neural activation. *American Journal of Physiology-Heart and Circulatory Physiology*, *287*(1), H414–H418.
- Alvarez, G. E., Beske, S. D., Ballard, T. P., & Davy, K. P. (2002). Sympathetic Neural Activation in Visceral Obesity. *Circulation*, *106*(20), 2533–2536.
- Angi, A., & Chiarelli, F. (2020). Obesity and Diabetes: A Sword of Damocles for Future Generations. *Biomedicines*, 8(11), 478.
- Arone, L. J., Mackintosh, R., Rosenbaum, M., Leibel, R. L., & Hirsch, J. (1995). Autonomic nervous system activity in weight gain and weight loss. *American Journal of Physiology-Regulatory, Integrative and Comparative Physiology*, 269(1), R222–R225.
- Bae, J., Chen, J., & Zhao, L. (2015). Chronic activation of pattern recognition receptors suppresses brown adipogenesis of multipotent mesodermal stem cells and brown preadipocytes. *Biochemistry and Cell Biology*, *93*(3), 251–261.

- Barbosa, T. C., Kaur, J., Holwerda, S. W., Young, C. N., Curry, T. B., Thyfault, J. P., Joyner, M. J., Limberg, J. K., & Fadel, P. J. (2018). Insulin increases ventilation during euglycemia in humans. *American Journal of Physiology Regulatory, Integrative and Comparative Physiology*, 315(1).
- Beltowski, J. (2006). Leptin and atherosclerosis. Atherosclerosis, 189(1), 47-60.
- Bertholet, A. M., Kazak, L., Chouchani, E. T., Bogaczyńska, M. G., Paranjpe, I., Wainwright, G. L., Bétourné, A., Kajimura, S., Spiegelman, B. M., & Kirichok, Y. (2017). Mitochondrial Patch-Clamp of Beige Adipocytes Reveals UCP1-positive and UCP1-negative Cells Both Exhibiting Futile Creatine Cycling. *Cell metabolism*, *25*(4), 811-822.e4.
- Bidulescu, A., Dinh, P. C., Sarwary, S., Forsyth, E., Luetke, M. C., King, D. B., Liu, J., Davis, S. K., & Correa, A. (2020). Associations of leptin and adiponectin with incident type 2 diabetes and interactions among African Americans: The Jackson heart study. *BMC Endocrine Disorders*, 20, 31.
- Bin-Jaliah, I., Maskell, P. D., & Kumar, P. (2004). Indirect sensing of insulin-induced hypoglycaemia by the carotid body in the rat. *The Journal of Physiology*, *556*(Pt 1), 255–266.
- Blaak, E. E., van Baak, M. A., Kemerink, G. J., Pakbiers, M. T. W., Heidendal, G. A. K., & Saris, W. H. M. (1995). β-adrenergic stimulation and abdominal subcutaneous fat blood flow in lean, obese, and reduced-obese subjects. *Metabolism*, *44*(2), 183–187.
- Blondin, D. P., Nielsen, S., Kuipers, E. N., Severinsen, M. C., Jensen, V. H., Miard, S., Jespersen, N. Z., Kooijman, S., Boon, M. R., Fortin, M., Phoenix, S., Frisch, F., Guérin, B., Turcotte, É. E., Haman, F., Richard, D., Picard, F., Rensen, P. C. N., Scheele, C., & Carpentier, A. C. (2020). Human Brown Adipocyte Thermogenesis Is Driven by β2-AR Stimulation. *Cell Metabolism*, *32*(2), 287-300.e7.
- Boucher, J., Kleinridders, A., & Kahn, C. R. (2014). Insulin Receptor Signaling in Normal and Insulin-Resistant States. *Cold Spring Harbor Perspectives in Biology*, *6*(1), a009191.

- Braun, K., Oeckl, J., Westermeier, J., Li, Y., & Klingenspor, M. (2018). Non-adrenergic control of lipolysis and thermogenesis in adipose tissues. *Journal of Experimental Biology*, *221*(Suppl 1), jeb165381.
- Brunner, E. j., Hemingway, H., Walker, B. r., Page, M., Clarke, P., Juneja, M., Shipley, M. j., Kumari, M., Andrew, R., Seckl, J. r., Papadopoulos, A., Checkley, S., Rumley, A., Lowe, G. d. o., Stansfeld, S. a., & Marmot, M. g. (2002). Adrenocortical, Autonomic, and Inflammatory Causes of the Metabolic Syndrome. *Circulation*, *106*(21), 2659–2665.
- Buemann, B., Toubro, S., & Astrup, A. (2000). Effects of the two β 3 -agonists, ZD7114 and ZD2079 on 24 hour energy expenditure and respiratory quotient in obese subjects. *International Journal of Obesity*, *24*(12), 1553–1560.
- Bukowiecki, L. J., Geloen, A., & Collet, A. J. (1986). Proliferation and differentiation of brown adipocytes from interstitial cells during cold acclimation. *American Journal of Physiology-Cell Physiology*.
- Caballero-Eraso, C., Shin, M., Pho, H., Kim, L. J., Pichard, L. E., Wu, Z., Gu, C., Berger, S., Pham, L., Yeung, H. (Bonnie), Shirahata, M., Schwartz, A. R., Tang, W. (Winnie), Sham, J. S. K., & Polotsky, V. Y. (2019). Leptin acts in the carotid bodies to increase minute ventilation during wakefulness and sleep and augment the hypoxic ventilatory response. *The Journal of Physiology*, *597*(1), 151–172.
- Calderon-Dominguez, M., Alcalá, M., Sebastián, D., Zorzano, A., Viana, M., Serra, D., & Herrero, L. (2017). Brown Adipose Tissue Bioenergetics: A New Methodological Approach. *Advanced Science*, *4*(4), 1600274.
- Cancello, R., Tordjman, J., Poitou, C., Guilhem, G., Bouillot, J. L., Hugol, D., Coussieu, C., Basdevant, A., Hen, A. B., Bedossa, P., Guerre-Millo, M., & Clement, K. (2006). Increased Infiltration of Macrophages in Omental Adipose Tissue Is Associated With Marked Hepatic Lesions in Morbid Human Obesity. *Diabetes*, *55*(6), 1554–1561.
- Cannon, B., & Nedergaard, J. (2004). Brown Adipose Tissue: Function and Physiological Significance. *Physiological Reviews*, *84*(1), 277–359.

- Cantarin, M. P. M., Waldman, S., Doria, C., Frank, A. M., Maley, W. R., Ramirez, C. B., Keith, S. W., & Falkner, B. (2013). The adipose tissue production of adiponectin is increased in end stage renal disease. *Kidney international*, *83*(3), 487–494.
- Castillo-Quan, J. I. (2012). From white to brown fat through the PGC-1 α -dependent myokine irisin: Implications for diabetes and obesity. *Disease Models & Mechanisms*, *5*(3), 293–295.
- Chadt, A., Immisch, A., de Wendt, C., Springer, C., Zhou, Z., Stermann, T., Holman, G. D., Loffing-Cueni, D., Loffing, J., Joost, H.-G., & Al-Hasani, H. (2015). "Deletion of both Rab-GTPase—activating proteins TBC1D1 and TBC1D4 in mice eliminates insulin- and AlCAR-stimulated glucose transport [corrected]. *Diabetes*, *64*(3), 746–759.
- Chait, A., & den Hartigh, L. J. (2020). Adipose Tissue Distribution, Inflammation and Its Metabolic Consequences, Including Diabetes and Cardiovascular Disease. *Frontiers in Cardiovascular Medicine*, 7, 22.
- Chan, J. L., Heist, K., DePaoli, A. M., Veldhuis, J. D., & Mantzoros, C. S. (2003). The role of falling leptin levels in the neuroendocrine and metabolic adaptation to short-term starvation in healthy men. *Journal of Clinical Investigation*, *111*(9), 1409–1421.
- Cho, K. W., Zamarron, B. F., Muir, L. A., Singer, K., Porsche, C. E., DelProposto, J. B., Geletka, L., Meyer, K. A., O'Rourke, R. W., & Lumeng, C. N. (2016). Adipose Tissue Dendritic Cells are Independent Contributors to Obesity-Induced Inflammation and Insulin Resistance*. *Journal of immunology (Baltimore, Md. : 1950), 197*(9), 3650–3661.
- Choi, C. S., Kim, Y.-B., Lee, F. N., Zabolotny, J. M., Kahn, B. B., & Youn, J. H. (2002). Lactate induces insulin resistance in skeletal muscle by suppressing glycolysis and impairing insulin signaling. *American Journal of Physiology-Endocrinology and Metabolism*, 283(2).
- Cohen, P., & Spiegelman, B. M. (2015). Brown and Beige Fat: Molecular Parts of a Thermogenic Machine. *Diabetes*, *64*(7), 2346–2351.
- Cohen, P., Zhao, C., Cai, X., Montez, J. M., Rohani, S. C., Feinstein, P., Mombaerts, P., & Friedman, J. M. (2001). Selective deletion of leptin receptor in neurons leads to obesity. *Journal of Clinical Investigation*, *108*(8), 1113–1121.

- Collins, S., Kuhn, C. M., Petro, A. E., Swick, A. G., Chrunyk, B. A., & Surwit, R. S. (1996). Role of leptin in fat regulation. *Nature*, *380*(6576), 677–677.
- Conde, S. V., Sacramento, J. F., Guarino, M. P., Gonzalez, C., Obeso, A., Diogo, L. N., Monteiro, E. C., & Ribeiro, M. J. (2014). Carotid body, insulin, and metabolic diseases: Unraveling the links. *Frontiers in Physiology*, *5*, 418.
- Considine, R. V., Kriauciunas, A., Ohannesian, J. P., & Bauer, T. L. (1996). Serum Immunoreactive-Leptin Concentrations in Normal-Weight and Obese Humans. *THE NEW ENGLAND JOURNAL OF MEDICINE*, 334(5), 4.
- Cracchiolo, M., Sacramento, J. F., Mazzoni, A., Panarese, A., Carpaneto, J., Conde, S. V., & Micera, S. (2019a). Decoding Neural Metabolic Markers From the Carotid Sinus Nerve in a Type 2 Diabetes Model. *IEEE Transactions on Neural Systems and Rehabilitation Engineering*, *27*(10), 2034–2043.
- Cracchiolo, M., Sacramento, J. F., Mazzoni, A., Panarese, A., Carpaneto, J., Conde, S. V., & Micera, S. (2019b). High frequency shift in Carotid Sinus Nerve and Sympathetic Nerve activity in Type 2 Diabetic Rat Model*. *2019 9th International IEEE/EMBS Conference on Neural Engineering (NER)*, 498–501.
- Cramer, J. A., Wiggins, R. H., Fudim, M., Engelman, Z. J., Sobotka, P. A., & Shah, L. M. (2014). Carotid body size on CTA: Correlation with comorbidities. *Clinical Radiology*, *69*(1), e33–e36. https://doi.org/10.1016/j.crad.2013.08.016
- Cunha-Guimaraes, J. P., Guarino, M. P., Timóteo, A. T., Caires, I., Sacramento, J. F., Ribeiro, M. J., Selas, M., Santiago, J. C. P., Mota-Carmo, M., & Conde, S. V. (2020). Carotid body chemosensitivity: Early biomarker of dysmetabolism in humans. *European Journal of Endocrinology*, *182*(6), 549–557.
- Cypess, A. M., Weiner, L. S., Roberts-Toler, C., Elía, E. F., Kessler, S. H., Kahn, P. A., English, J., Chatman, K., Trauger, S. A., Doria, A., & Kolodny, G. M. (2015). Activation of Human Brown Adipose Tissue by a β3-Adrenergic Receptor Agonist. *Cell metabolism*, *21*(1), 33–38.

- de Meis, L., Ketzer, L. A., da Costa, R. M., de Andrade, I. R., & Benchimol, M. (2010). Fusion of the Endoplasmic Reticulum and Mitochondrial Outer Membrane in Rats Brown Adipose Tissue: Activation of Thermogenesis by Ca2+. *PLoS ONE*, *5*(3), e9439.
- DeFronzo, R. A., & Tripathy, D. (2009). Skeletal Muscle Insulin Resistance Is the Primary Defect in Type 2 Diabetes. *Diabetes Care*, *32*(Suppl 2), S157–S163.
- Del Rio, R., Marcus, N. J., & Schultz, H. D. (2013a). Inhibition of hydrogen sulfide restores normal breathing stability and improves autonomic control during experimental heart failure. *Journal of Applied Physiology*, *114*(9), 1141–1150.
- Del Rio, R., Marcus, N. J., & Schultz, H. D. (2013b). CAROTID CHEMORECEPTOR ABLATION IMPROVES SURVIVAL IN HEART FAILURE: RESCUING AUTONOMIC CONTROL OF CARDIORESPIRATORY FUNCTION. *Journal of the American College of Cardiology*, *62*(25), 10.1016/j.jacc.2013.07.079.
- Dick, T. E., Hsieh, Y.-H., Wang, N., & Prabhakar, N. (2007). Acute intermittent hypoxia increases both phrenic and sympathetic nerve activities in the rat. *Experimental Physiology*, *92*(1), 87–97.
- Enerbäck, S., Jacobsson, A., Simpson, E. M., Guerra, C., Yamashita, H., Harper, M.-E., & Kozak, L. P. (1997). Mice lacking mitochondrial uncoupling protein are cold-sensitive but not obese. *Nature*, *387*(6628), 90–94.
- Engin, A. (2017). Adipose Tissue Hypoxia in Obesity and Its Impact on Preadipocytes and Macrophages: Hypoxia Hypothesis. Em A. B. Engin & A. Engin (Eds.), *Obesity and Lipotoxicity* (Vol. 960, pp. 305–326). Springer International Publishing.
- Esler, M., Rumantir, M., Wiesner, G., Kaye, D., Hastings, J., & Lambert, G. (2001). Sympathetic Nervous System and Insulin Resistance: From Obesity to Diabetes. *American Journal of Hypertension*, *14*(S7), 304S-309S.
- Fagius, J. (2003). Sympathetic nerve activity in metabolic control some basic concepts. *Acta Physiologica Scandinavica*, *177*(3), 337–343.
- Fedorenko, A., Lishko, P. V., & Kirichok, Y. (2012). Mechanism of Fatty-Acid-Dependent UCP1 Uncoupling in Brown Fat Mitochondria. *Cell*, *151*(2), 400–413.

- Fielding, B. A., & Frayn, K. N. (1998). Lipoprotein lipase and the disposition of dietary fatty acids. *British Journal of Nutrition*, *80*(6), 495–502.
- Fitzgerald, R. S., Shirahata, M., Chang, I., & Kostuk, E. (2009). The impact of hypoxia and low glucose on the release of acetylcholine and ATP from the incubated cat carotid body. *Brain Research*, 1270, 39–44.
- Franck, N., Stenkula, K. G., Öst, A., Lindström, T., Strålfors, P., & Nystrom, F. H. (2007). Insulin-induced GLUT4 translocation to the plasma membrane is blunted in large compared with small primary fat cells isolated from the same individual. *Diabetologia*, 50(8), 1716–1722.
- Frayn, K. (2002). Adipose tissue as a buffer for daily lipid flux. *Diabetologia*, *45*(9), 1201–1210.
- Frayn, K. N., Karpe, F., Fielding, B. A., Macdonald, I. A., & Coppack, S. W. (2003). Integrative physiology of human adipose tissue. *International Journal of Obesity*, *27*(8), 875–888.
- Freeman, A. M., & Pennings, N. (2021). Insulin Resistance. Em *StatPearls*. StatPearls Publishing. http://www.ncbi.nlm.nih.gov/books/NBK507839/
- Frontini, A., & Cinti, S. (2010). Distribution and Development of Brown Adipocytes in the Murine and Human Adipose Organ. *Cell Metabolism*, *11*(4), 253–256.
- Giannoni, A., Emdin, M., Bramanti, F., Iudice, G., Francis, D. P., Barsotti, A., Piepoli, M., & Passino, C. (2009). Combined Increased Chemosensitivity to Hypoxia and Hypercapnia as a Prognosticator in Heart Failure. *Journal of the American College of Cardiology*, *53*(21), 1975–1980.
- Glick, Z., & Raum, W. J. (1986). Norepinephrine turnover in brown adipose tissue is stimulated by a single meal. *American Journal of Physiology-Regulatory, Integrative and Comparative Physiology*, 251(1), R13–R17.
- Gonzalez, C., Agapito, M. T., Rocher, A., Gomez-Niño, A., Rigual, R., Castañeda, J., Conde, S. V., & Obeso, A. (2010). A revisit to O2 sensing and transduction in the carotid body chemoreceptors in the context of reactive oxygen species biology. *Respiratory Physiology & Neurobiology*, *174*(3), 317–330.

- Gonzalez, C., Almaraz, L., Obeso, A., & Rigual, R. (1994). Carotid body chemoreceptors: From natural stimuli to sensory discharges. *Physiological Reviews*, *74*(4), 829–898.
- Goossens, G. H., Bizzarri, A., Venteclef, N., Essers, Y., Cleutjens, J. P., Konings, E., Jocken, J. W. E., Čajlaković, M., Ribitsch, V., Clément, K., & Blaak, E. E. (2011). Increased Adipose Tissue Oxygen Tension in Obese Compared With Lean Men Is Accompanied by Insulin Resistance, Impaired Adipose Tissue Capillarization, and Inflammation. *Circulation*, 124(1), 67–76.
- Goossens, G. H., & Blaak, E. E. (2015). Adipose Tissue Dysfunction and Impaired Metabolic Health in Human Obesity: A Matter of Oxygen? *Frontiers in Endocrinology*, *6*, 55.
- Granneman, J. G. (1995). Why do adipocytes make the β 3 adrenergic receptor? *Cellular Signalling*, 7(1), 9–15.
- Granneman, J. G., Burnazi, M., Zhu, Z., & Schwamb, L. A. (2003). White adipose tissue contributes to UCP1-independent thermogenesis. *American Journal of Physiology-Endocrinology and Metabolism*, 285(6), E1230–E1236.
- Grassi, G., Dell'Oro, R., Facchini, A., Quarti Trevano, F., Bolla, G. B., & Mancia, G. (2004). Effect of central and peripheral body fat distribution on sympathetic and baroreflex function in obese normotensives. *Journal of Hypertension*, *22*(12), 2363–2369.
- Grassi, G., Seravalle, G., Cattaneo, B. M., Bolla, G. B., Lanfranchi, A., Colombo, M., Giannattasio, C., Brunani, A., Cavagnini, F., & Mancia, G. (1995). Sympathetic Activation in Obese Normotensive Subjects. *Hypertension*, *25*(4), 560–563.
- Grassi, G., Seravalle, G., Dell'Oro, R., Turri, C., Pasqualinotto, L., Colombo, M., & Mancia, G. (2001). Participation of the Hypothalamus-Hypophysis Axis in the Sympathetic Activation of Human Obesity. *Hypertension*, *38*(6), 1316–1320.
- Greenberg, H. E., Sica, A., Batson, D., & Scharf, S. M. (1999). Chronic intermittent hypoxia increases sympathetic responsiveness to hypoxia and hypercapnia. *Journal of Applied Physiology*, *86*(1), 298–305.

- Halaas, J., Gajiwala, K., Maffei, M., Cohen, S., Chait, B., Rabinowitz, D., Lallone, R., Burley, S., & Friedman, J. (1995). Weight-reducing effects of the plasma protein encoded by the obese gene. *Science*, *269*(5223), 543–546.
- Halaas, J. L., Boozer, C., Blair-West, J., Fidahusein, N., Denton, D. A., & Friedman, J. M. (1997). Physiological response to long-term peripheral and central leptin infusion in lean and obese mice. *Proceedings of the National Academy of Sciences of the United States of America*, *94*(16), 8878–8883.
- Hany, T. F., Gharehpapagh, E., Kamel, E. M., Buck, A., Himms-Hagen, J., & von Schulthess, G. K. (2002). Brown adipose tissue: A factor to consider in symmetrical tracer uptake in the neck and upper chest region. *European Journal of Nuclear Medicine and Molecular Imaging*, *29*(10), 1393–1398.
- Harald, G., Meier, S., Brown, R. H., O'Donnell, C. P., Wayne, M., & Tankersley, C. G. (2004). The Effect of Leptin on the Ventilatory Responseto Hyperoxia. *Experimental Lung Research*, *30*(7), 559–570.
- Harms, M., & Seale, P. (2013). Brown and beige fat: Development, function and therapeutic potential. *Nature Medicine*, *19*(10), 1252–1263.
- Harris, C. A., Haas, J. T., Streeper, R. S., Stone, S. J., Kumari, M., Yang, K., Han, X., Brownell, N., Gross, R. W., Zechner, R., & Farese, R. V. (2011). DGAT enzymes are required for triacylglycerol synthesis and lipid droplets in adipocytes. *Journal of Lipid Research*, *52*(4), 657–667.
- Hashimoto, T., Hussien, R., Oommen, S., Gohil, K., & Brooks, G. A. (2007). Lactate sensitive transcription factor network in L6 cells: Activation of MCT1 and mitochondrial biogenesis. *The FASEB Journal*, *21*(10), 2602–2612.
- Haynes, W. G., Morgan, D. A., Walsh, S. A., Mark, A. L., & Sivitz, W. I. (1997a). Receptor-mediated regional sympathetic nerve activation by leptin. *Journal of Clinical Investigation*, 100(2), 270–278.

- Haynes, W. G., Morgan, D. A., Walsh, S. A., Mark, A. L., & Sivitz, W. I. (1997b). Receptor-mediated regional sympathetic nerve activation by leptin. *Journal of Clinical Investigation*, 100(2), 270–278.
- He, L., Chen, J., Dinger, B., Sanders, K., Sundar, K., Hoidal, J., & Fidone, S. (2002). Characteristics of carotid body chemosensitivity in NADPH oxidase-deficient mice. *American Journal of Physiology-Cell Physiology*, 282(1), C27–C33.
- Hosogai, N., Fukuhara, A., Oshima, K., Miyata, Y., Tanaka, S., Segawa, K., Furukawa, S., Tochino, Y., Komuro, R., Matsuda, M., & Shimomura, I. (2007). Adipose Tissue Hypoxia in Obesity and Its Impact on Adipocytokine Dysregulation. *Diabetes*, *56*(4), 901–911.
- Hsieh, K., Lee, Y. K., Londos, C., Raaka, B. M., Dalen, K. T., & Kimmel, A. R. (2012). Perilipin family members preferentially sequester to either triacylglycerol- or cholesteryl esterspecific intracellular lipid storage droplets. *Journal of Cell Science*, jcs.104943.
- Hukshorn, C. J., Saris, W. H. M., Westerterp-Plantenga, M. S., Farid, A. R., Smith, F. J., & Campfield, L. A. (2000). *Weekly Subcutaneous Pegylated Recombinant Native Human Leptin (PEG-OB) Administration in Obese Men.* 85(11), 7.
- IDF Diabetes Atlas Eighth Edition 2017. [(accessed on 10 October 2018)];2018 Available online: https://www.idf.org/aboutdiabetes/what-is-diabetes/facts-figures.html.
- Inokuma, K., Ogura-Okamatsu, Y., Toda, C., Kimura, K., Yamashita, H., & Saito, M. (2005).

 Uncoupling Protein 1 Is Necessary for Norepinephrine-Induced Glucose Utilization in

 Brown Adipose Tissue. *Diabetes*, *54*(5), 1385–1391.
- Ip, M. S. M., Lam, K. S. L., Ho, C., Tsang, K. W. T., & Lam, W. (2000). Serum Leptin and Vascular Risk Factors in Obstructive Sleep Apnea. *CHEST*, *118*(3), 580–586.
- Iturriaga, R., Rey, S., & Del Río, R. (2005). Cardiovascular and ventilatory acclimatization induced by chronic intermittent hypoxia: A role for the carotid body in the pathophysiology of sleep apnea. *Biological Research*, *38*(4), 335–340.
- Kadowaki, T., Yamauchi, T., Kubota, N., Hara, K., Ueki, K., & Tobe, K. (2006). Adiponectin and adiponectin receptors in insulin resistance, diabetes, and the metabolic syndrome. *Journal of Clinical Investigation*, *116*(7), 1784–1792.

- Kajimura, S., & Saito, M. (2014). A New Era in Brown Adipose Tissue Biology: Molecular Control of Brown Fat Development and Energy Homeostasis. *Annual review of physiology*, *76*, 225–249.
- Kajimura, S., Seale, P., Kubota, K., Lunsford, E., Frangioni, J. V., Gygi, S. P., & Spiegelman, B. M. (2009). Initiation of myoblast/brown fat switch through a PRDM16-C/EBP-β transcriptional complex. *Nature*, *460*(7259), 1154–1158.
- Kalil, G. Z., & Haynes, W. G. (2012). Sympathetic nervous system in obesity-related hypertension: Mechanisms and clinical implications. *Hypertension research*: official journal of the Japanese Society of Hypertension, 35(1), 4–16.
- Kazak, L., Chouchani, E. T., Jedrychowski, M. P., Erickson, B. K., Shinoda, K., Cohen, P., Vetrivelan, R., Lu, G. Z., Laznik-Bogoslavski, D., Hasenfuss, S. C., Kajimura, S., Gygi, S. P., & Spiegelman, B. M. (2015). A Creatine-Driven Substrate Cycle Enhances Energy Expenditure and Thermogenesis in Beige Fat. *Cell*, *163*(3), 643–655.
- Kersten, S. (2014). Physiological regulation of lipoprotein lipase. *Biochimica et Biophysica Acta (BBA) Molecular and Cell Biology of Lipids*, 1841(7), 919–933.
- Kim, S. M., Lun, M., Wang, M., Senyo, S. E., Guillermier, C., Patwari, P., & Steinhauser, M. L. (2014). Loss of White Adipose Hyperplastic Potential Is Associated with Enhanced Susceptibility to Insulin Resistance. *Cell metabolism*, *20*(6), 1049–1058.
- Kim, W., & Kaelin, W. G. (2003). The von Hippel–Lindau tumor suppressor protein: New insights into oxygen sensing and cancer. *Current Opinion in Genetics & Development*, 13(1), 55–60.
- Klok, M. D., Jakobsdottir, S., & Drent, M. L. (2007). The role of leptin and ghrelin in the regulation of food intake and body weight in humans: A review. *Obesity Reviews*, 8(1), 21–34.
- Kojta, I., Chacińska, M., & Błachnio-Zabielska, A. (2020). Obesity, Bioactive Lipids, and Adipose Tissue Inflammation in Insulin Resistance. *Nutrients*, *12*(5), 1305.

- Konstantinides, S., Schäfer, K., Koschnick, S., & Loskutoff, D. J. (2001). Leptin-dependent platelet aggregation and arterial thrombosis suggests a mechanism for atherothrombotic disease in obesity. *Journal of Clinical Investigation*, *108*(10), 1533–1540.
- Koopman, F. A., Stoof, S. P., Straub, R. H., van Maanen, M. A., Vervoordeldonk, M. J., & Tak, P. P. (2011). Restoring the Balance of the Autonomic Nervous System as an Innovative Approach to the Treatment of Rheumatoid Arthritis. *Molecular Medicine*, *17*(9–10), 937–948.
- Koyama, Y., Coker, R. H., Stone, E. E., Lacy, D. B., Jabbour, K., Williams, P. E., & Wasserman, D. H. (2000). Evidence that carotid bodies play an important role in glucoregulation in vivo. *Diabetes*, *49*(9), 1434–1442.
- Kumar, P., & Bin-Jaliah, I. (2007). Adequate stimuli of the carotid body: More than an oxygen sensor? *Respiratory Physiology & Neurobiology*, *157*(1), 12–21.
- Kuryłowicz, A., & Puzianowska-Kuźnicka, M. (2020). Induction of Adipose Tissue Browning as a Strategy to Combat Obesity. *International Journal of Molecular Sciences*, *21*(17), 6241.
- Ladoux, A., Peraldi, P., Chignon-Sicard, B., & Dani, C. (2021). Distinct Shades of Adipocytes Control the Metabolic Roles of Adipose Tissues: From Their Origins to Their Relevance for Medical Applications. *Biomedicines*, *9*(1), 40.
- Lambert, E. A., Straznicky, N. E., & Lambert, G. W. (2013). A sympathetic view of human obesity. *Clinical Autonomic Research*, *23*(1), 9–14.
- LeBlanc, J., & Brondel, L. (1985). Role of palatability on meal-induced thermogenesis in human subjects. *American Journal of Physiology-Endocrinology and Metabolism*, *248*(3), E333–E336.
- Lee, Z. S. K., Critchley, J. A. J. H., Tomlinson, B., Young, R. P., Thomas, G. N., Cockram, C. S., Chan, T. Y. K., & Chan, J. C. N. (2001). Urinary epinephrine and norepinephrine interrelations with obesity, insulin, and the metabolic syndrome in Hong Kong Chinese. *Metabolism Clinical and Experimental*, *50*(2), 135–143.

- Lembo, G., Napoli, R., Capaldo, B., Rendina, V., Iaccarino, G., Volpe, M., Trimarco, B., & Saccà, L. (1992). Abnormal sympathetic overactivity evoked by insulin in the skeletal muscle of patients with essential hypertension. *Journal of Clinical Investigation*, *90*(1), 24–29.
- Lempesis, I. G., van Meijel, R. L. J., Manolopoulos, K. N., & Goossens, G. H. (2020). Oxygenation of adipose tissue: A human perspective. *Acta Physiologica (Oxford, England)*, 228(1), e13298.
- Li, Y., Fromme, T., Schweizer, S., Schöttl, T., & Klingenspor, M. (2014). Taking control over intracellular fatty acid levels is essential for the analysis of thermogenic function in cultured primary brown and brite/beige adipocytes. *EMBO Reports*, *15*(10), 1069–1076.
- Lin, Q., Lee, Y.-J., & Yun, Z. (2006). Differentiation Arrest by Hypoxia*. *Journal of Biological Chemistry*, *281*(41), 30678–30683.
- Lindström, P. (2007). The Physiology of Obese-Hyperglycemic Mice [ob/ob Mice]. *The Scientific World Journal*, *7*, 666–685.
- Liu, A., McLaughlin, T., Liu, T., Sherman, A., Yee, G., Abbasi, F., Lamendola, C., Morton, J., Cushman, S. W., Reaven, G. M., & Tsao, P. S. (2009). Differential Intra-abdominal Adipose Tissue Profiling in Obese, Insulin-resistant Women. *Obesity surgery*, *19*(11), 1564–1573.
- Liu, C., Wu, J., Zhu, J., Kuei, C., Yu, J., Shelton, J., Sutton, S. W., Li, X., Yun, S. J., Mirzadegan, T., Mazur, C., Kamme, F., & Lovenberg, T. W. (2009). Lactate Inhibits Lipolysis in Fat Cells through Activation of an Orphan G-protein-coupled Receptor, GPR81. *Journal of Biological Chemistry*, 284(5), 2811–2822.
- Liu, F., He, J., Wang, H., Zhu, D., & Bi, Y. (2020). Adipose Morphology: A Critical Factor in Regulation of Human Metabolic Diseases and Adipose Tissue Dysfunction. *Obesity Surgery*, *30*(12), 5086–5100.
- Liu, J., Divoux, A., Sun, J., Zhang, J., Clément, K., Glickman, J. N., Sukhova, G. K., Wolters, P. J., Du, J., Gorgun, C. Z., Doria, A., Libby, P., Blumberg, R. S., Kahn, B. B., Hotamisligil, G. S., & Shi, G.-P. (2009). Deficiency and pharmacological stabilization of mast cells reduce dietinduced obesity and diabetes in mice. *Nature medicine*, *15*(8), 940–945.

- Longo, M., Zatterale, F., Naderi, J., Parrillo, L., Formisano, P., Raciti, G. A., Beguinot, F., & Miele, C. (2019). Adipose Tissue Dysfunction as Determinant of Obesity-Associated Metabolic Complications. *International Journal of Molecular Sciences*, *20*(9), 2358.
- Luo, L., & Liu, M. (2016). Adipose tissue in control of metabolism. *The Journal of endocrinology*, *231*(3), R77–R99.
- Mahmoud, A. D., Lewis, S., Juričić, L., Udoh, U.-A., Hartmann, S., Jansen, M. A., Ogunbayo, O. A., Puggioni, P., Holmes, A. P., Kumar, P., Navarro-Dorado, J., Foretz, M., Viollet, B., Dutia, M. B., Marshall, I., & Evans, A. M. (2016). AMP-activated Protein Kinase Deficiency Blocks the Hypoxic Ventilatory Response and Thus Precipitates Hypoventilation and Apnea. *American Journal of Respiratory and Critical Care Medicine*, 193(9), 1032–1043.
- Marin, J. M., Carrizo, S. J., Vicente, E., & Agusti, A. G. N. (2005). Long-term cardiovascular outcomes in men with obstructive sleep apnoea-hypopnoea with or without treatment with continuous positive airway pressure: An observational study. *Lancet (London, England)*, 365(9464), 1046–1053.
- Marshall, J. A., Grunwald, G. K., Donahoo, W. T., Scarbro, S., & Shetterly, S. M. (2000). Percent Body Fat and Lean Mass Explain the Gender Difference in Leptin: Analysis and Interpretation of Leptin in Hispanic and Non-Hispanic White Adults. *Obesity Research*, 8(8), 543–552.
- Marshall, J. M. (1994). Peripheral chemoreceptors and cardiovascular regulation. *Physiological Reviews*, *74*(3), 543–594.
- Masuzaki, H., Ogawa, Y., Hosoda, K., Kawada, T., Fushiki, T., & Nakao, K. (1995). Augmented Expression of the obese Gene in the Adipose Tissue from Rats Fed High-Fat Diet. *Biochemical and Biophysical Research Communications*, *216*(1), 355–358.
- McBryde, F. D., Abdala, A. P., Hendy, E. B., Pijacka, W., Marvar, P., Moraes, D. J. A., Sobotka, P. A., & Paton, J. F. R. (2013). The carotid body as a putative therapeutic target for the treatment of neurogenic hypertension. *Nature Communications*, *4*(1), 2395.
- Meis, L. de. (2003). Brown Adipose Tissue Ca2+-ATPase: UNCOUPLED ATP HYDROLYSIS AND THERMOGENIC ACTIVITY *. *Journal of Biological Chemistry*, *278*(43), 41856–41861.

- Meis, L. de, Arruda, A. P., Costa, R. M. da, & Benchimol, M. (2006). Identification of a Ca2+-ATPase in Brown Adipose Tissue Mitochondria: REGULATION OF THERMOGENESIS BY ATP AND Ca2+*. *Journal of Biological Chemistry*, *281*(24), 16384–16390.
- Messenger, S. A., Moreau, J. M., & Ciriello, J. (2012). Intermittent hypoxia and systemic leptin administration induces pSTAT3 and Fos/Fra-1 in the carotid body. *Brain Research*, *1446*, 56–70.
- Miranda, S., González-Rodríguez, Á., Revuelta-Cervantes, J., Rondinone, C. M., & Valverde, Á. M. (2010). Beneficial effects of PTP1B deficiency on brown adipocyte differentiation and protection against apoptosis induced by pro- and anti-inflammatory stimuli. *Cellular Signalling*, *22*(4), 645–659.
- Mittendorfer, B., Horowitz, J. F., DePaoli, A. M., McCamish, M. A., Patterson, B. W., & Klein, S. (2011). Recombinant Human Leptin Treatment Does Not Improve Insulin Action in Obese Subjects With Type 2 Diabetes. *Diabetes*, *60*(5), 1474–1477.
- Mugabo, Y., & Lim, G. E. (2018). Scaffold Proteins: From Coordinating Signaling Pathways to Metabolic Regulation. *Endocrinology*, *159*(11), 3615–3630.
- Muntzel, M. S., Al-Naimi, O. A. S., Barclay, A., & Ajasin, D. (2012). THE CAFETERIA DIET INCREASES FAT MASS AND CHRONICALLY ELEVATES LUMBAR SYMPATHETIC NERVE ACTIVITY IN RATS. *Hypertension*, *60*(6), 1498–1502.
- Murano, I., Barbatelli, G., Parisani, V., Latini, C., Muzzonigro, G., Castellucci, M., & Cinti, S. (2008). Dead adipocytes, detected as crown-like structures, are prevalent in visceral fat depots of genetically obese mice. *Journal of Lipid Research*, *49*(7), 1562–1568.
- Nakamura, K. (2011). Central circuitries for body temperature regulation and fever. American Journal of Physiology-Regulatory, Integrative and Comparative Physiology, 301(5), R1207–R1228.
- Narkiewicz, K., Montano, N., Cogliati, C., van de Borne, P. J. H., Dyken, M. E., & Somers, V. K. (1998). Altered Cardiovascular Variability in Obstructive Sleep Apnea. *Circulation*, *98*(11), 1071–1077.

- Narkiewicz, K., Ratcliffe, L. E. K., Hart, E. C., Briant, L. J. B., Chrostowska, M., Wolf, J., Szyndler, A., Hering, D., Abdala, A. P., Manghat, N., Burchell, A. E., Durant, C., Lobo, M. D., Sobotka, P. A., Patel, N. K., Leiter, J. C., Engelman, Z. J., Nightingale, A. K., & Paton, J. F. R. (2016). Unilateral Carotid Body Resection in Resistant Hypertension. *JACC: Basic to Translational Science*, 1(5), 313–324.
- Narkiewicz, K., van de Borne, P. J. H., Cooley, R. L., Dyken, M. E., & Somers, V. K. (1998). Sympathetic Activity in Obese Subjects With and Without Obstructive Sleep Apnea. *Circulation*, *98*(8), 772–776.
- Narkiewicz, K., van de Borne, P. J. H., Montano, N., Dyken, M. E., Phillips, B. G., & Somers, V. K. (1998). Contribution of Tonic Chemoreflex Activation to Sympathetic Activity and Blood Pressure in Patients With Obstructive Sleep Apnea. *Circulation*, *97*(10), 943–945.
- Nielsen, T. S., Jessen, N., Jørgensen, J. O. L., Møller, N., & Lund, S. (2014). Dissecting adipose tissue lipolysis: Molecular regulation and implications for metabolic disease. *Journal of Molecular Endocrinology*, *52*(3), R199–R222.
- Nikolaos Perakakis, M. D., Olivia M. Farr, P., & Christos S. Mantzoros, M. D. (2021). Leptin in Leanness and Obesity: JACC State-of-the-Art Review. *Journal of the American College of Cardiology*.
- Nurse, C. A. (2014). Synaptic and paracrine mechanisms at carotid body arterial chemoreceptors. *The Journal of Physiology*, *592*(16), 3419–3426.
- O'Dea, K., Esler, M., Leonard, P., Stockigt, J. R., & Nestel, P. (1982). Noradrenaline turnover during under- and over-eating in normal weight subjects. *Metabolism Clinical and Experimental*, *31*(9), 896–899.
- O'Donnell, C. P., Schaub, C. D., Haines, A. S., Berkowitz, D. E., Tankersley, C. G., Schwartz, A. R., & Smith, P. L. (1999). Leptin Prevents Respiratory Depression in Obesity. *American Journal of Respiratory and Critical Care Medicine*, *159*(5), 1477–1484.
- Ogawa, Y., Masuzaki, H., Ebihara, K., Shintani, M., Aizawa-Abe, M., Miyanaga, F., & Nakao, K. (2002). Pathophysiogical role of leptin in lifestyle-related diseases: Studies with

- transgenic skinny mice overexpressing leptin. *Journal of Diabetes and Its Complications*, 16(1), 119–122.
- Okamatsu-Ogura, Y., Fukano, K., Tsubota, A., Nio-Kobayashi, J., Nakamura, K., Morimatsu, M., Sakaue, H., Saito, M., & Kimura, K. (2017). Cell-cycle arrest in mature adipocytes impairs BAT development but not WAT browning, and reduces adaptive thermogenesis in mice. *Scientific Reports*, 7(1), 6648.
- Olea, E., Ribeiro, M. J., Gallego-Martin, T., Yubero, S., Rigual, R., Masa, J. F., Obeso, A., Conde, S. V., & Gonzalez, C. (2015). The Carotid Body Does Not Mediate the Acute Ventilatory Effects of Leptin. Em C. Peers, P. Kumar, C. Wyatt, E. Gauda, C. A. Nurse, & N. Prabhakar (Eds.), *Arterial Chemoreceptors in Physiology and Pathophysiology* (pp. 379–385). Springer International Publishing.
- O'Rourke, R., Metcalf, M., White, A., Madala, A., Winters, B., Maizlin, I., Jobe, B., Roberts, C., Slifka, M., & Marks, D. (2009). Depot-specific differences in inflammatory mediators and a role for NK cells and IFN-γ in inflammation in human adipose tissue. *International journal of obesity (2005)*, *33*(9), 978–990.
- Ortega-Sáenz, P., & López-Barneo, J. (2020). Physiology of the Carotid Body: From Molecules to Disease. *Annual Review of Physiology*, 82(1), 127–149.
- Ortega-Sáenz, P., Moreno-Domínguez, A., Gao, L., & López-Barneo, J. (2020). Molecular Mechanisms of Acute Oxygen Sensing by Arterial Chemoreceptor Cells. Role of Hif2α. *Frontiers in Physiology*, *11*.
- Ortega-Sáenz, P., Pascual, A., Gómez-Díaz, R., & López-Barneo, J. (2006). Acute Oxygen Sensing in Heme Oxygenase-2 Null Mice. *The Journal of General Physiology*, *128*(4), 405–411.
- Pardal, R., & López-Barneo, J. (2002). Low glucose—sensing cells in the carotid body. *Nature Neuroscience*, *5*(3), 197–198.
- Pardal, R., Ortega-Sáenz, P., Durán, R., & López-Barneo, J. (2007). Glia-like Stem Cells Sustain Physiologic Neurogenesis in the Adult Mammalian Carotid Body. *Cell*, *131*(2), 364–377.

- Park, M.-Y., Kim, J., Chung, N., Park, H.-Y., Hwang, H., Han, J., So, J.-M., Lee, C.-H., Park, J., & Lim, K. (2020). Dietary Factors and Eating Behaviors Affecting Diet-Induced Thermogenesis in Obese Individuals: A Systematic Review. *Journal of Nutritional Science and Vitaminology*, 66(1), 1–9.
- Peppard, P. E., Young, T., Palta, M., & Skatrud, J. (2000). Prospective Study of the Association between Sleep-Disordered Breathing and Hypertension. *New England Journal of Medicine*, *342*(19), 1378–1384.
- Periasamy, M., Maurya, S. K., Sahoo, S. K., Singh, S., Reis, F. C. G., & Bal, N. C. (2017). Role of SERCA Pump in Muscle Thermogenesis and Metabolism. Em *Comprehensive Physiology* (pp. 879–890). American Cancer Society.
- Peterson, R. T., & Schreiber, S. L. (1999). Kinase phosphorylation: Keeping it all in the family. *Current Biology*, *9*(14), R521–R524.
- Pfannenberg, C., Werner, M. K., Ripkens, S., Stef, I., Deckert, A., Schmadl, M., Reimold, M., Häring, H.-U., Claussen, C. D., & Stefan, N. (2010). Impact of Age on the Relationships of Brown Adipose Tissue With Sex and Adiposity in Humans. *Diabetes*, *59*(7), 1789–1793.
- Phillips, B. G., Kato, M., Narkiewicz, K., Choe, I., & Somers, V. K. (2000). Increases in leptin levels, sympathetic drive, and weight gain in obstructive sleep apnea. *American Journal of Physiology-Heart and Circulatory Physiology*, *279*(1), H234–H237.
- Platero-Luengo, A., González-Granero, S., Durán, R., Díaz-Castro, B., Piruat, J. I., García-Verdugo, J. M., Pardal, R., & López-Barneo, J. (2014). An O2-Sensitive Glomus Cell-Stem Cell Synapse Induces Carotid Body Growth in Chronic Hypoxia. *Cell*, *156*(1), 291–303.
- Poher, A.-L., Altirriba, J., Veyrat-Durebex, C., & Rohner-Jeanrenaud, F. (2015). Brown adipose tissue activity as a target for the treatment of obesity/insulin resistance. *Frontiers in Physiology*, *6*, 4.
- Ponikowski, P., Chua, T. P., Anker, S. D., Francis, D. P., Doehner, W., Banasiak, W., Poole-Wilson, P. A., Piepoli, M. F., & Coats, A. J. S. (2001). Peripheral Chemoreceptor Hypersensitivity. *Circulation*, *104*(5), 544–549.

- Porzionato, A., Rucinski, M., Macchi, V., Stecco, C., Castagliuolo, I., Malendowicz, L. K., & De Caro, R. (2011). Expression of leptin and leptin receptor isoforms in the rat and human carotid body. *Brain Research*, *1385*, 56–67.
- Qatanani, M., & Lazar, M. A. (2007). Mechanisms of obesity-associated insulin resistance: Many choices on the menu. *Genes & Development*, *21*(12), 1443–1455.
- Rahmouni, K., Morgan, D. A., Morgan, G. M., Mark, A. L., & Haynes, W. G. (2005). Role of Selective Leptin Resistance in Diet-Induced Obesity Hypertension. *Diabetes*, *54*(7), 2012–2018.
- Rausch, M. E., Weisberg, S., Vardhana, P., & Tortoriello, D. V. (2008). Obesity in C57BL/6J mice is characterized by adipose tissue hypoxia and cytotoxic T-cell infiltration. *International Journal of Obesity*, *32*(3), 451–463.
- Reeves, S. R., Gozal, E., Guo, S. Z., Sachleben, L. R., Brittian, K. R., Lipton, A. J., & Gozal, D. (2003). Effect of long-term intermittent and sustained hypoxia on hypoxic ventilatory and metabolic responses in the adult rat. *Journal of Applied Physiology*, *95*(5), 1767–1774.
- Ribeiro, M. J., Sacramento, J. F., Gallego-Martin, T., Olea, E., Melo, B. F., Guarino, M. P., Yubero, S., Obeso, A., & Conde, S. V. (2018). High fat diet blunts the effects of leptin on ventilation and on carotid body activity. *The Journal of Physiology*, *596*(15), 3187–3199.
- Ribeiro, M. J., Sacramento, J. F., Gonzalez, C., Guarino, M. P., Monteiro, E. C., & Conde, S. V. (2013). Carotid Body Denervation Prevents the Development of Insulin Resistance and Hypertension Induced by Hypercaloric Diets. *Diabetes*, *62*(8), 2905–2916.
- Richard, A. J., White, U., Elks, C. M., & Stephens, J. M. (2000). Adipose Tissue: Physiology to Metabolic Dysfunction. Em K. R. Feingold, B. Anawalt, A. Boyce, G. Chrousos, W. W. de Herder, K. Dhatariya, K. Dungan, A. Grossman, J. M. Hershman, J. Hofland, S. Kalra, G. Kaltsas, C. Koch, P. Kopp, M. Korbonits, C. S. Kovacs, W. Kuohung, B. Laferrère, E. A. McGee, ... D. P. Wilson (Eds.), *Endotext*. MDText.com, Inc. http://www.ncbi.nlm.nih.gov/books/NBK555602/
- Rio, R. D. (2015). The carotid body and its relevance in pathophysiology. *Experimental Physiology*, 100(2), 121–123.

- Rooney, K., & Trayhurn, P. (2011). Lactate and the GPR81 receptor in metabolic regulation: Implications for adipose tissue function and fatty acid utilisation by muscle during exercise. *British Journal of Nutrition*, *106*(9), 1310–1316.
- Sacramento, J. F., Andrzejewski, K., Melo, B. F., Ribeiro, M. J., Obeso, A., & Conde, S. V. (2020). Exploring the Mediators that Promote Carotid Body Dysfunction in Type 2 Diabetes and Obesity Related Syndromes. *International Journal of Molecular Sciences*, 21(15), 5545.
- Sacramento, J. F., Chew, D. J., Melo, B. F., Donegá, M., Dopson, W., Guarino, M. P., Robinson, A., Prieto-Lloret, J., Patel, S., Holinski, B. J., Ramnarain, N., Pikov, V., Famm, K., & Conde, S. V. (2018). Bioelectronic modulation of carotid sinus nerve activity in the rat: A potential therapeutic approach for type 2 diabetes. *Diabetologia*, *61*(3), 700–710.
- Sacramento, J. F., Ribeiro, M. J., Rodrigues, T., Olea, E., Melo, B. F., Guarino, M. P., Fonseca-Pinto, R., Ferreira, C. R., Coelho, J., Obeso, A., Seiça, R., Matafome, P., & Conde, S. V. (2017). Functional abolition of carotid body activity restores insulin action and glucose homeostasis in rats: Key roles for visceral adipose tissue and the liver. *Diabetologia*, *60*(1), 158–168.
- Saito, M., Minokoshi, Y., & Shimazu, T. (1989). Metabolic and sympathetic nerve activities of brown adipose tissue in tube-fed rats. *American Journal of Physiology-Endocrinology and Metabolism*, *257*(3), E374–E378.
- Sakamoto, T., Nitta, T., Maruno, K., Yeh, Y.-S., Kuwata, H., Tomita, K., Goto, T., Takahashi, N., & Kawada, T. (2016). Macrophage infiltration into obese adipose tissues suppresses the induction of UCP1 level in mice. *American Journal of Physiology-Endocrinology and Metabolism*, *310*(8), E676–E687.
- Salans, L. B., Knittle, J. L., & Hirsch, J. (1968). The role of adipose cell size and adipose tissue insulin sensitivity in the carbohydrate intolerance of human obesity. *Journal of Clinical Investigation*, 47(1), 153–165.

- Sanner, B. M., Kollhosser, P., Buechner, N., Zidek, W., & Tepel, M. (2004). Influence of treatment on leptin levels in patients with obstructive sleep apnoea. *European Respiratory Journal*, *23*(4), 601–604.
- Santoleri, D., & Titchenell, P. M. (2018). Resolving the Paradox of Hepatic Insulin Resistance. *Cellular and Molecular Gastroenterology and Hepatology, 7*(2), 447–456.
- Satoh, N., Ogawa, Y., Katsuura, G., Numata, Y., Tsuji, T., Hayase, M., Ebihara, K., Masuzaki, H., Hosoda, K., Yoshimasa, Y., & Nakao, K. (1999). Sympathetic activation of leptin via the ventromedial hypothalamus: Leptin-induced increase in catecholamine secretion. *Diabetes*, *48*(9), 1787–1793.
- Schmidt, M. I., Duncan, B. B., Vigo, A., Pankow, J. S., Couper, D., Ballantyne, C. M., Hoogeveen, R. C., Heiss, G., & For the ARIC Investigators. (2006). Leptin and incident type 2 diabetes: Risk or protection? *Diabetologia*, *49*(9), 2086–2096.
- Schreiber, R., Diwoky, C., Schoiswohl, G., Feiler, U., Wongsiriroj, N., Abdellatif, M., Kolb, D., Hoeks, J., Kershaw, E. E., Sedej, S., Schrauwen, P., Haemmerle, G., & Zechner, R. (2017). Cold-Induced Thermogenesis Depends on ATGL-Mediated Lipolysis in Cardiac Muscle, but Not Brown Adipose Tissue. *Cell Metabolism*, *26*(5), 753-763.e7.
- Schultz, H. D., & Sun, S. Y. (2000). Chemoreflex function in heart failure. *Heart Failure Reviews*, *5*(1), 45–56.
- Schwartz, R. S., Jaeger, L. F., Silberstein, S., & Veith, R. C. (1987). Sympathetic nervous system activity and the thermic effect of feeding in man. *International Journal of Obesity*, *11*(2), 141–149.
- Seale, P., Bjork, B., Yang, W., Kajimura, S., Chin, S., Kuang, S., Scimè, A., Devarakonda, S., Conroe, H. M., Erdjument-Bromage, H., Tempst, P., Rudnicki, M. A., Beier, D. R., & Spiegelman, B. M. (2008). PRDM16 controls a brown fat/skeletal muscle switch. *Nature*, 454(7207), 961–967.
- Semenza, G. L. (1999). Regulation of Mammalian O ₂ Homeostasis by Hypoxia-Inducible Factor 1. *Annual Review of Cell and Developmental Biology*, *15*(1), 551–578.

- Shao, M., Wang, Q. A., Song, A., Vishvanath, L., Busbuso, N. C., Scherer, P. E., & Gupta, R. K. (2019). Cellular Origins of Beige Fat Cells Revisited. *Diabetes*, *68*(10), 1874–1885.
- Shapiro, H., Pecht, T., Shaco-Levy, R., Harman-Boehm, I., Kirshtein, B., Kuperman, Y., Chen, A., Blüher, M., Shai, I., & Rudich, A. (2013). Adipose Tissue Foam Cells Are Present in Human Obesity. *The Journal of Clinical Endocrinology & Metabolism*, *98*(3), 1173–1181.
- Sharma, B. K., Patil, M., & Satyanarayana, A. (2014). Negative Regulators of Brown Adipose Tissue (BAT)-Mediated Thermogenesis. *Journal of cellular physiology*, *229*(12), 1901–1907.
- Shimba, S., Wada, T., Hara, S., & Tezuka, M. (2004). EPAS1 Promotes Adipose Differentiation in 3T3-L1 Cells. *Journal of Biological Chemistry*, *279*(39), 40946–40953.
- Shin, H., Ma, Y., Chanturiya, T., Cao, Q., Wang, Y., Kadegowda, A. K. G., Jackson, R., Rumore, D., Xue, B., Shi, H., Gavrilova, O., & Yu, L. (2017). Lipolysis in Brown Adipocytes Is Not Essential for Cold-Induced Thermogenesis in Mice. *Cell metabolism*, *26*(5), 764-777.e5.
- Shin, M.-K., Eraso, C. C., Mu, Y.-P., Gu, C., Yeung, B. H. Y., Kim, L. J., Liu, X.-R., Wu, Z.-J., Paudel, O., Pichard, L. E., Shirahata, M., Tang, W.-Y., Sham, J. S. K., & Polotsky, V. Y. (2019). Leptin Induces Hypertension Acting on Transient Receptor Potential Melastatin 7 Channel in the Carotid Body. *Circulation research*, *125*(11), 989–1002.
- Siddle, K., & Hales, C. N. (1975). Hormonal control of adipose tissue lipolysis. *Proceedings* of the Nutrition Society, 34(3), 233–239.
- Sidossis, L., & Kajimura, S. (2015). Brown and beige fat in humans: Thermogenic adipocytes that control energy and glucose homeostasis. *The Journal of Clinical Investigation*, *125*(2), 478–486.
- Simonds, S. E., Pryor, J. T., & Cowley, M. A. (2017). Does leptin cause an increase in blood pressure in animals and humans?: *Current Opinion in Nephrology and Hypertension*, *26*(1), 20–25.
- Singh, A., Wirtz, M., Parker, N., Hogan, M., Strahler, J., Michailidis, G., Schmidt, S., Vidal-Puig, A., Diano, S., Andrews, P., Brand, M. D., & Friedman, J. (2009). Leptin-mediated

- changes in hepatic mitochondrial metabolism, structure, and protein levels. *Proceedings* of the National Academy of Sciences, 106(31), 13100–13105.
- Siński, M., Lewandowski, J., Przybylski, J., Bidiuk, J., Abramczyk, P., Ciarka, A., & Gaciong, Z. (2012). Tonic activity of carotid body chemoreceptors contributes to the increased sympathetic drive in essential hypertension. *Hypertension Research: Official Journal of the Japanese Society of Hypertension*, *35*(5), 487–491.
- Somers, V. K., Mark, A. L., & Abboud, F. M. (1988). Potentiation of sympathetic nerve responses to hypoxia in borderline hypertensive subjects. *Hypertension*, *11*(6_pt_2), 608–612.
- Sternini, C. (1997). Organization of the Peripheral Nervous System: Autonomic and Sensory Ganglia. *Journal of Investigative Dermatology Symposium Proceedings*, *2*(1), 1–7. https://doi.org/10.1038/jidsymp.1997.2
- Straznicky, N. E., Eikelis, N., Lambert, E. A., & Esler, M. D. (2008). Mediators of sympathetic activation in metabolic syndrome obesity. *Current Hypertension Reports*, *10*(6), 440–447.
- Straznicky, N. E., Lambert, E. A., Lambert, G. W., Masuo, K., Esler, M. D., & Nestel, P. J. (2005). Effects of Dietary Weight Loss on Sympathetic Activity and Cardiac Risk Factors Associated with the Metabolic Syndrome. *The Journal of Clinical Endocrinology & Metabolism*, *90*(11), 5998–6005. https://doi.org/10.1210/jc.2005-0961
- Streijger, F., Pluk, H., Oerlemans, F., Beckers, G., Bianco, A. C., Ribeiro, M. O., Wieringa, B., & Van der Zee, C. E. E. M. (2009). Mice lacking brain-type creatine kinase activity show defective thermoregulation. *Physiology & behavior*, *97*(1), 76–86.
- Subramanian, S., Han, C. Y., Chiba, T., McMillen, T. S., Wang, S. A., Haw, A., Kirk, E. A., O'Brien, K. D., & Chait, A. (2008). Dietary cholesterol worsens adipose tissue macrophage accumulation and atherosclerosis in obese LDL receptor-deficient mice. *Arteriosclerosis, thrombosis, and vascular biology*, *28*(4), 685–691.
- Sztalryd, C., & Brasaemle, D. L. (2017). The perilipin family of lipid droplet proteins: Gatekeepers of intracellular lipolysis. *Biochimica et biophysica acta*, *1862*(10 Pt B), 1221–1232.

- Taniguchi, C. M., Emanuelli, B., & Kahn, C. R. (2006). Critical nodes in signalling pathways: Insights into insulin action. *Nature Reviews Molecular Cell Biology*, *7*(2), 85–96.
- Tankersley, C. G., O'Donnell, C., Daood, M. J., Watchko, J. F., Mitzner, W., Schwartz, A., & Smith, P. (1998). Leptin attenuates respiratory complications associated with the obese phenotype. *Journal of Applied Physiology*, *85*(6), 2261–2269.
- Tappy, L. (1996). Thermic effect of food and sympathetic nervous system activity in humans. *Reproduction, Nutrition, Development*, *36*(4), 391–397.
- Tchkonia, T., Thomou, T., Zhu, Y., Karagiannides, I., Pothoulakis, C., Jensen, M. D., & Kirkland, J. L. (2013). Mechanisms and Metabolic Implications of Regional Differences among Fat Depots. *Cell metabolism*, *17*(5), 644–656.
- Thorp, A. A., & Schlaich, M. P. (2015). Relevance of Sympathetic Nervous System Activation in Obesity and Metabolic Syndrome. *Journal of Diabetes Research*, *2015*, 341583.
- Trayhurn, P. (2013). Hypoxia and Adipose Tissue Function and Dysfunction in Obesity. *Physiological Reviews*, *93*(1), 1–21.
- Trayhurn, P., Wang, B., & Wood, I. S. (2008). Hypoxia in adipose tissue: A basis for the dysregulation of tissue function in obesity? *British Journal of Nutrition*, *100*(2), 227–235.
- Ukropec, J., Anunciado, R. P., Ravussin, Y., Hulver, M. W., & Kozak, L. P. (2006). UCP1-independent Thermogenesis in White Adipose Tissue of Cold-acclimated Ucp1-/- Mice *. *Journal of Biological Chemistry*, *281*(42), 31894–31908.
- Vague, J. (1996). A Determinant Factor of the Forms of Obesity. *Obesity Research*, 4(2), 201–203.
- Valladares, A., Alvarez, A. M., Ventura, J. J., Roncero, C., Benito, M., & Porras, A. (2000). P38 mitogen-activated protein kinase mediates tumor necrosis factor-alpha-induced apoptosis in rat fetal brown adipocytes. *Endocrinology*, *141*(12), 4383–4395.
- Vaz, M., Jennings, G., Turner, A., Cox, H., Lambert, G., & Esler, M. (1997). Regional Sympathetic Nervous Activity and Oxygen Consumption in Obese Normotensive Human Subjects. *Circulation*, *96*(10), 3423–3429.

- Vidal, M. L., Freixas, J. L. C., Chávez, H. R. T., Chávez, E. U. M., Sánchez, J. E. M., Villegas, S. A. M., Rubio, C. Z. V., Melgoza, J. A. M., Cruz, S. A. M., & Dorronsoro, E. R. (2019). Insulin In The Carotid Sinus Increases Suprahepatic And Arterial Glucose Levels. *Revista Cubana de Investigaciones Biomédicas*, *38*(1), Article 1.
- Villarroya, F., Cereijo, R., Gavaldà-Navarro, A., Villarroya, J., & Giralt, M. (2018). Inflammation of brown/beige adipose tissues in obesity and metabolic disease. *Journal of Internal Medicine*, *284*(5), 492–504.
- Vollenweider, P., Tappy, L., Randin, D., Schneiter, P., Jéquier, E., Nicod, P., & Scherrer, U. (1993). Differential effects of hyperinsulinemia and carbohydrate metabolism on sympathetic nerve activity and muscle blood flow in humans. *Journal of Clinical Investigation*, *92*(1), 147–154.
- Wang, Z. V., & Scherer, P. E. (2008). Adiponectin, Cardiovascular Function, and Hypertension. *Hypertension*, *51*(1), 8–14.
- Waxenbaum, J. A., Reddy, V., & Varacallo, M. (2021). Anatomy, Autonomic Nervous System. Em *StatPearls*. StatPearls Publishing. http://www.ncbi.nlm.nih.gov/books/NBK539845/
- Weigle, D. S., Bukowski, T. R., Foster, D. C., Holderman, S., Kramer, J. M., Lasser, G., Lofton-Day, C. E., Prunkard, D. E., Raymond, C., & Kuijper, J. L. (1995). Recombinant ob protein reduces feeding and body weight in the ob/ob mouse. *Journal of Clinical Investigation*, *96*(4), 2065–2070.
- Weyer, C., Tataranni, P. A., Snitker, S., Danforth, E., & Ravussin, E. (1998). Increase in insulin action and fat oxidation after treatment with CL 316,243, a highly selective beta3-adrenoceptor agonist in humans. *Diabetes*, 47(10), 1555–1561.
- Winer, D. A., Winer, S., Shen, L., Wadia, P. P., Yantha, J., Paltser, G., Tsui, H., Wu, P., Davidson, M. G., Alonso, M. N., Leong, H., Glassford, A., Caimol, M., Kenkel, J. A., Tedder, T. F., McLaughlin, T., Miklos, D. B., Dosch, H.-M., & Engleman, E. G. (2011). B Lymphocytes Promote Insulin Resistance through Modulation of T Lymphocytes and Production of Pathogenic IgG Antibody. *Nature Medicine*, *17*(5), 610–617.

- World Health Organization—Obesity and overweight. (2021, Junho 9). https://www.who.int/news-room/fact-sheets/detail/obesity-and-overweight
- Wu, H., & Ballantyne, C. M. (2020). Metabolic Inflammation and Insulin Resistance in Obesity. *Circulation research*, *126*(11), 1549–1564.
- Wu, J., Boström, P., Sparks, L. M., Ye, L., Choi, J. H., Giang, A.-H., Khandekar, M., Nuutila, P., Schaart, G., Huang, K., Tu, H., van Marken Lichtenbelt, W. D., Hoeks, J., Enerbäck, S., Schrauwen, P., & Spiegelman, B. M. (2012). Beige Adipocytes are a Distinct Type of Thermogenic Fat Cell in Mouse and Human. *Cell*, *150*(2), 366–376.
- Yao, Q., Pho, H., Kirkness, J., Ladenheim, E. E., Bi, S., Moran, T. H., Fuller, D. D., Schwartz, A. R., & Polotsky, V. Y. (2016). Localizing Effects of Leptin on Upper Airway and Respiratory Control during Sleep. *Sleep*, *39*(5), 1097–1106.
- Ye, J., Gao, Z., Yin, J., & He, Q. (2007). Hypoxia is a potential risk factor for chronic inflammation and adiponectin reduction in adipose tissue of *ob / ob* and dietary obese mice. *American Journal of Physiology-Endocrinology and Metabolism*, *293*(4), E1118–E1128.
- Yin, J., Gao, Z., He, Q., Zhou, D., Guo, Z., & Ye, J. (2009). Role of hypoxia in obesity-induced disorders of glucose and lipid metabolism in adipose tissue. *American Journal of Physiology Endocrinology and Metabolism*, *296*(2), E333–E342.
- Yoneshiro, T., Aita, S., Matsushita, M., Kameya, T., Nakada, K., Kawai, Y., & Saito, M. (2011). Brown Adipose Tissue, Whole-Body Energy Expenditure, and Thermogenesis in Healthy Adult Men. *Obesity*, *19*(1), 13–16.
- Young, J. B., & Macdonald, I. A. (1992). Sympathoadrenal activity in human obesity: Heterogeneity of findings since 1980. *International Journal of Obesity and Related Metabolic Disorders: Journal of the International Association for the Study of Obesity,* 16(12), 959–967.
- Yudkin, J. S., Kumari, M., Humphries, S. E., & Mohamed-Ali, V. (2000). Inflammation, obesity, stress and coronary heart disease: Is interleukin-6 the link? *Atherosclerosis*, 148(2), 209–214.

Zhang, F., Hao, G., Shao, M., Hassan, G., An, Y., Wang, Q., Zhu, Y., Kusminski, C. M., Nham, K., Gupta, R. K., Zhai, Q., Sun, X., Scherer, P. E., & Oz, O. K. (2018). An Adipose Tissue Atlas: An Image Guided Identification of Human-like BAT and Beige Depots in Rodents. *Cell metabolism*, *27*(1), 252-262.e3.

Zhang, M., Buttigieg, J., & Nurse, C. A. (2007). Neurotransmitter mechanisms mediating low-glucose signalling in cocultures and fresh tissue slices of rat carotid body. *The Journal of Physiology*, *578*(Pt 3), 735–750.